



UNIVERSITÀ DEGLI STUDI DI TORINO

Scuola di Dottorato in Scienze della Vita e della Salute
Programma in Scienze Biomediche e Oncologia Umana
Indirizzo di Genetica Umana

TESI DI DOTTORATO

Therapeutic approaches in gastric cancer based on genetic and biological analysis

Candidato:

Tânia Isabel de Miranda CAPELÔA

Relatore:

Prof.ssa Claudia GIACHINO

Co-relatore:

Prof.ssa Silvia GIORDANO

Coordinatore del dottorato

Prof Emilio HIRSCH

Coordinatore di Genetica Umana:

Prof Giuseppe MATULLO

ANNI ACCADEMICI: 2014-2017

Index

Abstract	5
1- Introduction	8
1.1- Gastric cancer: Clinical aspects	8
1.1.1- Epidemiology	8
1.1.2- Genetics	9
1.1.3- Risk factors	10
1.1.4- Clinical presentation and diagnosis	11
1.1.5- Therapeutic approaches	12
1.2- Classification systems	13
1.2.1- Lauren's classification	14
1.2.2- WHO classification	14
1.2.3- Molecular classifications	15
1.3- Therapeutic molecular targets	18
1.3.1- HER2	19
1.3.2 - EGF/EGFR	21
1.3.3 - VEGF/VEGFR-2	23
1.3.4 - HGF/MET	24
1.3.5 - Other targets	28
1.4- KRAS	29
1.4.1 - KRAS activation and Signaling	29
1.4.2 - KRAS mutations	31
1.4.3 - KRAS THERAPIES	32
1.4.4 - KRAS in gastric cancer	35
1.5- Translational cancer research	36
1.5.1 - Patient-derived cancer xenografts (PDX)	37
1.5.2 - Outstanding characteristic of PDX models	38
1.5.3 - Limitations of PDX models	38
1.6- Patients –derived cell models as preclinical tools	39
1.6.1 - Cancer stem cells	40
1.6.2 - Origin of Gastric Cancer Stem Cells (GCSCs)	42
1.6.3 - Gastric cancer stem cells markers	42
1.6.4 - Gastric cancer stem cells and therapies	43
2- Aim of the work	46
3- Material and methods	48
3.1- Patient and tumor samples	48
3.2 - Animals	48
3.3 - Xenograft transplantation	48
3.4 - Drugs	49

3.5 - Primary Cell culture	49
3.6 - Sphere isolation	49
3.7 - Anchorage-independent cell growth assay	50
3.8 - Cell viability	50
3.9 - Gene copy number and gene expression analysis by real-time PCR	50
3.10 - Sanger sequencing	51
3.11 - Gene silencing	51
3.12 - Western blot analysis	51
3.13 - Pull-down assay for RAS	52
3.14 - Lactate uptake	52
3.15 - Lactate production	52
3.16 - Xenotrials	52
3.17 - Immunohistochemistry	54
3.18 - Statistical Analysis	54
4- Results	56
4.1 - The “GEA PLATFORM” project	56
4.1.1 - Establishment of PDX models	56
4.1.2 - Factors influencing PDX generation	57
4.1.3 - PDX characterization	57
4.2 - PDX-derived <i>in vitro</i> models	58
4.2.1 - Xenospheres characterization	58
4.3 - <i>MET</i> amplified PDX model	62
4.3.1 - <i>MET</i> amplified PDX model characterization	62
4.3.2 - <i>MET</i> amplified PDX- derived cells response to <i>MET</i> inhibition	64
4.3.3 - <i>MET</i> amplified PDX response to <i>MET</i> inhibition <i>in vivo</i>	66
4.3.4 <i>In vivo</i> generation of a <i>MET</i> amplified xenopatient model resistant to the <i>MET</i> inhibitor JNJ-605	69
4.4 - <i>KRAS</i> PDX models	71
4.4.1 - <i>KRAS</i> amplified and mutated gastric tumors	71
4.4.2 Characterization of <i>KRAS</i> mutated and amplified models	72
4.4.3 - RAS activation state in <i>KRAS</i> mutated and amplified cells	74
4.4.4 – Changes in glycolytic metabolism in <i>KRAS</i> mutated and amplified <i>in vitro</i> models	77
4.4.5 - <i>KRAS</i> mutated and amplified models are addicted to <i>KRAS</i>	78
4.4.6 - <i>In vitro</i> response to <i>KRAS</i> downstream inhibitors of <i>KRAS</i> mutated and amplified models	80
4.4.7 - <i>KRAS</i> mutated model <i>in vivo</i> response to <i>KRAS</i> downstream inhibitors	83
5- Discussion	88
6- Conclusions	95
6.1 - Future perspectives	95
7- References	97

Acknowledgments.....	112
PhD Report.....	113

Abstract

Gastric cancer is the fifth most common malignancy in the world and represents the third leading cause of cancer-related death. The overall clinical outcome for patients with advanced gastric cancer is poor, and Trastuzumab is the only therapy targeting tumor molecular alterations added to the cytotoxic treatments, which has anyway given unsatisfactory results.

In the last decades several preclinical models have been developed to better understand the mechanisms of tumor drug response. Patient-derived tumor xenografts (PDXs) are *in vivo* models that recapitulate the histological and molecular characteristics of the patient tumor and can be used to generate *in vitro* models for drug screens. Among these *in vitro* models, 2D/3D cell cultures and cancer stem cells have been isolated from tumors and studied due to their importance for understanding tumor resistance to antitumor therapies.

In this work we took advantage of our recently generated and characterized gastric cancer PDX platform, and explored the response to target therapies in different models. In particular, we focused on three main issues: i) the isolation, characterization and response to target therapies of gastric cancer stem cells; ii) the mechanisms of response and resistance to MET inhibitors using PDXs and gastric cells lines with *MET* amplification and addiction to this oncogene, and finally, iii) the characterization of *KRAS* amplified and mutated PDX models. *KRAS* mutations and amplifications have been poorly studied in gastric cancer, so in this work we explored whether *KRAS* could be a target in gastric cancer, and if the differences between *KRAS* amplified and mutated models could have relevance on therapy. Since no strategy has already been defined to target *KRAS*, *KRAS* pathway inhibition was explored *in vitro* and *in vivo* using *KRAS* downstream effectors inhibitors (MEK, AKT, and mTOR) or PARP inhibitors, alone or in combination.

From the *MET* amplified PDX we obtained a cohort of tumor-bearing animals that were treated with anti-MET drugs. The performed preclinical trial in the PDXs showed that i) even in the presence of more than 26 *MET* gene copies, anti-MET drugs induced only a partial response due to the activation of EGFR; ii) treatment with a combined anti-MET/anti-EGFR therapy resulted in a durable, complete response and prevented the onset of resistance. From the *MET* amplified PDXs we were also able to isolate and characterize stem like cells that maintained *MET* amplification and responded in the same way to MET inhibition as the PDX and PDX-derived cells.

Regarding the *KRAS* PDX models, we found that *KRAS* amplified models displayed high levels of RAS activation, were addicted to *KRAS* and, *in vitro*, presented a response to *KRAS*

downstream pathway inhibitors similar to that observed in *KRAS* mutated models. Indeed, they showed a partial response to MEK inhibition, which increased when drugs targeting AKT, mTOR or PARP were added to the MEK inhibitor. One preclinical trial was performed in a PDX with a G12D *KRAS* homozygous mutation. Single treatment with Trametinib (MEKi) or Everolimus (mTORi) and their combinations led to a delay in the tumor growth while single treatments with MK-2206 and Olaparib were ineffective. The effects of the single in vivo treatments recapitulate those obtained in vitro experiments

Overall, these results support the use of PDX models as a potent investigational platform for better understanding resistance to target therapies in gastric cancer which could be translated to patients.

Key words: Gastric Cancer, Target Therapy, Translational Oncology, Gastric Cancer Stem Cells, c-MET, KRAS.

CHAPTER I

INTRODUCTION

1- Introduction

1.1- Gastric cancer: Clinical aspects

1.1.1- Epidemiology

Gastric cancer is the fifth most common cause of cancer worldwide, after lung, breast, colorectal and prostate cancer. Despite a significant decline in incidence and mortality during the second half of the 20th century, gastric cancer still represents the third leading cause of cancer-related death in both sexes worldwide (723,000 deaths, 8.8% of the total) (1). The most recent data account for more than 26,000 new cases and 10,500 deaths ([Figure 1](#)) occurred in the United States in 2016 (2); both values are estimated to increase in 2017 (28,000 new cases and 10,960 deaths) (3). Although the number of deaths is still high, a substantial change occurred since 1975 when stomach cancer was the most common neoplasm (1).

In the last 10 years, the rates for new stomach cancer cases have been falling on average 1.5% each year, while death rates have dropped on average 2.4% each year over 2005-2014, reaching 3% in US (4). Stomach cancer is most frequently diagnosed among people aged 65-74 (median age at diagnosis is 68 years) (4). Age-standardized incidence is twofold higher in males than females (2) (3) as one in 27 men and 1 in 68 women developed gastric cancer before age 79 years in 2013 (5). Male incidence rate ranges from 3.3 in Western Africa to 35.4 in Eastern Asia, and in developing countries (70% of total cases, 456,000 in men, 221,000 in women) (1). Age-standardized incidence rates (ASIRs) per 100 000 in both sexes are 17 and 14 in developing and developed countries, respectively (6).

Gastric cancer remains one of the most common neoplasms worldwide, showing a stable trend due to both the decreasing incidence and the increasing 5-year survival rates (6). In patients with localized, operable disease, the 5 years relative overall survival ranges from 62.7% to 30.7% (4). However, in patients with metastatic disease the 5 years relative overall survival is 5.2% only (4); palliative chemotherapy improves survival compared to best supportive care (BSC) enhancing median survival from 4.3 months (weighed average in BSC) to 11 months (with chemotherapy) (7).

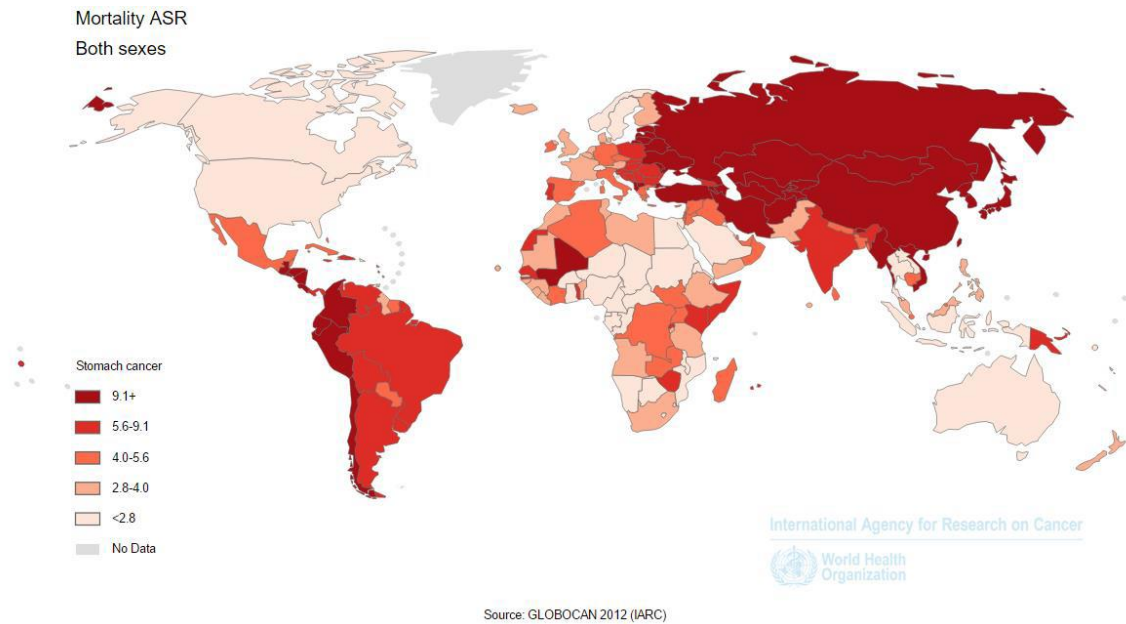


Figure 1 - World gastric cancer mortality. Age-standardized ratios. Adapted from <http://globocan.iarc.fr>

1.1.2- Genetics

The majority of gastric cancer cases is sporadic; only 10% are familial and at least three hereditary syndromes exist including gastric cancer: hereditary diffuse gastric cancer (HDGC), gastric adenocarcinoma and proximal polyposis of the stomach (GAPPS), and familial intestinal gastric cancer (FIGC). HDGC is caused by an autosomal dominant heterozygous germline mutation in the gene *CDH1* that encodes the E-cadherin protein, which is involved in cell-to-cell adhesion. This is a loss of function mutation that contributes to neoplastic progression as well as facilitating tumor metastases through spread of cancer cells across the tissue basement membrane. This condition predisposes patients not only to early-onset diffuse gastric cancer but also to lobular breast cancer (8). Prophylactic total gastrectomy is highly recommended for individuals with pathogenic *CDH1* mutations (9). Another hereditary syndrome linked to gastric cancer is GAPPS, a gastric polyposis syndrome with a significant risk of gastric adenocarcinoma, characterized by the autosomal dominant transmission of fundic gland polyposis, which demonstrates areas of dysplasia or intestinal type gastric cancer, restricted to the proximal stomach, without evidence of colorectal or duodenal polyposis or other heritable gastrointestinal cancer syndromes (10). FIGC is also inherited with an autosomal dominant pattern but, unlike GAPPS, there is no evidence of gastric polyposis. Nevertheless, the genetic factors involved in GAPPS and FIGC are still unclear (8). Epigenetic methylation of *CDH1* was reported in approximately 17% of cases, and loss of heterozygosity in 9.4% of cases (11) Gastric cancer is also related to a multiplicity of cancer-associated syndromes with known genetic

causes, such as Lynch, familial adenomatous polyposis, Li-Fraumeni, Peutz-Jeghers, juvenile polyposis and BRCA1 and BRCA2 hereditary breast and ovarian cancer syndromes (12).

1.1.3- Risk factors

Innumerable risk factors have been associated with the onset of gastric cancer. They include: *Helicobacter pylori* infection, genetics predisposition, high salt and nitrite-containing foods consumption, smoking, obesity, pernicious anemia and chronic atrophic gastritis (8). In 1994, *Helicobacter pylori* was recognized as a “Group 1 human carcinogen” by the International Agency for Research on Cancer (13). Indeed, *H. pylori* infection doubles the risk of developing gastric cancer (14). In *H. pylori* infected patients, some combinations of single nucleotide polymorphisms (SNPs) in immune-related genes (interleukin 1-b [IL-1 b], interleukin 1 receptor antagonist [IL-1RN], tumor necrosis factor-a [TNF-a] and interleukin 10 [IL-10]) increase the risk of experiencing gastric cancer (15). Besides *H. pylori* there is another infectious agent that plays a relevant role in gastric cancer onset. According to the most recent GC classification proposed by The Cancer Genome Atlas (TCGA), about 10% of gastric cancers are EBV-positive (Epstein-Barr virus). EBV may directly contribute to the development of EBV-associated gastric cancer through multiple mechanisms since EBV affects several host proteins and pathways that normally promote apoptosis and regulate cell proliferation. EBV-associated gastric carcinomas have some distinctive clinicopathological characteristics: they occur predominately in men and in younger individuals, and present a diffuse histological type. Furthermore, most cases exhibit rich lymphocyte infiltration (16).

The role of diet is still controversial: it has been demonstrated that diets rich in complex carbohydrates and poor in proteins, with a small intake of fresh fruit and vegetables may promote tumorigenesis through acid-catalyzed nitrosation in the stomach as well as mechanical damage of the gastric mucosa (17). A meta-analysis of seven prospective studies demonstrated that a direct correlation between dietary salt intake and risk of gastric cancer exists and this risk progressively increases with salt consumption levels (18). Intake of large amounts of salt and salt-preserved foods facilitates *H. pylori* colonization, and increases the risk of gastric cancer through direct damage to the gastric mucus and hence to the mucosa. Salt is also known to increase the production of gastrin and to induce endogenous mutations, promoting epithelial cell proliferation (19). Epidemiological data also suggest that high intake of nitrosamines, processed meat products, salted foods, overweight and obesity are associated with increased risk for gastric cancer. (20) Nitrosamines and N-nitrosornicotine can also be found in tobacco products, which have demonstrated carcinogenic effects both in animals and in humans (21).

Being a man is also a risk factor for gastric cancer, since the relative risk (RR) of developing gastric cancer is 1.62 and 1.20 in men and women, respectively, according to the European Prospective Investigation into Cancer and Nutrition group studies (22).

1.1.4- Clinical presentation and diagnosis

Gastric cancer is a type of cancer that mainly does not present characteristic clinical features or pathognomonic symptoms in early stages; for this reason it is often diagnosed in advanced stages. As the disease progresses, some symptoms can appear, such as abdominal pain, nausea and dyspepsia, usually associated with weight loss, early satiety, or digestive hemorrhage. Gastric tumors present a local invasion that can lead to external compression and distal obstructive symptoms, gastro-intestinal bleeding, colonic invasion, and subsequent fistulisation or obstruction, or gastric perforation. Lymph nodes, liver, lungs and the peritoneal surface are the most common sites of metastasis. In early stages, physical investigation is often silent, while in advanced disease a palpable abdominal mass, ascites, left supraclavicular adenopathy (Virchow node), periumbilical lesions (Sister Mary Joseph sign), and can appear (8).

According to the European Society for Medical Oncology (ESMO) clinical practice guidelines (23), the diagnostic imaging procedure of choice in the work-up of gastric cancer is EGDS (Esophagogastroduodenoscopy), mainly because it allows direct visualization of the disease. Moreover, biopsies can be performed for histological confirmation and identification of any precancerous lesions or *H. pylori* infection (23) Even though EGDS is excellent for recognizing developed or large tumor masses, it lacks sensitivity when identifying early lesions. For this reason, in order to support the identification of microscopic lesions, some new techniques such as high-resolution endoscopy with narrow band imaging and image-enhanced endoscopy, have been introduced (24). Endoscopy is also used for screening in some Eastern Countries with high prevalence of gastric tumors, such as Japan and Korea. In these areas, the screening is a useful and cost-effective tool since it allows the diagnosis at an early stage of approximately 50% of the gastric cancer cases (25). EUS (Endoscopic Ultrasound) is also a useful tool, particularly to assess tumor and nodal staging, allowing biopsies of suspected and endoscopically accessible lymph nodes (23). CT and FDG-PET are required for the disease staging. Diagnostic laparoscopy may be performed to evaluate specifically peritoneal metastases (23).

1.1.5- Therapeutic approaches

Surgical resection is still the only curative treatment for gastric cancer, although many therapeutic approaches have been proposed and used through the years (8). Partial or total gastrectomy, with or without lymphadenectomy, are the two principal surgical options and the decision between them is dictated by the stage of the disease (8).

Endoscopic mucosal resection and endoscopic mucosal dissection are other types of potentially curative and mini-invasive treatments for early gastric cancer resection (8). An important and debated problem is the type of lymphadenectomy (D1 vs D2 or even D3). The incidence rates of lymph node metastases are reported to be 52.2%, 66.9%, 74.4%, and 82.6% when the neoplasm is spread through the muscularis propria, subserosa, serosa, and adjacent structures, respectively (26). Lymph node dissection decreases locoregional recurrence, improves staging of the disease and possibly has some benefits in overall survival (27) (28) (29). Nevertheless, there is no agreement among Western and Eastern countries about the best type of lymphadenectomy that should be performed (8), even if D1 dissections are usually followed by adjuvant chemoradiation.

Surgery remains the keystone of treatment for gastric cancer, as the only therapeutic tool in early stages and in combination with other types of treatments in later stages. The majority of patients with advanced cancer relapse even after complete surgical resection, and these patients may eventually die of this disease (30). For this reason, numerous randomized clinical trials have been carried out in order to evaluate the best perioperative treatment. In Europe, the randomized studies MAGIC (31) and FNCLCC (32) are the principal reference for integrated protocols: these studies have demonstrated a survival benefit for neoadjuvant and perioperative treatment in GC staged >T1 and/or N+ (33). Chemotherapy schemes in these studies were based on preoperative and postoperative cycles of intravenous cisplatin alone or in combination with epirubicin and a continuous intravenous infusion of fluorouracil (31) (32). Treatment options are limited, since patients often progress after first-line chemotherapy and usually have a worsened performance status. However, recent studies established that irinotecan or docetaxel monotherapy as second-line therapy, determine a survival advantage compared to BSC (34).

Besides standard therapy, two targeted drugs have been approved for metastatic gastric cancer by EMA (European Medicine Agency) and FDA (Food and Drug Administration, USA): Trastuzumab, an anti-HER2 monoclonal antibody, and Ramucirumab, an anti-VEGFR2 monoclonal antibody, which exerts an antiangiogenic activity (35). Additionally, Apatinib, an oral tyrosine kinase inhibitor against VEGFR2, was approved in 2014 by CFDA (China Food

and Drug Administration) for patients with metastatic gastric cancer after second-line chemotherapy (36). According to guidelines, Trastuzumab should be offered to HER2-positive gastric cancer patients (Figure 2). Immunohistochemistry (IHC) and *in situ* hybridization (ISH) analysis are required to assess HER2 positivity. A strong, complete, basolateral or lateral membranous staining in $\geq 10\%$ of tumor cells (in surgical specimens) and a tumor cell cluster with a strong, complete, basolateral or lateral membranous reactivity (in biopsy specimens) is defined as IHC strongly positive (IHC3+): this is sufficient to consider a sample as HER positive. IHC0/1+ is considered negative, whereas IHC2+ requires ISH assessment (HER2/CEP17 ratio ≥ 2 is defined as positive) (37).

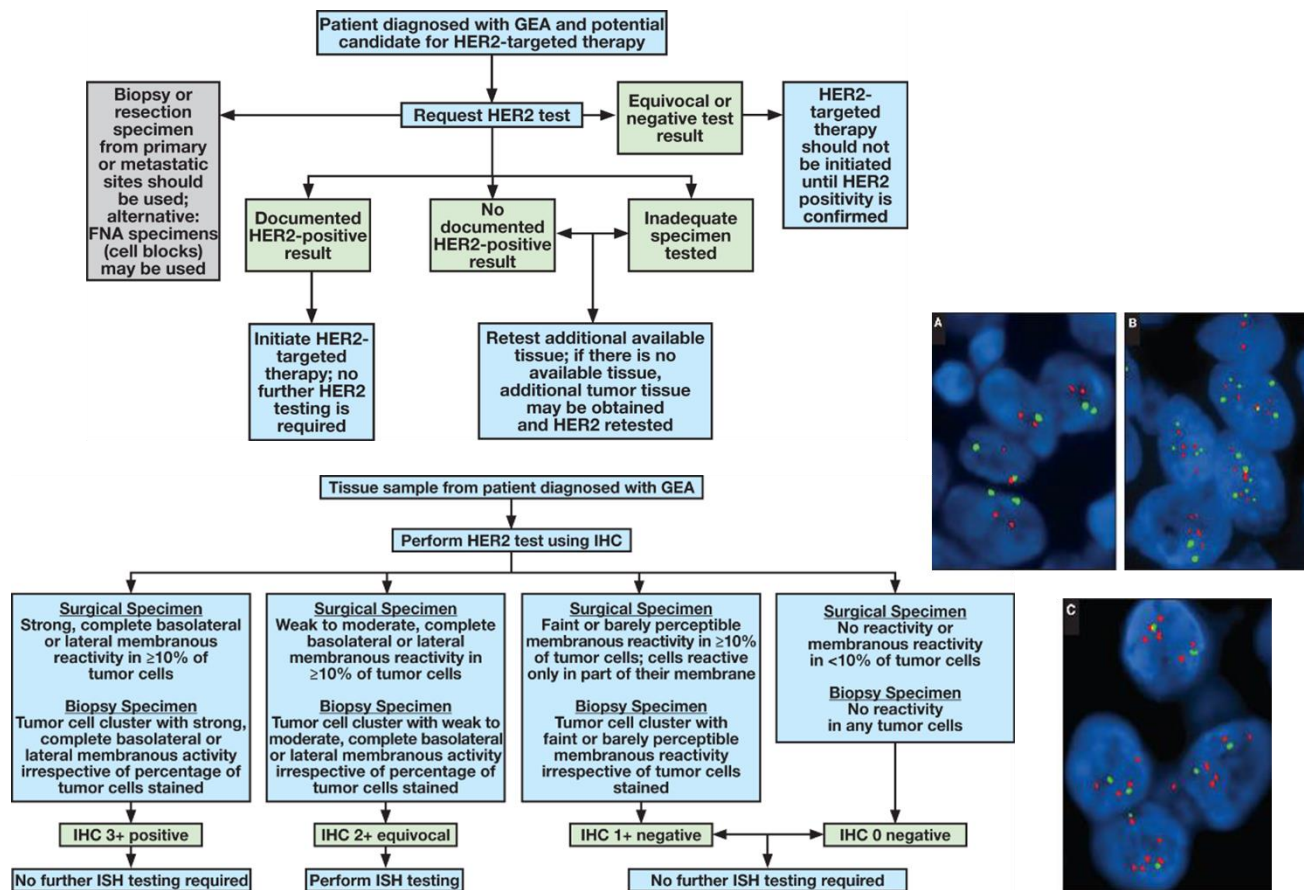


Figure 2 - Flow chart to assess HER2 positivity in gastric cancer. GEA: Gastro-Esophageal Adenocarcinoma. FNA: Fine Needle Aspiration. IHC: Immunohistochemistry. Modified from Bartley *et al.*, 2016.

1.2- Classification systems

Stomach cancer refers to any malignant neoplasm that arises from the region extending between the gastroesophageal junction and the pylorus. The largest part of stomach tumors is of epithelial origin (approximately 95%) and are classified as adenocarcinomas. Histological types such as undifferentiated carcinomas, adenosquamous and squamous are rare entities (38). The

most used classification systems for gastric cancer are based on the tumor histology, namely Lauren's classification and the World Health Organization (WHO) system (8).

1.2.1- Lauren's classification

Lauren's classification divides gastric adenocarcinomas in two main subtypes: intestinal and diffuse (39). The intestinal subtype is more common in men and older people in high-risk regions and is characterized by a better prognosis (38). It is often associated with *H. Pylori* infection and is defined as the last step after a precancerous cascade which consists of i) non-atrophic gastritis, which is the result of acute inflammation with infiltration of polymorphonuclear cells within the gastric glands; ii) atrophic gastritis with a loss of parietal cells; iii) intestinal metaplasia in which injured gastric cells originate glands with intestinal phenotype; iv) dysplasia, that is characterized by nuclear atypia and architectural disorganization (8). The diffuse subtype may also be associated with *H. Pylori*, but precancerous lesions are not well defined (8). It is the predominant subtype in endemic areas, in which the incidence is low and it is more frequent in women and younger patients (38). The pathognomonic feature of this subtype is the presence of signet ring cells (40), where cell nuclei are displaced to the periphery by intracellular mucin (41). These cells are also characterized by loss of E-cadherin expression (42), which allows them to infiltrate more easily through the leathery and thickened stomach wall, giving rise to *linite plastica* (43).

1.2.2- WHO classification

According to WHO classification, gastric cancer can be divided in nine subtypes according to their predominant histological arrangement: I) adenocarcinoma intestinal; II) adenocarcinoma diffuse; III) papillary adenocarcinoma (with elongated, finger-like processes supported by fibrovascular stalks and lined by cuboidal or cylindrical cells); IV) tubular adenocarcinoma (with tubules of irregular shapes and sizes, lined by cuboidal, cylindrical or flattened cells); V) mucinous adenocarcinoma (in which mucin is the major component of the extracellular matrix and fills the gland lumen, compressing the epithelium and forming mucin lakes where cells float); VI) signet-ring cell carcinoma (in which mucin is intracellular) and other less frequent subtypes, such as VII) adenosquamous, VIII) squamous and IX) undifferentiated carcinoma (44).

A distinct classification proposed by the Japanese Endoscopic Society for Early Gastric Cancer, now exploited worldwide, describes four types of gastric cancer: type 1, with protruding growth; type 2, with superficial growth (further subdivided into 2a-c with respectively elevated,

flat, and depressed growth); type 3, with excavating growth; and type 4, with infiltrating growth with lateral spreading (45).

These types of classification systems based on the tumor histology do not have particular clinic applicability, since they do not have a prognostic or predictive role. For this reason, they cannot be used to guide the clinical management of the disease, either initially for potentially curative treatment, or for advanced disease (46). In order to overcome this need, The Cancer Genome Atlas (TCGA) Research Network and the Asian Cancer Research Group (ACRG) proposed two different but related classifications, based on molecular profiling data.

1.2.3- Molecular classifications

The first molecular classification of gastric cancer was proposed by the TCGA Research Network with the objective of identifying deregulated pathways and candidate drivers of distinct classes of gastric cancer. In this study 295 gastric adenocarcinoma samples derived from patients not treated with chemotherapy or radiotherapy were analyzed. Somatic alterations of the germline DNA were also studied by analyzing matched blood or normal mucosa of each case (47). The authors performed six different types of analyses: somatic copy number alterations evaluation, DNA methylation profiling, messenger RNA sequencing, microRNA (miRNA) sequencing and proteomic analysis. They also performed microsatellite instability (MSI) testing on tumor DNAs, and low-pass whole genome sequencing on 107 tumor/germline pairs.

From this integrated analysis they identified four molecularly distinct subtypes ([Figure 3](#)). The first subtype, called EBV (Epstein-Barr Virus)-positive, is characterized by a high EBV burden and extensive DNA promoter hypermethylation. The second subtype, named MSI (microsatellite instable), shows elevated mutation rates and hypermethylation and is enriched for MSI (microsatellite instability). The remaining two groups are distinguished by the presence or absence of extensive somatic copy-number aberrations (SCNAs), being called CIN or chromosomal instable and GS or genomically stable group, respectively.

The EBV subtype accounts for 9% of all the analyzed gastric cancers (47). This subtype has a typical CIMP (CpG island methylator phenotype) methylation profile and the highest prevalence of DNA hypermethylation among all the 295 described human tumor types. This subcategory is characterized by the highest frequency of *PIK3CA* (phosphatidylinositol-4,5-bisphosphate 3-kinase catalytic subunit α) mutations (80% of cases); mutations in genes like *ARID1A* (AT-rich interaction domain 1A gene) and *BCOR* (BCL6 corepressor gene) account for 55% and 23% cases, respectively (47). Specific gene aberrations detected in the EBV subtype, such as amplification of a locus containing *JAK2* (Janus kinase) and *PDL1/2* (Programmed cell

death 1 ligand 1 and 2; inhibitory immune checkpoint) genes may be functionally implicated in the identification of strong IL-12 mediated signaling molecular signatures, an event that suggests the presence and/or communication with immune cells (46). EBV subtype tumors are mainly found in the gastric fundus or body and in male patients (47).

The second subtype, the MSI group, represents 22% of gastric adenocarcinomas, is enriched for MSI, shows elevated mutation rate and is characterized by a hypermethylated pattern (47). In this subtype, mutations of kinases such as *PIK3CA* (42%), *HER3* (14%), *JAK2* (11%), *EGFR* (5%), *HER2* (5%), *MET* (3%) and *FGFR2* (2%) are present. Additionally, MSI tumors present common alterations in major histocompatibility complex class I genes, such as *B2M* and *HLA-B*, potentially suggesting reduced tumor antigen presentation to cells of the immune system (46). MSI tumours are diagnosed at relatively older ages and patients tend to be female (47).

The GS subtype accounts for 20% of the studied cases. Tumors belonging to this group, present frequent alterations in genes involved in cell adhesion, such as mutations in *RHOA* (15%), *CDH1* (26%), and *CLDN18/ARHGAP* fusion (15%), while extensive somatic copy number aberrations are not frequent (46). In the GS subtype, expression of cell adhesion pathways, including the B1/B3 integrins, syndecan-1 mediated signaling, and angiogenesis related pathways, is significantly increased (47). Genomically stable tumors prevalently show a diffuse histological subtype and are diagnosed at an earlier age (median age 59 years) (47).

The majority of the studied tumors belongs to the CIN group (50%) (47). The most frequently mutated gene is *TP53*, while the most frequently amplified genes are *KRAS/NRAS* (18%), *HER2* (24%), *EGFR* (10%), *PIK3CA* (10%), *HER3* (8%), *FGFR2* (8%), *MET* (8%), and *JAK2* (5%) (45). CIN tumors are more frequently found in the gastroesophageal junction/cardia (Figure 3) (47).

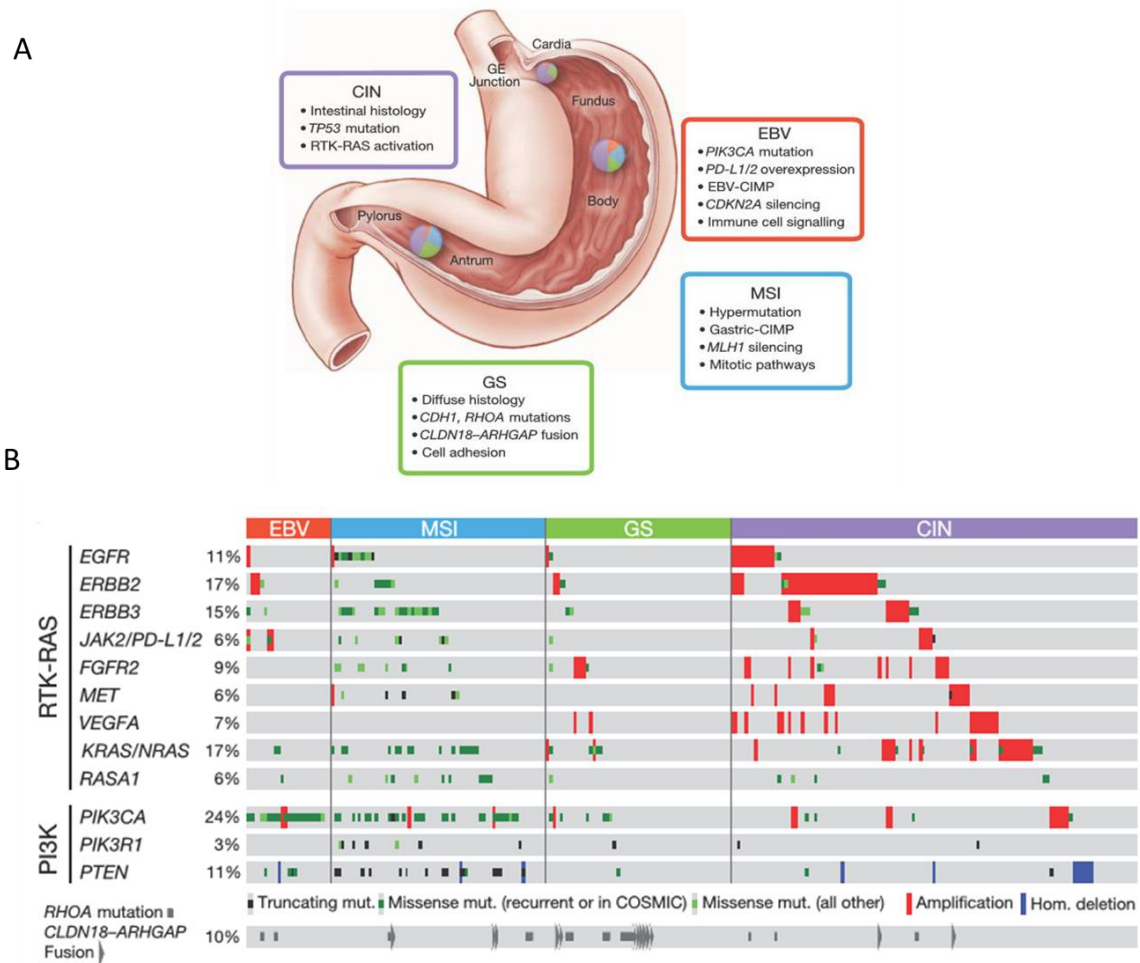


Figure 3 - Key features of gastric cancer subtypes and their integrated molecular analysis. A) This scheme represents some of the salient characteristics of each of the four described molecular subtypes. The distribution of the molecular subtypes in tumors obtained from distinct regions of the stomach is represented in insert charts; colors of the inserts refer to the subtype frames. CIN= chromosomal instable; EBV= Epstein-Barr Virus-positive; MSI= microsatellite instable; GS= genomically stable. B) Mutations, copy-number changes and translocations for selected genes are shown across samples organized by molecular subtypes. Frequencies of the alterations are indicated as a percentage of all cases. Adapted from: The Cancer Genome Atlas Research Network, 2014.

Only a short time after the first TCGA Research Network molecular classification for gastric cancer (47), the Asian Cancer Research Group (ACRG) proposed a second one (48). In this work 300 samples of adenocarcinoma of the stomach were collected, examined and submitted to gene expression profiling, genome-wide copy number microarrays and targeted gene sequencing (48). Specimens were derived from patients who did not receive neoadjuvant chemotherapy or chemoradiation. From the analysis of all these data, ACRG proposed a new classification system which consists of four subtypes: MSI, MSS/EMT, MSS/TP53+ (p53 active) and MSS/TP53- (p53 inactive) (Figure 4) (49). Differently from the TCGA classification, the molecular subtypes of the ACRG classification are correlated with clinical prognosis (46).

The MSI subtype is characterized by the loss of MLH1 and presents hypermutations in genes such as KRAS (23%), ALK (16.3%), ARID1A (44.2%), as well as in those involved in the PI3K pathway (42%). Tumors belonging to this group occur mainly in the antrum (75%), are preferentially of the intestinal type (>60%), and are mostly diagnosed at early stages.

Interestingly, MSI tumors show the best prognosis. The MSS/EMT subtype is distinguished by microsatellite stability and epithelial–mesenchymal transition. This group presents a lower mutation rate compared with the other MSS groups ($P < 0.001$), and lacks CNV alterations. MSS/EMT tumors occur at a younger age, mainly display a diffuse histology with loss of cadherin, are often diagnosed at late stages, and are related with the worst prognosis. The MSS/EMT type is associated with a higher chance of recurrence compared with MSI subtype (63% versus 23%). The MSS/TP53– group presents the highest prevalence of *TP53* mutations (60%) and genomic instability. Recurrent focal amplifications in genes such as *HER2*, *EGFR*, *CCNE1*, *CCND1*, *MDM2*, *ROBO2*, *GATA6* and *MYC* are common and significantly enriched in these types of tumors. Instead, in the MSS/TP53+ subtype the genes more frequently mutated are *APC*, *ARID1A*, *KRAS*, *PIK3CA*, and *SMAD4*. This is the group in which the EBV infection occurs more frequently. Concerning prognosis, the MSS/TP53+ and MSS/TP53– subtypes present an intermediate prognosis (49).

Each one of these two classifications, in its own way, represents an important step forward in advancing knowledge of the molecular basis and subtyping of gastric cancer.

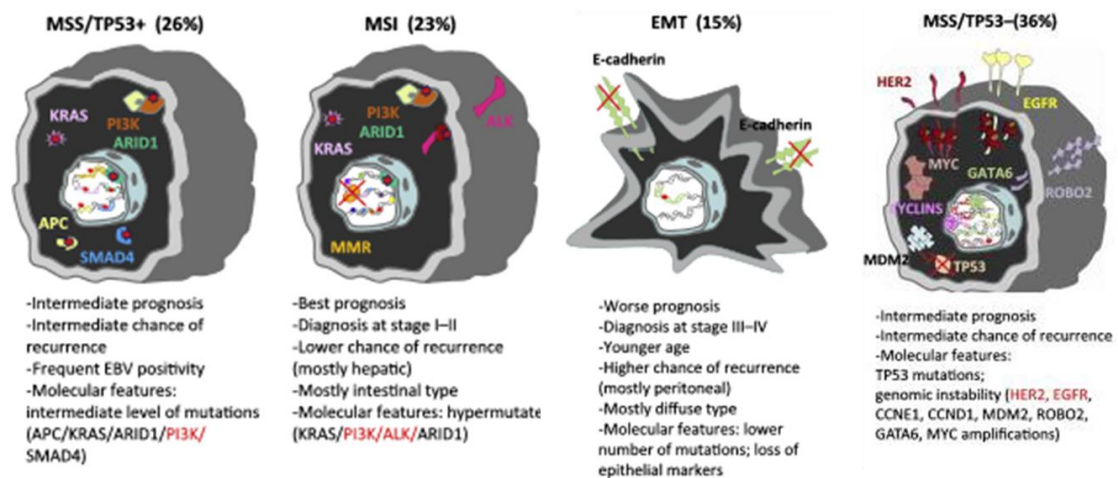


Figure 4 - Gastric Cancer Classification Proposed by the Asian Cancer Research Group. MSI, tumors with microsatellite instability; EMT, tumors with epithelial–mesenchymal transition; MSS/TP53+, tumors with microsatellite stability and p53 activity; MSS/TP53–, tumors with microsatellite stability and loss of p53 activity. Major molecular alterations are shown, those currently targetable are highlighted in red. Modified from Corso S. *et al.*, 2016

1.3- Therapeutic molecular targets

It is clearly recognized that gastric cancer is a heterogeneous disease, that has been divided into different subgroups based on anatomical, epidemiological, histological and, more recently, molecular classifications. The molecular subtyping of gastric cancer can extensively provide uncovered potentially targetable features and it is fundamental for the development of rational molecular therapies. The modest efficacy of conventional therapies together with their

toxicity has prompted to pursue novel systemic strategies (46). Up to date, only two target therapies have been approved. Nonetheless, most patients have seen limited benefit from these drugs (50) (51) (52). Moreover, recent trials with other targeted therapies have failed, probably because of an inappropriate patient selection.

1.3.1- HER2

HER2 (or ErbB2) is a receptor tyrosine kinase of the Epidermal Grow Factor family, and its gene *ERBB2* is localized at chromosome 17q21 (53). The HER2 receptor, contrarily to other members of EGF family, is not activated by a ligand, but functions as a co-receptor for other members of its family (heterodimerization) (54). HER2-containing heterodimers are preferentially formed and HER2 receptor homodimerization can spontaneously occur in cells with HER2 overexpression (55).

Some of the most common tumor types bear *HER2* alterations. *HER2* can be overexpressed and amplified in breast, pancreatic and colorectal tumors, and, as several studies suggest, in gastric carcinomas, with a frequency ranging 16-34% in intestinal subtype and 2-7% in the diffuse subtype (35). *HER2* overexpression is significantly associated with older age, male gender, intestinal histology, location in the upper third of the stomach, higher nodal involvement, and advanced stage (56). A recent study (GASTHER1) involving unresectable or metastatic gastric cancer, demonstrated that HER2 positivity is also correlated with diffuse gastric, Borrmann type IV as well as with liver metastases (57).

HER2 overexpression has been shown to predict response to Trastuzumab, one of the two targeted drugs approved for gastric cancer. Trastuzumab is a recombinant humanized IgG1 monoclonal antibody against the HER2 ectodomain, which blocks ligand-dependent HER2 activation (by heterodimerization) and stimulates ADCC (antibody-dependent cellular cytotoxicity) (58). The ToGA trial, a phase III open-label, randomized-controlled, multicentre study including 584 patients with HER2 positive tumors, allowed the approval of Trastuzumab in HER2+ metastatic gastric cancer ([Figure 5](#)) (59). This study was based on the comparison of first-line fluoropyrimidine/cisplatin chemotherapy doublet with or without Trastuzumab, in patients with HER-2 over-expressing unresectable or metastatic gastric cancer. The primary endpoint of the study was reached: overall survival (OS) was significantly longer in patients receiving Trastuzumab plus chemotherapy than in patients receiving chemotherapy alone (13.8 months vs 11.1). Progression free survival (PFS) (6.7 vs 5.5 months), overall response rate (47% vs 35%) and duration of response (6.9 vs 4.8 months) were increased as well in patients receiving targeted therapy (50).

Recently, the first antibody-drug conjugate targeting the HER2 receptor, trastuzumab emtansine (T-DM1) has been approved. T-DM1 is a conjugate of Trastuzumab and a cytotoxic moiety (DM1), a derivative of maytansine, which inhibits microtubule assembly. This drug was approved for HER2+ breast cancer and favorably tested in preclinical studies in gastric cancer models (35). For these reasons, a randomized, open-label, phase II/III study of T-DM1 versus a taxane in patients with previously treated HER2+ locally advanced or metastatic gastroesophageal tumors (GATSBY) was performed, but did not show significant efficacy benefit (60). This negative result could be justified by the fact that systemic chemotherapy plus Trastuzumab performs better than T-DM1 because the first can be efficient also against low-level/HER2- clones (inpatient tumor heterogeneity). Alternatively, or in addition, as up to 35% of gastric tumors lost their HER2+ status after first line therapy, a decreased level of HER2 could impair the activity of T-DM1 but not that of taxanes and could make archived samples, as used in GATSBY, inadequate for selecting appropriate HER2 patients in second line (53) (35).

Trastuzumab is not the only anti-HER2 monoclonal antibody evaluated in gastric cancer treatment. The humanized monoclonal antibody directed against the extracellular subdomain 2 of HER2, Pertuzumab, is characterized by its capacity of inhibiting ligand-dependent heterodimerization of HER2 with other HER family members (61). Pertuzumab and Trastuzumab may be efficaciously combined because they are able to bind different HER2 epitopes (61). Actually, the combination of the two antibodies produces synergistic effects, providing complementary mechanisms for disrupting HER2 signalling and enhancing the antitumor effects of trastuzumab on HER2-positive tumors (62) (63). Two studies performed in HER2-positive human gastric cancer mouse xenograft models demonstrated an enhanced efficacy of the Trastuzumab-Pertuzumab combination characterized by a higher cell growth inhibition, increased ADCC activity and more pronounced antiangiogenic activity (62) (63). The efficacy of Pertuzumab in combination with Trastuzumab and chemotherapy, in HER2+ metastatic gastric cancer, was evaluated by an international phase III (JACOB) trial (NCT01774786). Contrarily to what was seen in pre-clinical trials, the results of this study revealed no statistically significant improvement in OS with the addition of Pertuzumab to Trastuzumab + chemotherapy, yet, a 3.3-month increase in median OS was observed (64). There are two more monoclonal antibodies under evaluation: Nimotuzumab (a humanized monoclonal antibody that acts by binding with high affinity and specificity to the HER receptors) is being tested for advanced esophageal and gastric carcinomas, while Ertumaxomab (a trifunctional monoclonal antibody which targets CD3 and HER2, thus linking T lymphocytes, macrophages

and tumor cells causing their phagocytosis by T-lymphocyte activation) is being tested in patients with HER2 positive advanced solid tumors (59).

Monoclonal antibodies have not been the only HER2 inhibitors studied to target gastric cancer. Lapatinib, a dual intracellular tyrosine kinase inhibitor (TKI) of HER2 and EGFR, was also evaluated in first- and second-line gastric cancer therapy (TRIO-013/LOGiC and TyTAN). However, these studies suggest that Lapatinib, as single targeted therapy, is poorly active in gastric cancer, maybe because, differently from Trastuzumab, it cannot rely on the contribution of antibody-dependent cell-mediated cytotoxicity (ADCC). Nevertheless, further studies are needed to evaluate if, as shown in preclinical setting, Lapatinib synergizes with Trastuzumab (35). Additional TKIs, have been studied at different levels to assess their activity in gastric cancer. They include MM-111, a bispecific antibody fusion protein comprising anti-HER2 and anti-HER3 antibodies linked by modified human serum albumin, Dacomitinib, an irreversible pan-HER tyrosine kinase inhibitor, and Afatinib, an irreversible inhibitor of EGFR and HER2 (58).

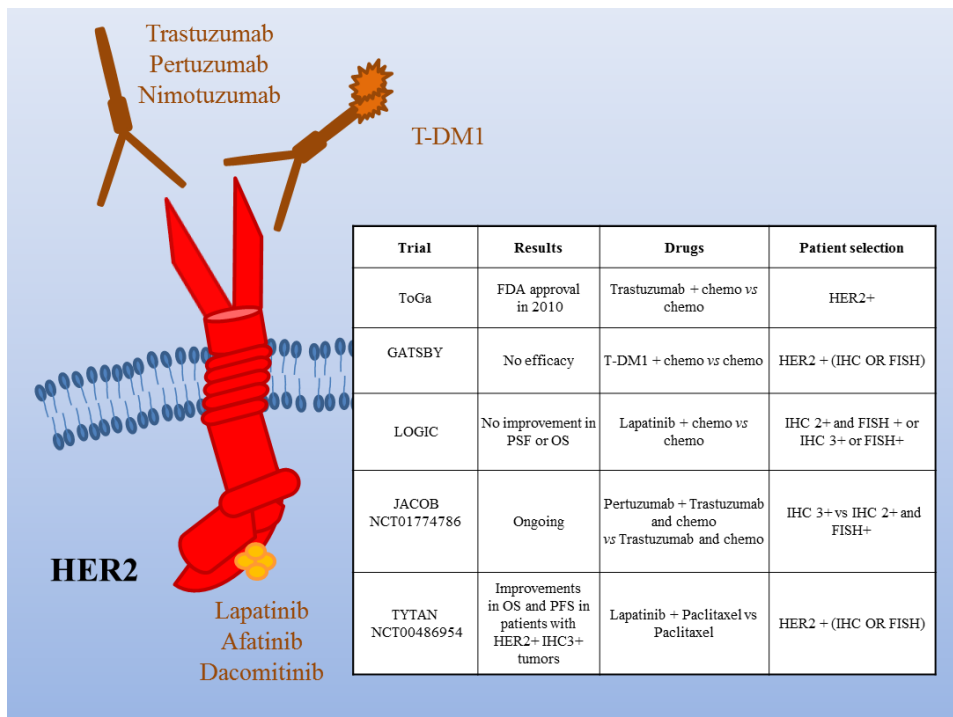


Figure 5 - HER2 as a target in gastric cancer. Schematic illustration of the HER2 receptor and the targeted drugs tested in clinical trials (the mAbs Pertuzumab and Trastuzumab -and its emtansine conjugated, T-DM1-and the dual HER1/HER2 small kinase inhibitor Lapatinib). The insert table shows the major trials targeting HER2. PFS = Progression Free Survival; OS = Overall Survival. Modified from Apicella *et al.*, 2017.

1.3.2 - EGF/EGFR

Epidermal growth factor receptor (EGFR) is a receptor tyrosine kinase member of the ErbB/HER family. The activation of EGFR can be triggered by the binding of seven growth factors that can be broadly divided in two groups: I) group I growth factors, that bind only

EGFR: epidermal growth factor (EGF), epigen (EPG), transforming growth factor- α (TGF α), and amphiregulin (AR); II) group II growth factors that bind to both EGFR and ErbB4: betacellulin (BTC), heparin-binding epidermal growth factor-like growth factor (HB-EGF), and epiregulin (EPR). The EGF receptor plays an important role in tumorigenesis, sustaining neoplasm growth and progression (65). Overexpression of EGFR, as well as EGFR amplification, detected by fluorescence *in situ* hybridization (FISH) analysis are more common in esophageal cancer with respect to gastric tumors (66). Overexpression of this tyrosine kinase receptor is present in approximately 30% of gastric cancer (53), whereas EGFR amplification is found in around 5% of gastric cancers (47). Amplification is mostly present in the CIN subtype, according to TCGA classification (47). Multiple studies have shown that increased EGFR expression is associated with an overall decrease in survival in patients with esophageal cancer (66). Based on these findings, multiple phase I/II studies of small molecule tyrosine kinase inhibitors and monoclonal antibodies have been initiated for patients with esophageal and gastric cancers.

At least three tyrosine kinase inhibitors were used in clinical trials for gastric cancer, two of first generation and one of second generation: Erlotinib (67), Gefitinib (68) (69) and Afatinib (70). Nonetheless the results obtained were not encouraging. Upon non-promising clinical benefit of TKIs, EGFR monoclonal antibodies have been tested in several studies. Cetuximab, extensively used in colorectal cancer, is a recombinant, chimeric monoclonal antibody (IgG1) directed against EGFR that shows ADCC (Antibody-dependent cell-mediated cytotoxicity) activity (71). It has been tested in several phase II/III trials in oesophagogastric cancers, but it showed limited activity (72) (73) (74) (75) (76) (77) (78). Nevertheless, as seen before in other trials, the lack of patients selection could be the cause of failure in this studies, because a subset of patients from a previous phase II clinical study possessing more than four EGFR copies showed a clinical improvement upon cetuximab (79). Similarly, survival benefit has been described in the small patient subgroup of the EXPAND trial that showed extremely high EGFR expression by IHC (80).

Not only Cetuximab had demonstrated poor results in clinical trials for gastric cancer, but also the antibodies anti-EGFR Panitumumab (81) (82) and Matuzumab (58) did not demonstrate any improvement. Nimotuzumab, instead, showed interesting results in initial phase I/II studies, having a good toxicity profile and demonstrating good response rates in combination with radiotherapy or chemoradiotherapy (58). Promising results were also obtained treating advanced gastric cancer patients with Nimotuzumab in combination with chemotherapy (S-1 and cisplatin) in a phase II study (83). Interestingly, a phase III study is ongoing in preselected advanced

gastric cancer patients with high EGFR expression to compare Nimotuzumab in combination with irinotecan with chemotherapy alone as second line treatment (NCT01813253).

1.3.3 - VEGF/VEGFR-2

Vascular Endothelial Grow Factor/Vascular Endothelial Grow Factor Receptor 2 (VEGF/VEGFR2)-dependent signalling plays an important role in tumor angiogenesis. Until now there are no selection factors that predict how and if a patient could benefit from an anti-angiogenic therapy; nevertheless, those drugs have significantly prolonged gastrointestinal cancer patients' median survival (84). Similarly to other types of cancer, in gastric carcinomas a deregulated angiogenesis is involved in tumor development and progression. Studies demonstrated that VEGF expression and serum levels correlate with more advanced stage disease and poor outcome (35). Additionally, the expression of VEGF and VEGF receptor (VGFR) was reported in 40 and 36% of cases, respectively (84) and VEGF-A gene amplification was found in 7% of TCGA samples (47).

One of the two target therapies approved for gastric cancer is Ramucirumab, a human immunoglobulin G1 (IgG1) monoclonal antibody that directly binds to VEGFR2 and inhibits VEGF binding. Its use in gastric cancers has been evaluated in several studies: in particular, the REGARD and RAINBOW trials, which led to the acknowledgment of Ramucirumab (alone or in combination with paclitaxel) as the second targeted drug approved for advanced or metastatic gastric cancer after progression followed by fluoropyrimidine or platinum containing regimens (35). The REGARD trial was performed on a cohort of patients with advanced, unresectable gastric and gastroesophageal tumors in order to evaluate safety and efficacy of Ramucirumab as second-line therapy after disease progression on a first line chemotherapy. Median OS was 5.2 months in patients treated with Ramucirumab and 3.8 months in those who received placebo; moreover, median PFS was 2.1 months for the first group and 1.3 for the second one (51). The RAINBOW study was quite similar to the previous one; it was performed in a cohort of patients with the same characteristics to investigate Ramucirumab plus paclitaxel or placebo plus paclitaxel as second line treatment. Median OS (9.6 vs 7.3 months) and PFS (4.4 vs 2.8 months) resulted superior in the Ramucirumab group (52). In another study, Apatinib, an oral tyrosine kinase inhibitor directed against VEGFR2, RET, c-Kit, and c-Src showed significant improvement of OS and PFS in patients progressed on second-line therapy (85). This drug has been recently approved in China by CFDA (China Food and Drug Administration) for patients with metastatic gastric cancer after second-line chemotherapy (36). In terms of targeting angiogenesis, it seems that it is more effective to target VEGFR-2 than VEGF-A, probably

because during tumor evolution cancer cells change the expression of VEGF ligands, leading to a decreased response to VEGF-A targeting drugs. Indeed, studies evaluating Bevacizumab, a recombinant humanized anti-VEGF-A monoclonal antibody, such as AVAGAST (86) and AVATAR (87) failed their primary endpoint. Many other multi-target TKIs are being studied as possible approaches to suppress angiogenesis in this disease. Some examples are Sunitinib, Sorafenib, Cediranib and Foretinib (XL-880). The latter target drug is a powerful orally available multitarget compound that inhibits VEGFR2, c-MET, AXL, RON, Kit and TIE2, and recently demonstrated some kind of activity in advanced gastric cancer patients (88).

1.3.4 - HGF/MET

The Hepatocyte growth factor (HGF) is the natural ligand of the cell surface tyrosine kinase receptor c-MET (encoded by the *MET* gene). The HGF/c-MET axis is involved in multiple biological activities such as organ morphogenesis, protection and regeneration in a wide range of cellular targets, including epithelial and endothelial cells, hematopoietic cells, neurons, melanocytes and hepatocytes (89). Aberrant HGF/c-MET signaling significantly contributes to oncogenesis and tumor progression, leading to tumor growth, proliferation and metastasis (90). The MET-associated aberrant signaling could be triggered by a variety of mechanisms, such as mutations, gene amplification, increased gene copy number and MET/HGF protein expression. The most common genetic alteration of *MET* in human tumors is gene amplification, leading to receptor over-expression. Cancer cell lines exhibiting *MET* gene amplification are “addicted” to *MET* (which means that they are dependent on this receptor for their growth and survival) and, in this context, MET inhibition results in either a block of proliferation or cell death.

Several strategies have been tried to inhibit MET activation ([Figure 6](#)). These strategies are based on the use of monoclonal antibodies directed against HGF or c-Met receptor, and small-molecule tyrosine kinase inhibitors directed against c-Met.

Anti-HGF monoclonal antibodies act by binding and neutralizing HGF, preventing HGF binding to the MET receptor, thus avoiding the activation of the downstream pathway. Among them there are Ficlaturumab, Rilotumumab, and TAK701. Rilotumumab (AMG102) is a fully humanized IgG2 monoclonal antibody that has undergone phase I and II clinical trials (91) (92). In a phase II trial, in patients with advanced gastric cancer, rilotumumab -in combination with epirubicin, cisplatin, and capecitabine (ECX)- showed improved efficacy outcomes (PFS and OS) compared to ECX alone (93). Considering the good results from phase I and II trails, two phase III clinical trials (RILOMET-1 and RILOMET-2) were initiated. However, RILOMET-1 was prematurely stopped due to lack of efficacy. No subgroup benefited from rilotumumab

treatment, including patients with higher *MET* expression (94). Another anti-HGF antibody tested in clinical trials is Ficlatusumab (AV299), a humanized anti-HGF IgG1 monoclonal antibody that has completed phase I and II trials as single agent or in combination with gefitinib (95) (96). Further, the promising humanized IgG1 monoclonal antibody TAK701, that successfully overcame Gefitinib resistance in EGFR-mutated human NSCLC cell lines (97), has just completed phase I testing in patients with advanced solid malignancies (98).

Activation of the HGF/MET pathway requires the dimerization of the MET receptor upon binding to the active form of HGF, which leads to kinase auto-activation. MET antagonists compete with HGF for MET binding, leading to the degradation of MET and subsequent inactivation. On these bases, antibodies which specifically bind MET, in order to prevent MET constitutive activation have been developed. One of them is Onartuzumab (OA-5D5 or OAM4558g or METMAb), a monovalent, humanized MET mAb, specifically designed to avoid agonistic activity that may occur when a bivalent antibody binds two MET molecules. Onartuzumab blocks HGF-induced MET dimerization and activation of the intracellular kinase domain. In the past, efforts to develop MET-directed antibodies failed due to the tendency of bivalent antibodies to cause receptor dimerization, thus displaying agonistic activity. This agonistic activity has been prevented by producing a monovalent human IgG1 antibody with murine variable domains (99) (100). The resulting monoclonal antibody, onartuzumab, is the only anti -MET monovalent antibody that has been tested in clinical studies to date. A randomized phase II trial comparing onartuzumab/erlotinib to erlotinib treatment in second- or third-line NSCLC (101) has given encouraging results in term of progression free survival (PSF) and overall survival (OS) in MET positive NSCLC (102). A phase III trial was stopped due to lack of clinical efficacy. At this time, further development of ornatusumab has been halted. Another anti-MET antibody tested in humans is Emibetuzumab, a bivalent humanized anti-cMET IgG4 mAb that blocks HGF binding to cMET. Binding of Emibetuzumab to cMET promotes internalization and degradation of cMET, in contrast to Onartuzumab, which does not induce cMET degradation. Recently, a first-in-human phase I clinical study testing single-agent Emibetuzumab in patients with solid tumors and Emibetuzumab in combination with Erlotinib in patients with NSCLC (NCT01287546) (103) showed no dose-limiting toxicities and adverse events. Phase II clinical studies (NCT01897480 and NCT02082210) are ongoing.

The MET pathway can also be inhibited through the use of MET kinase inhibitors, which target the intracellular portion of MET. Various small-molecule inhibitors of the MET receptor tyrosine kinase have been evaluated in the preclinical setting and several anti-MET TKIs have reached the clinic. Some inhibitors are selective, while others inhibit a panel of kinases. Selective

MET inhibitors share a common structure (an indolin-2-one-core) and have been refined over time in terms of specificity, based on co-crystal structure and early inhibitors with MET kinase domain (100). Among the selective MET kinase small molecules there are JNJ-38877605 (Johnson and Johnson), PHA-665752 (Tocris Bioscience) and AMG-337 (Amgen Inc). JNJ-38877605 is a small-molecule, ATP-competitive inhibitor of the catalytic activity of c-Met, able to potently inhibit HGF-stimulated and constitutively activated MET phosphorylation; however, renal toxicity has been detected in treated patients (100). Similarly, PHA-665752 has a powerful inhibitory effect in MET-amplified cancer cells *in vitro* by blocking MET activation, but it cannot be used *in vivo* in preclinical models due to its high toxicity (104). The drug AMG-337, is another cMET selective inhibitor, that demonstrated very promising results in terms of activity when tested in a multi-center Phase II study (NCT02016534) in patients with MET amplified gastroesophageal adenocarcinoma. However, this study was closed because of the low safety and tolerability of AMG-337 (105).

Other types of MET inhibitors in clinical development include non-selective, multikinase inhibitors. For example, Crizotinib, has been developed and marketed as an ALK inhibitor and it is recently being evaluated for its MET inhibitory activity. Crizotinib earned accelerated approval by United States Food and Drug Administration (US FDA) in 2011 due to its superiority of PSF and ORR compared with chemotherapy in ALK rearranged lung cancer patients (106). Recent analysis of previously unreported results has shown that Crizotinib produced either disease stabilization or tumor response in patients with NSCLC and high *MET* amplification, suggesting that Crizotinib can eventually be a potential agent for the treatment of MET-amplified NSCLC (107). Moreover, Crizotinib showed marked antitumor activity in patients with advanced NSCLC tumors carrying ROS-1 rearrangements (108) as well as clinical improvement and radiographic regression in patients with MET-amplified gastro-esophageal adenocarcinoma (109). Another TKI, Cabozantinib is a US FDA approved drug for treating patients with medullary thyroid cancer. This multikinase inhibitor of MET, VEGFR2, AXL, TIE2, KIT, FLT3 and RET is currently undergoing multiple phase III trials in a variety of indications, including castration-resistant prostate cancer, metastatic renal cell carcinoma, and HCC (127). Similar to Cabozantinib, Foretinib, Golvatinib and MGCD265 are dual MET/VEGFR2 inhibitors while BMS-777607 inhibits MET and RON. Clinical evaluations of the therapeutic benefit of these agents are currently ongoing.

Among the various MET alterations, *MET* exon 14 splicing abnormalities, causing the loss of the MET juxtamembrane (JM) domain, recently emerged as a new potential oncogenic driver and have been identified and validated among different tumors and histology subtypes.

Research in gastrointestinal malignancies demonstrated for the first time the existence of *MET* exon 14 deletion in gastric cancer. A recent study reported that *MET* exon 14 skipping mutations occur mutually exclusively with other validated drivers, supporting its oncogenic implication and defining a distinct molecular subgroup of gastrointestinal malignancies (110) (111). Aside from two independent preclinical studies that reported the presence of *MET* exon 14 deletion in gastric cancer cell lines (112) (113), other preclinical studies demonstrated that patient-derived tumor cell lines harboring *MET* exon 14 deletion were strongly inhibited by both MET TKIs and an anti-Met monoclonal antibody (110). These results suggest preliminary evidence that MET exon 14 skipping alterations might act as drivers in some gastrointestinal malignancies, indicating the clinical benefit of MET TKIs observed in NSCLC can potentially be expanded to gastric malignancies.

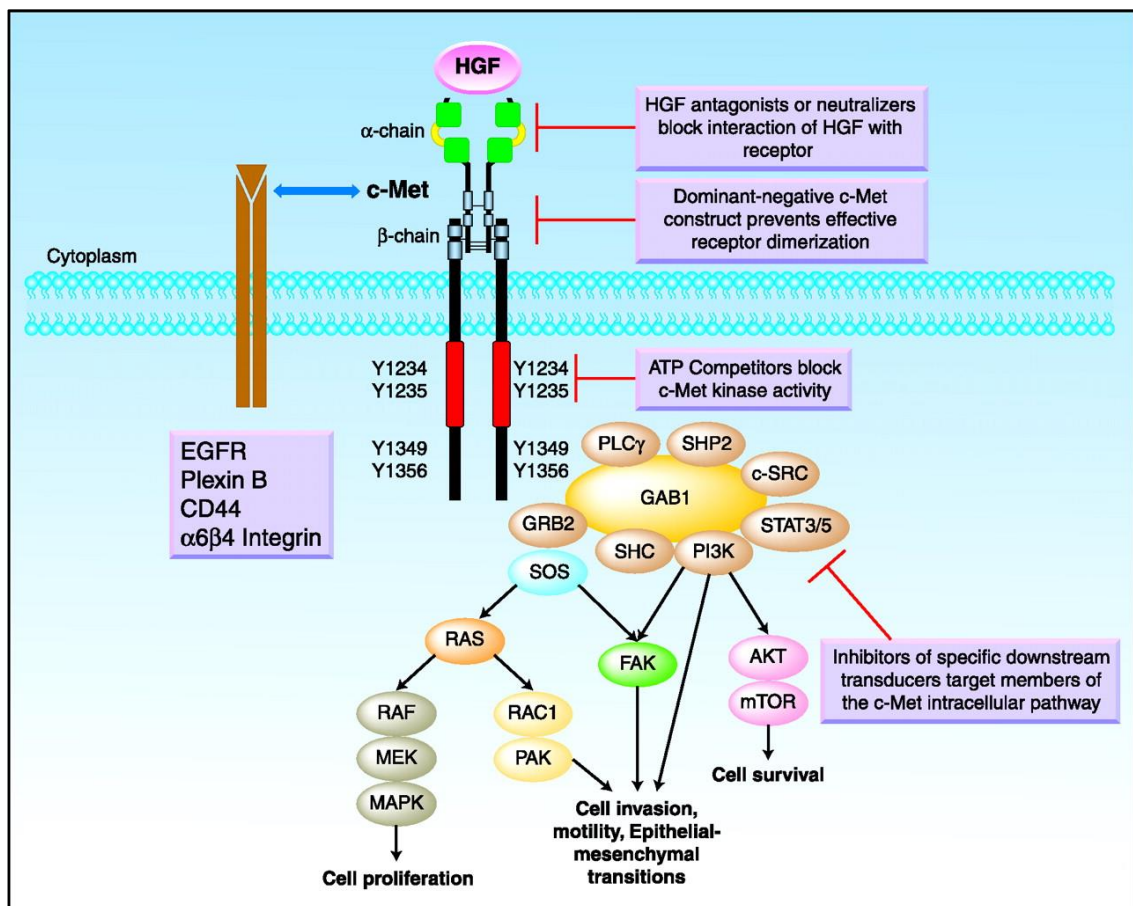


Figure 6 - Main signaling pathways activated through c-Met, interactions between c-Met and other membrane receptors, and c-Met signaling inhibition strategies. HGF binding results in c-Met autophosphorylation of tyrosines Y1234 and Y1235 leading to the activation loop of the kinase domain and subsequent phosphorylation of tyrosines Y1349 and Y1356 next to -COOH terminus. Adapter proteins and direct kinase substrates activated downstream in the c-Met pathway account for growth factor receptor-bound protein 2 (GRB2), Grb2-associated adaptor protein 1 (GAB1), phosphatidylinositol 3-kinase (PI3K), son of sevenless (SOS), rat sarcoma oncogene homolog (RAS), mitogen-activated protein kinase (MAPK), signal transducer and activator of transcription 3/5 (STAT 3/5), SRC, SRC homology protein tyrosine phosphatase 2 (SHP2), SRC homology domain c-terminal adaptor homolog (SHC), phospholipase c- γ (PLC), Ras-related C3 botulinum toxin substrate 1 (RAC1), p21-activated kinase (PAK), focal adhesion kinase (FAK), AKT, and mammalian target of rapamycin (mTOR). c-Met can crosstalk with some membrane protein partners, such as the epidermal growth factor receptor (EGFR), the plexin B family, $\alpha 6\beta 4$ integrin, and CD44, resulting in additional signaling response modulation. Adapted from Eder *et al.*, 2009 (114).

1.3.5 - Other targets

The Fibroblast Growth Factor 2 receptor tyrosine kinase (FGFR-2) is also considered as a target in gastric cancer since it is amplified in approximately 10% of cases (47) that are associated with lymphatic invasion and worse prognosis (115). Clinical trials involving FGFR2 TKIs were performed and while AZD4547 did not demonstrate clinical activity in the SHINE phase II trial (116), another small phase IIa trial showed response in 3 out of 9 patients with promising durability in FGFR2-amplified patients; these results show that high and homogeneous gene amplification may better predict therapeutic benefit (117).

Another pathway that is frequently altered and active in gastric cancer is the PI3K-AKT-mTOR pathway, determining resistance to target therapies (35). mTOR is an intracellular serine/threonine protein kinase that regulates cell growth and proliferation, cellular metabolism and angiogenesis, and is mainly activated via the PI3K pathway (84). *PIK3CA* (the PI3K encoding gene) activating mutations are present in 24% of gastric cancers, in particular in the EBV and the MSI subtypes (72% and 42%, respectively) (47). Moreover, genetic or functional loss of PTEN, a negative controller of the PI3K/AKT pathway, is present in 11% of tumors, especially in the MSI subtype (35). For these reasons, the mTOR orally available inhibitor Everolimus has been tested in a phase III study (GRANITE-1): despite positive results in an early study, Everolimus did not show any clinical improvements in unselected second-line or third-line patients (118) (119). Preclinical studies have been performed in order to evaluate PI3K inhibitors, which include drugs like BEZ235 and BKM120 (54). AZD5363 and Ipatasertib, AKT inhibitors, have been studied in combination, respectively, with paclitaxel in second-line therapy (NCT02451956/NCT02449655), and with FOLFOX in the first-line JAGUAR trial (NCT01896531). MK-2206, another inhibitor of AKT, has been tested in a phase II study but gave negative results (120).

In the last decade immune therapy provided an important step forward in cancer treatment. Studies demonstrated that reactivating the immune system against tumor cells can significantly increase patients survival (121). PD-L1 is the principal immunotherapy target. It normally binds to receptors on T lymphocytes, thereby inhibiting T-cell proliferation and inducing apoptosis (53). In gastric cancer the overexpression of PD-L1 and PD-L2 is mostly present in EBV-associated gastric tumors, mainly due to 9p24 amplification (122). MSI-high tumors are also good candidates for immunotherapy agents as they are associated with intense immune infiltration (47) (123). Since immunotherapy showed promising results in multiple types of cancer, it has been explored in gastric cancer as well. The human monoclonal antibodies

against PDL1 Pembrolizumab (124), Nivolumab (125), Avelumab (126), as well as Ipilimumab (127), and Tremelimumab (128), antibodies specific against CTLA-4 are examples of immunotherapeutic drugs that have been used and tested in phase I, II and III clinical trials, respectively. Indeed, a multicenter phase IB/II study evaluated and confirmed the antitumor activity and safety of Pembrolizumab in combination with anti-HER2 agents in patients with HER2 positive gastric cancer (NCT02901301 and NCT02689284), being now an approved therapies for GC.

1.4- KRAS

KRAS (chromosome 12p12.1) is a member of the canonical RAS family of genes that also includes *HRAS* (chromosome 11p15.5) and *NRAS* (chromosome 1p13.1). The importance of RAS in cancer pathogenesis was found for the first time more than thirty years ago when it was discovered that mutated versions of *KRAS* and *HRAS* are responsible for the transforming activities of sarcoma-inducing retroviruses. Nowadays it is known that somatic activating mutations in the cellular homologs of all three RAS family members occur in a multiplicity of human cancers.

The three RAS genes are highly conserved across different species and all RAS genes encode for 21-kDa monomeric GTPases that function to transduce extracellular signals to intracellular signal transduction cascades. These monomeric GTPases cycle between active (GTP-bound) and inactive (GDP-bound) state in response to extracellular stimuli. Unlike *HRAS* and *NRAS*, *KRAS* undergoes alternative splicing, giving rise to two proteins (*KRAS4A* and *KRAS4B*) that differ for their carboxyl termini. RAS proteins are 188/189 amino acids in length, and the sequence of the first 165 amino acids is almost identical. This region contains highly conserved domains that are responsible for GTP binding and hydrolysis, as well as functional interactions with regulators and downstream effectors.

1.4.1 - KRAS activation and Signaling

RAS signaling initiates upon the activation of a vast array of upstream receptors including receptor tyrosine kinases (RTKs) ([Figure 7](#)). Adaptor proteins (e.g. Grb2) interact with the intracellular domain of activated TK receptors and recruit guanine nucleotide exchange factors (GEFs) such as Son of Sevenless (SOS) to the cellular membrane where they can bind RAS and promote the exchange of GDP for GTP. RAS signaling ends upon the hydrolysis of GTP to GDP by the intrinsic GTPase activity of RAS through the interaction with GTPase-

activating proteins (GAPs). However, cancer-causing mutations in RAS drastically impair the GTPase activity, resulting in RAS proteins that are blocked in the active GTP-bound conformation, despite of upstream signals. In their active, GTP-bound conformations, the four RAS proteins engage and activate a large number of downstream signaling pathways which regulate several cellular responses, such as proliferation, survival, and differentiation. One of these pathways is the canonical RAS/RAF/MEK/ERK pathway, that controls cellular proliferation by modulating the levels of many cell cycle regulators and is frequently hyperactivated in tumors (129). RAS signaling also contributes to cell survival by activating PI3K/PDK1/AKT signaling, a pathway that is also often deregulated in numerous cancer types (130). Less usual proteins, such as RALGDS and RALGDS-like proteins and tumor invasion and metastasis-inducing protein 1 (TIAM1) can also be activated by RAS to control vesicle trafficking and cytoskeletal organization, respectively (131) (132). Both RalGDS and Tiam1 have been demonstrated to be required for Ras-dependent tumor formation in a mouse skin cancer model (133) (134). Many of these downstream signaling pathways are involved in feedback regulation and crosstalk that together further contribute to the complexity of the RAS signaling network.

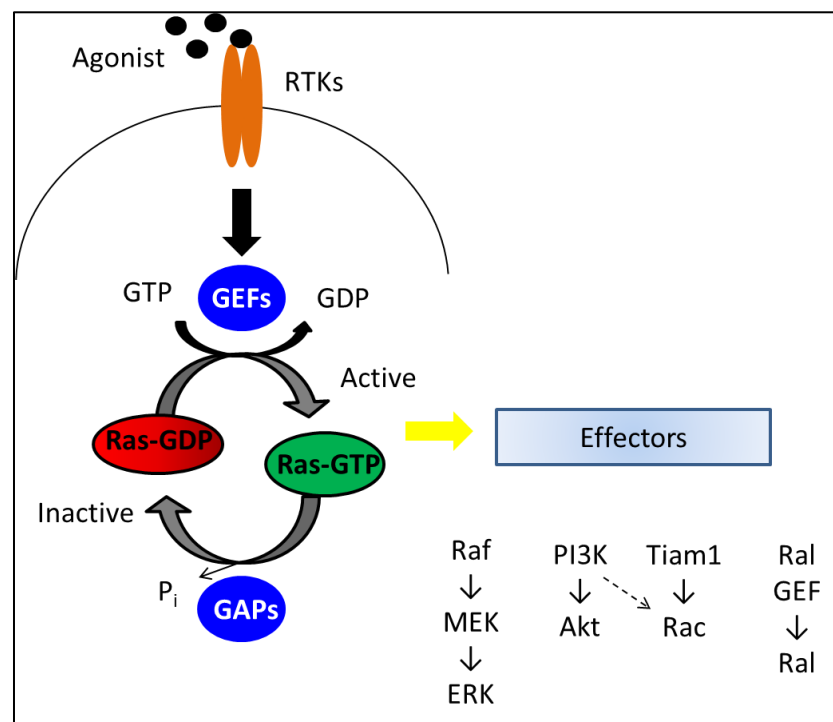


Figure 7 - Ras activation signaling. Activation of Receptors Tyrosine Kinases (RTKs) lead to the recruitment of guanine nucleotide exchange factors (GEFs) that can bind RAS and promote the exchange of GDP for GTP. RAS signaling ends upon the hydrolysis of GTP to GDP by the intrinsic GTPase activity of RAS through the interaction with GTPase-activating proteins (GAPs). RAS signaling activates pathways crucial for cell proliferation, survival, and differentiation, such as the canonical RAS/RAF/MEK/ERK pathway, PI3K/PDK1/AKT signaling as well as less usual proteins like RalGEF and tumor invasion and metastasis-inducing protein 1 (Tiam1). Modified from Mitin *et al.*, 2005 (135).

1.4.2 - *KRAS* mutations

The structural conformation of *KRAS*, and therefore its biological activity, is governed by its nucleotide binding state. The most common *KRAS*-activating mutations are localized in codons 12, 13, 61, 117, and 146, and they cluster around the nucleotide-binding pocket. Mutations in G12 and G13 are located the P loop, which is needed to stabilize the nucleotide in the active site; however, they have distinct effects in the biochemistry of *KRAS* (136) (137). Q61 is located at the N terminus of switch II, where it participates in the conformational changes associated with this region during the interconversion between structural states (136) (138). The K117N mutation enhances nucleotide exchange (139). Finally, the A146 mutation seems to play a role in nucleotide specificity, as this residue is present in a tightly packed space near the guanine base of the nucleotide (140). Mutations at A146 promote nucleotide exchange (1000-fold increase over WT) in the absence of GEF, but do not affect intrinsic GTPase activity (141). This indicates that *KRAS* can be activated by alleles that have large or subtle effects on hydrolysis or nucleotide exchange. This concept is demonstrated even more effectively by the mutations that arise in the RASopathies (e.g. neurofibromatosis type 1 (NF1)) that results from germ line mutations in genes of the mitogen-activated protein kinase pathway, such as *KRAS*. *KRAS* mutations are more common in pancreatic ductal adenocarcinoma (PDAC), colorectal cancer (CRC), and NSCLC, in particular those at codon 12, accounting for approximately 90% of all *KRAS* mutations. The frequency of mutations at the diverse codons is dependent on the cancer type. For example, mutations in codons 13, 146, and 117 are more common in CRC relative to NSCLC and PDAC (142) (143).

KRAS mutations are genetic events that occur early in tumors progression. Multiple genetically engineered mouse models of RAS-driven cancers have demonstrated the potent cancer-inducing activity of RAS mutations. However, an enhancement of tumor formation and progression was observed when RAS activation was associated with the loss of tumor suppressor function (loss of tumor protein p53 (TP53), LKB1 or adenomatous polyposis coli (APC)), suggesting that additional genetic alterations are needed to cooperate with mutant RAS to fully transform cells (144) (145) (146). In spite of the early onset of RAS mutations, several data suggest that continued expression of mutant RAS is necessary for tumor maintenance. It was observed in both in vitro and in vivo models (mouse models driven by inducible mutant RAS), that withdrawal of RAS expression leads to tumor regression (147) (148) (149) (150) (151).

One issue that cannot be neglected when regarding the oncogenic *KRAS* mutants is the function of the WT allele. Recent data, from genetically engineered mouse models suggest that loss of the WT *KRAS* allele enhances tumorigenesis induced by the mutants (152) (153). It is not

clear if the WT allele is not a fictitious tumor suppressor, or if the ratio of WT and mutant alleles is the most critical factor, but allelic imbalance due to loss of WT *KRAS* or amplification of mutant *KRAS* is frequently seen in tumors from mice and humans and seems to influence tumor response to therapy (154) (155).

1.4.3 - KRAS THERAPIES

During the last decades experimental compounds were identified with the challenging purpose of directly bind RAS and disrupt its signaling. The fact that RAS isoforms play a crucial role also in normal cell growth makes it even more difficult to develop a compound that directly binds RAS to selectively inhibit the oncogenic functions of RAS proteins. To date, no drug that can inhibit oncogenic RAS has been approved by FDA, so that RAS proteins continue to be called "undruggable".

However, the need to develop RAS-inhibitory molecules motivates the search for effective pharmacological strategies, and recent studies have renewed the hope of targeting RAS proteins.

The main promising strategies attempting RAS inhibition account for i) the use of direct inhibitors of RAS; ii) blocking RAS membrane association; iii) targeting RAS downstream effectors, which seems to be the most favorable current strategy; iv) search for synthetic lethal interactors of mutant RAS; and finally more recently, v) targeting RAS-mediated changes in cell metabolism.

Direct targeting of RAS was explored when some potential binding sites were identified using computational approaches (156) (157). Low affinity inhibitors, such as SCH-54292 or Sulindac analogues, were designed to compete with GDP for the nucleotide binding site of RAS (158) (159) (160), and even if they were able to inhibit nucleotide exchange and RAS-dependent cell growth, these compounds lack potency and metabolic stability, as well as own high toxicity. GEF inhibitors were also thought to be a very promising strategy, since RAS GTP-GDP cycle is negatively regulated by GAPs and positively regulated by GEFs, which facilitates the dissociation of GDP and consequently promote binding of the more abundant GTP portion (161). But as it was seen with RAF1 binding inhibitors, like Kobe 0065, GEF inhibitors demonstrated weak potency (162). A recent study reporting an attempt to direct targeting RAS demonstrated that is possible to design a molecule that covalently and selectively binds to the G12C form of *KRAS*. This small molecule was capable of blocking SOS-1 mediated nucleotide exchange, decreasing the binding of RAS to both BRAF and RAF1, and selectively killing cancer cells carrying the G12C mutation (163). Even though the mutation G12C is relatively less frequent

compared to the G12D mutation, this study demonstrates that it is possible to selectively target KRAS-G12C and this could result in the development of similar compounds (163).

The most encouraging small molecule which demonstrated to interact with several RAS effector proteins (including A-, B-, and c-RAF, the Ras-binding domains of RALGDS, PI3K- α , β and γ) is the Polo-like kinase inhibitor, Rigosertib. This compound is able to inhibit the interactions of both mutants and wild-type isoforms of K- or N-RAS with the downstream effectors (164). Rigosertib showed to be effective in inhibiting RAS-mediated activation of ERK1/2 and PI3K signaling pathways. Several clinical trials of Rigosertib treatment for hematologic and solid malignancies are ongoing.

The use of Farnesyltransferase Inhibitors (FTIs) was one of the early approaches developed in order to block the RAS membrane association. But, despite the promising activity in preclinical tumor models mutated for HRAS, FTIs inhibitors were ineffective in clinical trials (165). Since the response to these molecules can differ according to the RAS isoform, recent efforts have focused on the noncatalytic δ -subunit of the cyclic GMP phosphodiesterase (PDE) 6 isozyme, which functions as a chaperone, binding the prenyl group and shuttling RAS to the plasma membrane. A small-molecule inhibitor of PDE δ (deltarasin) inhibited KRAS signaling and pancreatic tumor cell growth *in vitro* and *in vivo* (166). However, its clinical utility has not been evaluated yet.

An encouraging strategy against KRAS activation has been targeting the downstream components of RAS signaling with inhibitors of the RAF/MEK/ERK kinase or the PI3K/AKT/mTOR pathway that demonstrated some effects in the context of different mutations of K-, N-, or HRAS isoforms, even if a complex feedback system gives rise to resistance mechanisms (165). For instance, at least 4 pharmaceutical inhibitors of RAF kinase were approved by the US FDA. Sorafenib, vemurafenib and dabrafenib are some examples. The last two inhibitors are ATP-competitive RAF inhibitors, approved for *BRAF*-mutant metastatic melanoma (167) (168). However, when tested in RAS-mutant cancer cells, activation, rather than inactivation, of ERK was reported (169) (170) (171). Better results were observed using Trametinib, a MEK inhibitor, another FDA approved drug for *BRAF*-mutant metastatic melanoma. This inhibitor seems to be more selective as it functions via allosteric regulation as a non-ATP competitive inhibitor of MEK-1 and MEK-2. But, despite its high efficacy in *BRAF*-mutant melanoma, this MEKi has only been partially effective in RAS-mutant cancers as well as in human cells lines and RAS-mutant mouse models (172). The MEK inhibitors GDC-0623 and G-573 are more efficient in RAS-mutant cancers and block MEK feedback phosphorylation by RAF. Primary or secondary resistance to MEKi by RAS-mutant cancer cells can occur due to

activation of RTKs or by amplification of upstream activators that consequently activate ERK (173). These data suggests that a combination of RAF+MEK+ERK inhibitors might provide an efficient inhibition of RAS constitutively active pathway. On another hand, the advantage of PI3K/AKT/mTOR inhibition in RAS-mutants is contradictory. There are evidences that PI3K activity can be modulated by RAS activation (174), but it is also known that PI3K is not always a key RAS effector, since the pharmaceutical inhibition of this pathway in RAS-driven models did not effectively block tumor growth (175). Furthermore, KRAS silencing in KRAS-mutant colorectal cancer cell lines did not reduce activation of the PI3K effector AKT, while effectively reduced ERK activation (174). Nevertheless, taking into consideration the complex feedback system of resistance upon inhibition of some RAS downstream effectors, targeting Pi3K-AKT signaling in RAS-mutant cancers, especially in combination with other pathways inhibition may have a clinical therapeutic value. Until now, inhibition of PI3K/AKT/mTOR alone did not show satisfactory results either in RAS-mutant tumors in preclinical trials or in clinical evaluations; however, in mouse models, encouraging synergistic activity with ERK and MAPK inhibitors has been seen (175).

As in other types of cancer, one possible approach to increase the therapeutic selectivity for RAS-mutant cancer cells would be the identification of targets that have synthetic lethal interactions with the *RAS* oncogene. These targets would be genes whose loss of function would have a lethal effect only in the presence of mutated *RAS*. In order to identify synthetic lethal interactors with *RAS* an initial screen is crucial and the synthetic lethal genes must encode proteins that function in different pathways of those involved in *RAS* pathway. These screenings were performed by short interfering RNAs (siRNA) (176), by the use of pool-based short hairpin RNAs (shRNA) or by chemicals (177). The last type of screening identified genes whose inhibition could sensitize KRAS mutant cancer models to one or more FDA-approved drug (e.g., Trametinib). In the last ten years multiple screenings have identify synthetic lethal genes that encode proteins involved in several cellular processes: i) associated with the cell cycle and mitosis (surviving (BIRC5)); ii) rho-associated kinase (ROCK) (178) (177), iii) targeting protein for XKLP2 (TPX2) (179), PLK1, and anaphase promoting complex, (180); iv) those associated with cell survival (Wilms' tumour protein homologue 1 (WT1) and BCL-XL) (181) (182); v) associated with collaborative transcriptional programs (GATA-binding protein 2 (GATA2) and SNAIL2 (also known as SNAI2)) (183) (184); vi) associated with parallel growth and survival signals (FGFR1, TBK1 and TAK1 (also known as NR2C2)) (185) (186) (187); vii) involved in nuclear export (exportin 1 (XPO1)) (176). However from the results obtained until now, it is clear that the existence of a universal mutant *RAS* synthetic lethal target that comes anywhere

close to the targeting of RAS proteins themselves among all the spectrum of RAS-mutant cancers is unlikely.

The most recent strategy against RAS-mutated tumors is the exploration of RAS mediated changes in cell metabolism. Recognized as one of the cancer hallmarks, neoplastic cells change their metabolism, consuming more glucose and producing more lactate even in the presence of oxygen (188) (180). Evidences have been shown that many metabolic changes driven by oncogenic RAS become crucial for tumor maintenance. Some of the metabolic changes that occur in RAS-mutated tumors and are required for their maintenance and aggressiveness are autophagy (189) (190), macropinocytosis (191), increase glucose uptake (192) and a shift in glutamine metabolism (193) (194) (195). This last type of metabolism switch was described mainly in *KRAS* mutated pancreatic tumors (193) but the inhibition of the aspartate aminotransferase in a breast cancer *in vitro* model with *KRAS* mutation also demonstrated antitumor effects (196). The strategy of targeting the altered metabolism of RAS-mutated tumors is potentially attractive, considering that normal cells do not experience the same reliance on these altered pathways. Thus, an encouraging therapeutic window is currently open.

1.4.4 - *KRAS* in gastric cancer

The first report of a *KRAS* mutation in gastric cancer was published in 1986. Researchers described the presence of a mutated *KRAS* allele (Gly-12 to Ser) together with an amplification of 30-50 fold of the other *KRAS* allele (197). Since this first publication, more than 50 studies reported the incidence of *KRAS* mutations in GC, with the majority of studies (61%) originating from Asia (198).

To date, a multiplicity of studies has investigated the status of *KRAS* gene mutations in gastric adenocarcinoma, with the frequency varying from 0 to 21% (199) (200) (201). Yet, it was evident that the frequency of mutations in the *KRAS* gene in different studies was markedly variable. Attempting to better understand the status of *KRAS* mutations in gastric cancer, a large international multi-center study, including 712 patients with gastric cancer, was performed in 2013 (202). The results of this study, which is the largest to date, demonstrated that the overall frequency of mutations in the *KRAS* gene was 4%, statistically not different between the different GC cohorts. Interestingly, in this study, *KRAS* mutation was not associated with clinicopathological features, including ethnicity, gender and stage of tumor differentiation (202). While it is still unclear if there is a relationship between *KRAS* mutation status and survival (203), this study reported a trend towards better survival in patients with a *KRAS* mutant GC. The disparity between previous studies and the multi-center study may be due to the different population size.

Data collected from eleven studies involving molecular characterization of gastroesophageal tumors, demonstrated that the most frequent mutations in gastric cancer were found at codons 12 (G12A/C/D/R/S/V) and 13 (G13D) accounting, respectively, for 2% and 1.62% of all KRAS mutations found in the gastric tumors studied. Less frequently detected mutations were Q61H, K117N, A59T, P121H, R135H, R135T and A146T, with a frequency that goes from 0.07 to 0.28 % (<http://cbioportal.org>) (204).

Gene amplification of *KRAS*, with or without mutation, has been evaluated in a limited number of cases (205) (206) (207). While the amplification of *KRAS* is rare in colon and pancreatic cancers, the incidence of *KRAS* gene amplification (greater than 4-fold) is higher in gastric cancer, and seems to be responsible for *KRAS* activation (208). A study involving 86 primary gastric tumors demonstrated that approximately 5% of them bear *KRAS* amplification (208), which is statistically similar to the frequency described in other studies (<http://cbioportal.org>) (204). The same study also showed that gene amplification coincided with intense *KRAS* immunoreactivity in the same tumor samples, potentially suggesting that gene amplification results in the overexpression of *KRAS* in primary gastric cancer. This was the first work reporting a potential relationship between gene amplification of WT *KRAS*, activation of *KRAS* signaling pathways, and cell growth in gastric cancer. While *KRAS* amplification had been described as a cause of resistance to EGFR target therapy in colorectal cancer (209) (210), its role in gastric cancer therapy is still unclear.

1.5- Translational cancer research

Translational research is an important bridge between basic research and clinics. Translational cancer research is mainly based on the biologic understanding of the disease with the aim of developing new treatments; consequently, preclinical models are required to investigate biological mechanisms and features. Murine models and cancer cell lines have been the most exploited models for preclinical testing of anticancer molecules both *in vivo* and *in vitro* (211) (212). Cancer cell lines have been characterized and collected all over the world since they are an essential tool for early drug screening and development (213). In spite of their advantages, cancer cell lines have important limitations (214). First of all they lack predictive value (gain and loss of genetic information, alteration of growth and acquisition of invasive properties) (215); second, they are representative of a subset of tumors but miss the ability to represent neoplastic heterogeneity (214); and, third, studies performed in cell lines miss the regulatory role of tumor microenvironment. To overcome these disadvantages, other preclinical cancer models have been

explored, such as patient-derived tumor xenografts that represent recent promising new tools in translational research (Figure 8) (214).

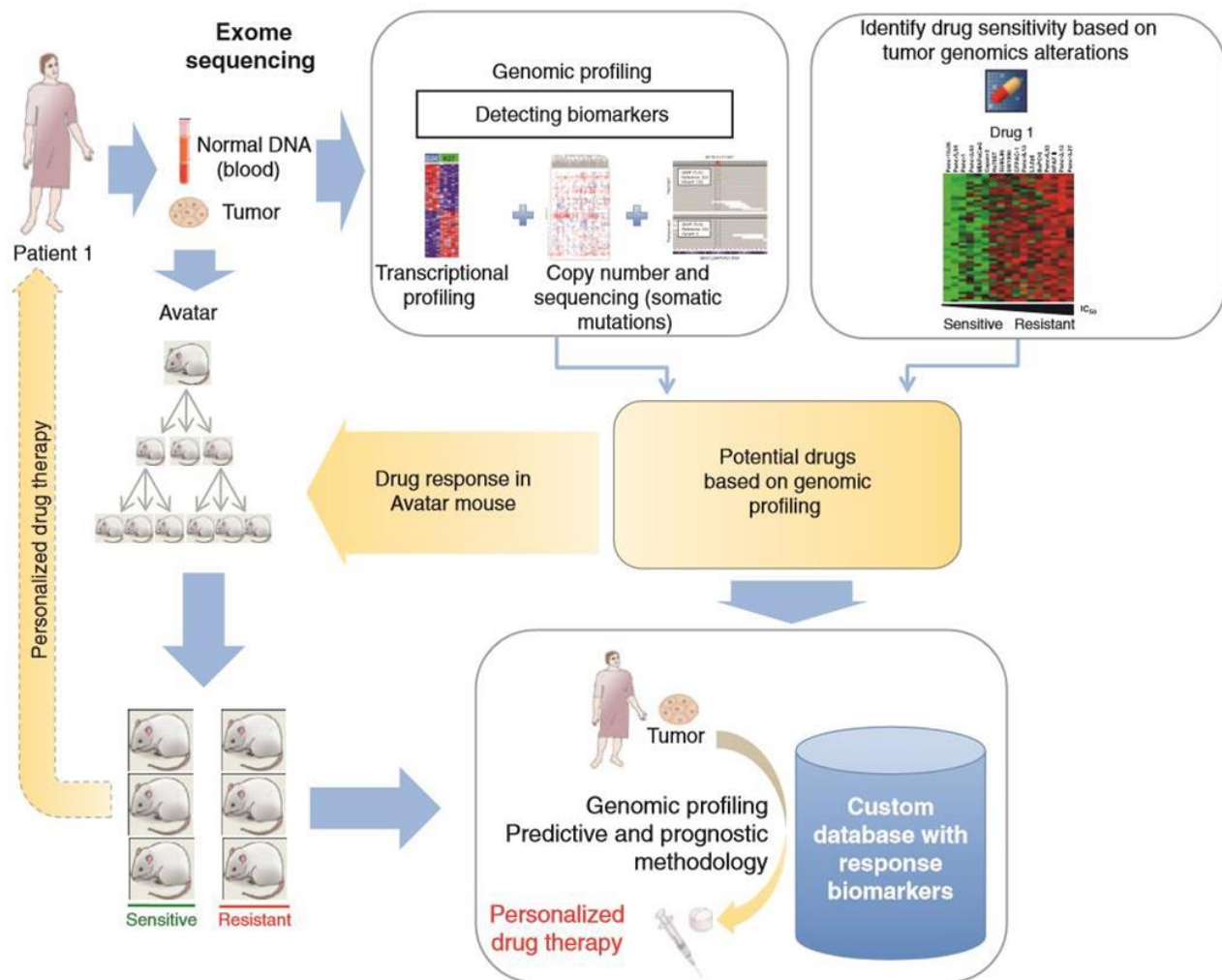


Figure 8 - Personalized medicine strategy. This figure shows a strategy for individualizing medicine that integrates genomic analysis of a patient tumor with testing in PDX models. Molecular analysis of a patient tumor can lead to the identification of potential therapeutically targetable alterations. Mining of genomic–drug response databases could result in several potential therapeutic regimens for a given patient. PDXs can be exploited to test and rank these potential treatments to be administered to the patient. A post hoc analysis of this information can be added to existing data to amplify the available databases. Adapted from Hidalgo M *et al.*, 2014

1.5.1 - Patient-derived cancer xenografts (PDX)

Patient-derived cancer xenografts can be originated by implanting patients' tumors as pieces (tumors resections or biopsies) or single-cell suspensions on the dorsal region of immunodeficient mice (subcutaneous implantation), or in the organ in which the original tumor developed (orthotopic implantation) (214). Metastases implantation are also performed and for some types of lesions the engraftment rate is higher (216) (217). The murine models with highest engraftment rates are NOD/SCID or NOD/SCID/IL2 λ - receptor null due to their severe immunosuppression (214).

Even though the subcutaneous method is more frequently exploited, because of the lower complexity of the implantation technique, the orthotopic tumor implantation provides a translational advantage, as the tumor develops in its original anatomic microenvironment (214). Advances in imaging tools made it possible to increase the number of trials performed in orthotopic PDXs.

1.5.2 - Outstanding characteristic of PDX models

PDX models are very important tools mainly due to their ability to retain the principal characteristics of the donor tumors, including tissue histology and molecular features, making them predictive of human cancer biology and patient response to treatments. Multiple studies, involving different types of tumors (214) which compared PDXs and the donor tumors demonstrated that PDX models show the same specific tissue structure and subtle microscopic details, per example gland architecture, mucin production, or cyst development of the original specimen. Additionally, gene expression profile analysis of donor tumors and the corresponding PDXs are mostly coincident, except for genes expressed in the stromal compartment and immune function, as the human stroma is replaced by murine elements. Regarding molecular features, an extraordinary concordance between PDXs and donor tumors was also observed. Studies evaluating copy-number alterations and exome sequencing report an even higher frequency of genomic alterations in the PDX model, as PDXs do not contain the normal DNA from the human stromal tissue (214). The functional features of the grafted tumor remain stable during mouse-to-mouse propagation; indeed, drug treatments of PDX models from different passages show the same effects across generation (218) (219). Very importantly, several studies emphasized the similarity between the activity of drugs in PDX models and in the corresponding clinical trials (214); in addition, recent studies in which human patients have been treated with drugs previously tested in their PDX analogue demonstrated a high predictive value. For these reasons PDXs are effective models with good correlation with clinical outcome (220).

1.5.3 - Limitations of PDX models

Despite the numerous advantages of PDX models, some critical issues are not settled. Concerning the size of the specimen to generate the PDX there is no consensus, since on one hand large surgical samples are preferred, yet on the other hand smaller ones may possess enhanced characteristics. Also the best strategy of implantation (subcutaneous vs. orthotopic) has to be assessed for different cancers, as well as the time that the tumor requires to engraft and to start to grow: these factors may negatively affect further evaluation of personalized treatments (214). Furthermore, it is also unclear if the patient-derived tumor is the expression of a selected

subpopulation (e.g. more aggressive) of cells existing in donor tumors that in some cases can change the drug response (214). It should also be taken in consideration that after the implant, human stroma is rapidly replaced by the murine one (214), possibly resulting in changes of microenvironment signals and limiting the testing of drugs targeting tumor stroma (221) (222). Lastly, the use of immunodeficient mice is a limitation, because it cannot be used for the screening of immune-mediating agents (214), even though recent studies have been initiated involving the development of humanized mouse tumor models (223).

1.6- Patients –derived cell models as preclinical tools

In some types of cancer the time for PDX establishment (that usually takes more than 4 months) is too long to bring therapeutic advantages to the patient, so faster alternative preclinical models are required. Generation of primary cell cultures in monolayer or in threedimensional matrices (3D, such as spheroids and organoids) have been used as a prediction tool for preclinical drug sensitivity (224). Several studies have demonstrated that also these models can recapitulate the histological and genomic features of primary patient tumors and show the same drug sensitivity compared with real-life clinical treatment outcomes (224).

Recently developed 3D models can overcome some PDX deficiencies. 3D models can not only be established directly from patients in a shorter period but can also be much cheaper than PDX models. These three dimensional models are also able to better replicate natural tissue mechanical stresses and provide a more representative pathophysiological condition than the classic monolayer cultures (225). 3D culture models in cancer can be divided in 4 types: organotypic multicellular spheroids, multicellular tumor spheroids, tumor-derived organoids and tumor-derived spheroids (TS) (226).

Tumor-derived organoids were recently generated by Sato *et al.* (227) and rapidly spread as a powerful *ex vivo* model of organogenesis and *in vitro* tool for drug screening (228) (227). Produced upon specific growth conditions, such as basement membrane matrix (Matrigel), tyrosine kinase receptor agonists, Wnt agonists and bone morphogenetic protein/transforming growth factor- β inhibitors, a diversity of tissues were reconstituted *in vitro* in the absence of non-tumor cells (228). Afterwards, identical culture protocols were developed also from malignant tissues of pancreas (229) (230), stomach (231), prostate (232) (233), and liver (234) (235). The capacity to culture patient-derived healthy and diseased organoids was widely recognized as a major improvement for the shift of biomedical research into more patient-focused approaches. After the setting of organoid culture protocols, many key papers have been published in which organoids have been used as a tool to augment the basic understanding of cancer (236) (237)

(238). These studies extensively suggest that organoid cultures have the ability to promote drug development and clinical practice (224).

Contrarily to the other 3D models that are mainly derived to study the heterogeneity within tumors as well as to provide a more representative platform for the testing of therapeutic strategies (239), the TS model does not seek to mimic cancer tissues but rather to study cancer stem cells (CSC) properties. These spheres are formed from clonal expansion of single cells suspended in non-adherent conditions supplemented with a specific cocktail of growth factors in the culture media (240). TS culture represents a selective population of cells known to be aggressive and likely to contribute to tumor regrowth (240) (226). Accordingly, TS may differ in drug response and growth kinetics relative to multicellular tumor spheroids owing to the enrichment of the CSC population. The investigation of tumor-derived spheroids may provide invaluable clues on the eradication of CSCs and it is likely to be of clinical importance due to their association with tumorigenicity or chemoresistance (226).

1.6.1 - Cancer stem cells

The theory of cancer stem cells was first mentioned in 1937 when Furth and Kahn (241), demonstrated that a single leukemic cell is capable of transmitting systemic disease in mice. But it was just sixty years later that Bonnet and Dick (242) first identified and isolated leukemic stem cells of acute myeloid leukemia (AML) using the surface markers CD34 and CD38. Here, for the first time, selected CD34+/CD38- leukemic cells from AML patients led to strong enhancement of tumorigenicity after serial xenografting into NOD/SCID mice. Since then, CSCs have been discovered in many solid tumors, including breast (243), brain (187), and prostate cancers (244), melanoma (245), liver (246), pancreatic (247) (248), colon (249) (250) and head and neck cancers (251).

Some years ago (2006), to enable researchers working in the same or different systems to compare cells exhibiting analogous sets of properties, a common recognition of the accurate definition for CSCs was proposed by the American Association for Cancer Research workshop. According to this definition a stem cell is “a cell within a tumor that possesses the capacity to self-renew and to cause the heterogeneous lineages of cancer cells that comprises the tumor” (252). In addition to the fundamental traits of normal stem cells, such as self-renewal by asymmetric division, proliferation, and differentiation into their progeny, CSCs have the potential to metastasize (253) (254). CSCs are a rare population within cancers, and highly tumorigenic in nude mice xenografts. This small population is often associated with therapy resistance (such as chemotherapy and radiation) because of activation of prosurvival and

antiapoptotic pathways, overexpression of drug efflux pumps, and increased DNA repair capacity. These cells may remain viable after treatment and may be responsible for relapse (255). For many cancers, CSCs represent a distinct population that can be prospectively isolated from the remainder of the tumor cells (252) (256). However, in some cancer types it has not been possible to distinguish CSCs from non-CSCs because most cells have CSC function. This kind of tumors seems to be homogeneous or possess a very superficial hierarchy. In the same way, some evidence is emerging that certain cancer cells exhibit plasticity by reversibly transitioning between a stem and non-stem-cell state (257). This hypothesis suggests that the tumor cell is a dynamic state with greatly adaptable CSCs and non-CSCs that are capable of transient evolution and plasticity (258). Nevertheless, the definition of CSCs remains dependent of operational and based on functional assays that evaluate their self-renewal and tumorigenic properties, mainly assessed by the formation of tumorspheres in restricted culture conditions *in vitro*, and the formation of differentiated tumors upon xenograft *in vivo* (259) (Figure 9).

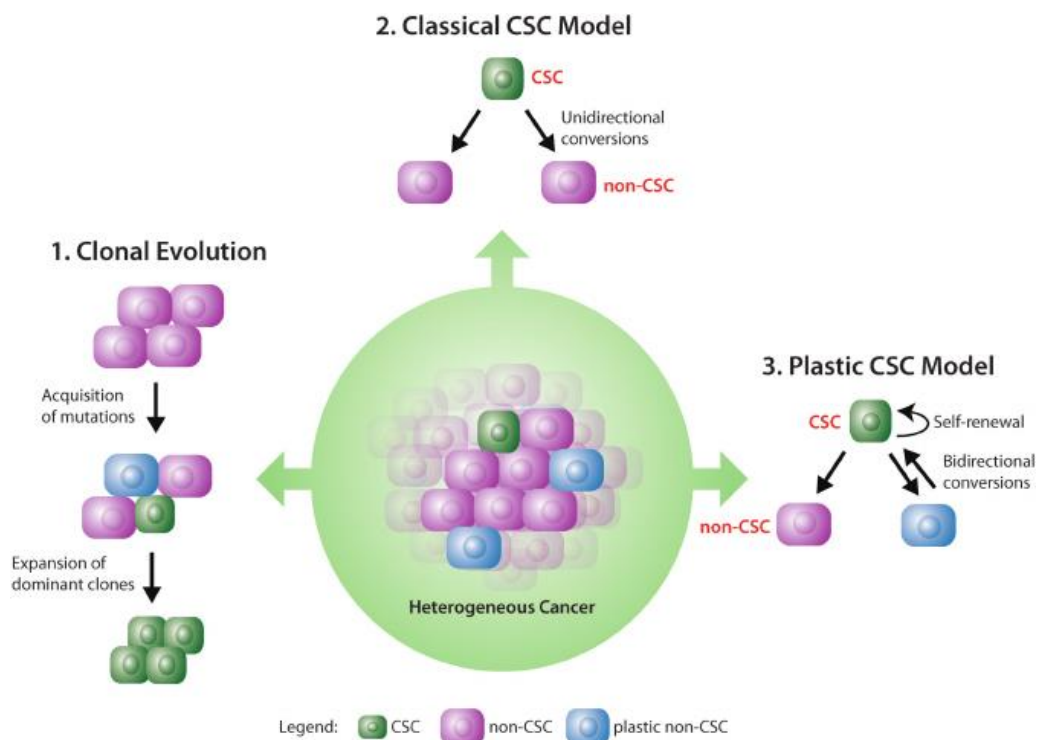


Figure 9 - Models of tumor heterogeneity and the role of CSCs. The clonal evolution theory was the first model to hypothesize a way in which cancer cells with diverse phenotypes could arise inside a tumor. In this model, different cancer cell populations evolve during tumorigenesis due to heritable genetic and epigenetic changes. A second model is described by the classical CSC theory, which proposes that tumor heterogeneity arises when cancer cells within a given tumor reside in different states of stemness or differentiation. While in this model the CSC-to-non-CSC conversion is a unidirectional process, in the plastic cancer stem cell model it is hypothesized that bidirectional conversions exist between non-CSCs and CSCs. This model is based on the fact that non-CSCs can continually create CSC populations throughout tumorigenesis. Adapted from Marjanovic *et al.*, 2013.

1.6.2 - Origin of Gastric Cancer Stem Cells (GCSCs)

In the stomach, the existence of GCSCs has been under debate. A theory suggests that gastric cancer stem cells may be closely associated with gastric stem cells. This hypothesis is based on the fact that gastric epithelial cells are constantly replacing the dead or injured cells, in order to maintain their own hemostasis (260). When an injury takes place, the epithelium renews faster, and it is here where stem cells play an essential role. In this process, the transformation of a stem cell that suffers genetic alterations will cause the development of gastric cancer (261). Another theory stands on the belief that GCSCs are originated from bone marrow-derived mesenchymal stem cells (BM-MSCs). BM-MSCS are adult stem cells that can migrate, regenerate and differentiate in several types of tissues and cells. When there is gastric injury caused by *Helicobacter felis* and *pylori* infection, the BM-MSCs migrate from the bone marrow to the epithelium and participate in the repair of injured tissues (262) (263). During the regeneration and repair process the development of gastric cancer can occur as a result of abnormal differentiation of BM-stem cells. A study performed by Varon *et al.*, demonstrated that green fluorescent protein (GFP)-labeled bone marrow-derived cells, upon *H. pylori*-induced chronic and atrophic gastritis and gastric cancer, were present in 90% of the mice, and 25% of tumor cells were derived from bone marrow-derived cells, proving that these cells participate in the development of gastric cancer and that BM-MSCs are a source of GCSCs (264). It is believed that bone-marrow-derived cells differentiate in the gastric mucosa by cell-cell fusion with local gastric epithelial cells and induce CSCs. However, the majority of dysplastic lesions do not arise from BMDCs (265). Overall, the issue is still debated and more studies are needed to fully understand the origin of GCSCs.

1.6.3 - Gastric cancer stem cells markers

Similar to the tumor bulk, CSCs may display endogenous heterogeneity, not only phenotypic but also genetic, so markers allowing their identification have been explored in different organs. Among the classic markers there are cluster of differentiation 44 (CD44), CD133, and CD24 (266) (249) (250) (243) (247) (244) (267). The activity and expression of aldehyde dehydrogenases (ALDH), which are enzymes involved in oxidation of aldehydes and retinoic acid signaling, were proposed to be a stemness marker in some tumors, like ovarian (230), breast (268), lung (269) or even colon (270). Concerning gastric tumors, several potential gastric CSC markers have been identified. These include CD44 and its variants; CD24/CD44; CD54/CD44; CXCR4; the epithelial cell adhesion molecule (EpCAM)/CD44; aldehyde

dehydrogenase 1 (ALDH1); sex-determining region Y-box 2 (Sox2); Oct4; CD90; CD71-negative; CD133; CD166 and leucine-rich, repeat-containing, G-protein– coupled receptor 5 (LGR5) (271). Recently, Nguyen and colleagues reported that CD44 and ALDH are the most specific biomarkers for isolation and detection of tumorigenic and chemoresistant gastric CSCs, independently from the histology of the tumor (271). CD133-positive CSCs have demonstrated resistance to standard chemotherapies (272) and qPCR analyses indicated that high CD133 expression is a marker for poor prognosis (273). Additionally, CD44 is expressed in up to 80% of primary gastric cancer resection specimens and is associated with advanced clinicopathologic features and also poorer prognosis (274). CD44 expression also denotes a subpopulation of gastric cancer cells in which Hedgehog signaling pathway proteins are up-regulated and also promote chemotherapy resistance, related with a poorer prognosis (274) (275).

1.6.4 - Gastric cancer stem cells and therapies

Standard therapies against gastric cancer, such as chemo and radiotherapy, have multiple limitations that lead to treatment failure and tumor recurrence. These drugs do not only cause high toxicity in the patients, but cannot kill all the tumor cells. It is believed that tumor relapse is due to the small population of CSCs that for their intrinsic characteristics are drug resistant and capable of reform again a tumor bulk. The identification of surface markers and the understanding of the molecular feature associated with GCSC phenotype are crucial for the design of effective treatments.

To date there is no solid consensus regarding specific gastric cancer stem cells markers. Several preclinical studies have indicated that targeting markers of CSCs, such as CD90 (276), LGR5 (277), CD44 and ALDH (271), may also be an effective approach to treat gastric cancer. For instance, cells expressing high levels of CD90 could be targeted by Trastuzumab, leading to significant reduction of the CD90+ population in tumor size and growth when combined with traditional chemotherapy. The finding that Trastuzumab targets the CSC population in gastric tumors suggests that HER2 signaling has a role in maintaining CSC populations, contributing to carcinogenesis and tumor invasion (276). Targeting CSCs with anti-LGR5 antibody-drug conjugates also demonstrated to be an effective strategy. The treatment with two anti-LGR5 antibodies induced cytotoxicity in LGR5-high gastrointestinal cancer cells, but not in LGR5- or LGR4-knockdown cancer cell lines (277). Metabolism modulating drugs, such as metformin (278) or all-trans retinoic acid (279) were as well successfully tested in GCSCs in in vivo and in vitro models with higher levels of CD44 and ALDH activity. Additionally, a clinical study has demonstrated the potential for targeting CSC markers in gastric cancer (280). A variant form of

CD44 (CD44v) was reported to interact with xCT, a cysteine-glutamate transporter subunit that maintains high levels of intracellular-reduced glutathione (GSH), which helps to defend the cell against oxidative stress. So, upon good results of Sulfasalazine (SSZ), an inhibitor of xCT that can suppress the survival of CD44v-positive stem-like cancer cells both *in vitro* (281) and *in vivo* (282), a clinical trial was performed. Half of the patients in that study which presented CD44v+ cells in their pretreatment biopsies, showed a reduction on the CD44v+ cancer cell population in the post-treatment biopsies. Intratumoral GSH levels were also decreased, consistent with the mode of action of this drug in CSCs. These data generate the hypothesis that SSZ may be a promising treatment for targeting CSCs in GC (280). Taking into consideration the emerging importance of gastric cancer stem cells it becomes urgent to identify and further validate biomarkers that better identify patients who have upregulated CSC pathways as well as specific markers as well as prioritize this evaluation during clinical development.

CHAPTER II

AIMS OF THE WORK

2- Aim of the work

As an alternative to standard therapies, targeted therapies represent a new perspective for cancer treatment. However, the efficacy of these therapies requires an accurate patient selection, on the basis of the molecular characteristics of the tumor, and the identification of the best drug combination effective in the different tumors. PDX platforms have provided important information on the activity of molecular drugs in the different tumor contexts and have shown to be endowed with translational activity.

In this work we took advantage of the gastro-esophageal tumor PDX platform that we have generated, to:

i) Investigate whether CSC share the genetic alterations identified in patient's tumors. As CSCs are believed to play a critical role in sustaining resistance to standard therapies, we explored if these cells respond to the targeted drugs as PDXs or PDX-derived cells;

ii) Study, in a PDX cohort characterized by *MET* gene amplification and addiction (SG16 PDX), the response to *MET* inhibition. *MET*, the tyrosine kinase receptor for HGF, is amplified in 2-4% of gastric tumors, characterized by a particularly aggressive disease. Even if *in vitro* and preclinical studies have shown the efficacy of *MET* inhibition in gastric cancer, clinical trials have provided negative results. In this study, we aimed at investigating the response to *MET* tyrosine kinase inhibitors and the mechanisms of resistance to the treatment.

iii) Identify and characterize *KRAS* amplified and mutated PDX, as well as to derive *in vitro* models. *KRAS* mutations and amplification have been poorly studied in gastric cancer, so in this work we explored whether *KRAS* could be targeted in gastric cancer, and if the presence of either *KRAS* amplification or mutation could have relevance for the treatment. *KRAS* pathway inhibition was explored *in vitro* and *in vivo* using *KRAS* downstream effectors inhibitors (MEK, AKT, and mTOR) and PARP inhibitors, alone or in combination.

CHAPTER III

MATERIAL AND METHODS

3- Material and methods

3.1- Patient and tumor samples

Gastric tumor and matched normal samples were obtained from patients undergoing surgery at the following Italian Hospitals: Candiolo Cancer institute- FPO, IRCCS; Ordine Mauriziano Hospital; San Giovanni Battista Hospital (Torino); Humanitas-IRCCS; San Raffaele Hospital (Milano); Treviglio-Caravaggio Hospital (Bergamo); Brescia Hospital, Borgo-Trento Hospital (Verona); Santa Maria delle Scotte Hospital (Siena); Forli' Hospital; Fondazione Macchi Hospital (Varese); Pisa Hospital. All the tumor samples were obtained through the 'Profiling protocol' approved by the Ethical Committee (Candiolo, Italy, Prot.5141, TitII Cat02 classe 01, 9 March 2011) and through the Gastroesophageal Annotated platform protocol (Candiolo, Italy, 006-IRCC-00II5-14; prat. n° 140/2014). All patients provided informed consent; samples were obtained and the study was conducted under the approval of the Review Boards of all the institutions. Clinical and pathologic data were entered and maintained in our prospective database.

3.2 - Animals

NOD (non-obese diabetic)/SCID (severe combined immunodeficient) mice were purchased by Charles River (Milan, Italy). Guidelines for Care and Use of Laboratory Animals were followed during the investigation. All animal procedures were approved by Ethical Commission of the IRCC in Candiolo and the Italian Ministry of Health.

3.3 - Xenograft transplantation

Tumor material not required for histopathologic analysis was collected and placed in medium 199 supplemented with 100 µg/mL levofloxacin. The surgical sample was cut into 25- to 30mm³ pieces in antibiotic-containing medium; some of the pieces were incubated overnight in RNAlater (Invitrogen, California, USA) and then frozen at -80°C for molecular analyses; two additional pieces were coated in Matrigel (BD Biosciences, Franklin Lakes, New Jersey, USA) and subcutaneously implanted in two different 4/6-week-old NOD/SCID female mice. After mass formation, tumors were analyzed for genetic identity with the original tumor (by short tandem repeat profiling, Cell ID) and for maintenance of *MET* amplification in the case of the PDX named SG16, and of *KRAS* mutations/amplifications in GTR10, GTR60A, GTR164, GTR165, GTR213, GTR245, GTR249 and GTR424.

3.4 - Drugs

Crizotinib and Lapatinib were purchased from Sequoia Research Products (Pangbourne, UK). Cetuximab was obtained from the Hospital Pharmacy. The MET inhibitor JNJ-38877605 (JNJ-605) was provided by Janssen Pharmaceutica NV (Beerse, Belgium). OSI-027 was purchased from Selleckchem (Munich, Germany) and Trametinib, MK-2206, Everolimus and Olaparib were purchased from Carbosynth (Berkshire, UK).

3.5 - Primary Cell culture

SG16, GTR10, GTR60A, GTR164, GTR165, GTR213, GTR245, GTR249 and GTR424 were derived from a chopped piece (approx. 3mm³) of the respective PDX after collagenase I digestion (Sigma-Aldrich, St Louis, MO, USA). After 1 h incubation at 37° in a shaking incubator, cells were centrifuged (1200 rpm for 10 min.) and the pellet was resuspended in L-15 medium (Sigma-Aldrich), supplemented with 100 units/ml penicillin and 100 µg/ml streptomycin (Sigma- Aldrich). After centrifugation (1200 rpm, for 5 min), cells were incubated for 5 min with DNase. Cells were washed in L-15 medium, centrifuged and the pellet was resuspended in 5 ml red blood lysis buffer. After 5 min incubation, cells were centrifuged and plated in a cell culture collagen coated dish. All the cells were cultured in ISCOVE medium (Sigma-Aldrich) supplemented with 10% fetal bovine serum, 100 units/ml penicillin and 100 µg/ml streptomycin.

Genetic identity between tumors and generated cells has been identified by short tandem repeat profiling (Cell ID, Promega, Madison, WI, USA). Maintenance of MET and KRAS amplification was evaluated by qRT-PCR as described above. 293T cells were obtained from ATCC.

3.6 - Sphere isolation

Cells dissociated from SG16, GTR10 and GTR165 PDXs were grown in suspension using T75 and T25 ultra low attachment flasks (Sigma-Aldrich) in stem-cell medium: DMEM/F-12 (Sigma-Aldrich) supplemented with 100 units/ml penicillin, 100 µg/ml streptomycin (Sigma - Aldrich), human recombinant EGF (20 ng/mL; Sigma-Aldrich), basic fibroblast growth factor (bFGF; 10 ng/mL; Peprotech) and insulin (2.5 mg/mL; Sigma-Aldrich); this medium was diluted 1:1 in LWRN medium (a conditioned medium from L-WRN cell line) (283).

3.7 - Anchorage-independent cell growth assay

For soft agar assays, 0.4% seaplaque soft agar (Lonza) was diluted with stem cell medium and was covered by a second 0.3% soft agar layer in which SG16 cells/spheres, GTR10 cells/spheres and GTR165 cells/spheres were embedded. After 20 days, colonies were counted using an optical microscope.

3.8 - Cell viability

For in vitro viability assays, GTR165, GTR213, GTR245 and GTR424 were seeded (5000 cells/well, three technical replicates) in the presence of Trametinib 5nM, MK-2206 500nM; OSI-027 250nM; Everolimus 25nM, Olaparib 3 μ M or vehicle (dimethyl sulphoxide) for 96h. After the end of treatment, cell medium was discarded and the CellTiter-Glo reagent (Promega Inc, Madison, WI, USA) was added and the plate was incubated for 10 min at room temperature. Luminescence was measured in a Multilabel Reader (PerkinElmer, Waltham, MT, USA). SG16 spheres (5000 cells/well, three technical replicates) and cells (2000/well; four technical replicates) were seeded in 96-well plastic culture plates, in the presence of the indicated drugs (JNJ-605 50 nM; LAP 500 nM; CmAb 1 μ g/ml) or vehicle (dimethyl sulphoxide) for 6 days. Cell viability was evaluated by CellTiter-Glo.

3.9 - Gene copy number and gene expression analysis by real-time PCR

mRNA and genomic DNA analyses were performed with standard techniques. mRNA was extracted using miRNeasy Mini Kit (Qiagen, Venlo, the Netherlands) and reverse transcribed into complementary DNA using the High Capacity complementary DNA Reverse Transcription Kit (Applied Biosystems, Carlsbad, CA, USA) and random primers, according to the manufacturer's protocol. Complementary DNA (500 ng) was amplified by Real-time qPCR using the TaqMan Universal PCR Master Mix, according to the manufacturer's protocol. Real-time qPCR was performed in triplicates using the following primers: ACTB (assay ID: Hs99999903_m1); HPRT (assay ID: Hs02800695_m1); MET (assay ID Hs01565584_m1); KRAS (assay ID Hs00364283_g1); ALDH (forward, 5'-CTGCTGGCGACAATGGAGT-3'; reverse, 3'-GTCAGCCCAACCTGCACAG-5'); NANOG (forward -5'-TGTTTGCCTTTGGGACTG-3' , reverse, 3'-ATACCTCAGCCTCCAGCAGA-5'); OCT4 (forward, 5'-GGGGTTCTATTTGGGAAGGT- 3'; reverse, 3'-CTGGTTCGCTTTCTCTTTTCG-5'); SOX2 (forward 5'- TGGGTTCGGTGGTCAAGTC- 3'; reverse 3'-GCTCTGGTAGTGCTGGGACA-5') (Syber). Genomic DNA samples were extracted by Wizard SV Genomic DNA Purification System (Promega). Quantitative PCR experiments for estimation

of *MET* and *KRAS* copy number variations were performed in triplicates using a Human TaqMan Copy Number Assay for *MET* (assay ID: hs01277655_cn), a Human TaqMan Copy Number Assay for *KRAS* (assay ID: Hs06936191_cn) and the TaqMan Copy Number Reference Assay RNase P (Applied Biosystems, Foster City, CA, USA). PCR runs were performed in triplicates with ABI Prism 7900HT (Applied Biosystems) using 2 ng total genomic DNA as a template.

3.10 - Sanger sequencing

Exon sequencing of *KRAS* (2, 3, 4) was performed by automated sequencing by ABI Prism 3730 (Applied Biosystems).

3.11 - Gene silencing

For *KRAS* transduction in GTR245 and GTR213 cells, viruses were produced as described elsewhere (284). 200 ng of concentrated virus was used to transduce the cells with sh*KRAS* or the pLKO empty vector. Twenty-four hours after transfection, cells were seeded at the appropriate density for biochemical or biological assays. For transient transfection GTR60A, GTR165 and GTR424 cells at 70% confluence were transfected using Lipofectamine 2000 (Invitrogen) with 0,1 $\mu\text{mol/mL}$ of synthetic *KRAS*/Ctrl siRNAs (Applied Biosystem) overnight. Then the following morning the medium was changed and 72h after RNA was extracted and cell viability was evaluated by CellTiter Glo (Promega Inc, Madison, WI, USA). CellTiter-Glo luminescence was measured in a Multilabel Reader (PerkinElmer, Waltham, MT, USA).

3.12 - Western blot analysis

Whole-protein extracts were prepared using LB buffer ($\frac{1}{2}$ vol. H₂O, $\frac{1}{4}$ vol. Tris HCl pH 6.8, $\frac{1}{4}$ vol. sodium dodecyl sulphate 10%) and quantified using the BCA Protein Assay kit (Pierce, Rockford, IL, USA). Primary antibodies: anti-EGFR (1005:sc-03), MCT4 (H90) and anti-*MET* (clone C28) were from Santa Cruz Biotechnology; antibodies against phosphorylated *MET* (Tyr1234/1235) (Clone D26), phosphorylated ERK (Thr202/Tyr204), GLUT1 (ab15309), HKII (C64G5), PKM2 (Tyr105) phosphorylated AKT (Ser473) (Clone D9E), total AKT, and ERK were from Cell Signaling; antibody against phosphorylated EGFR (Tyr1068) (ab5644) was from Abcam (Cambridge, UK) and antibodies against *KRAS* (3B10-2F2), Vinculin (1931) and Actin (A3854) from Sigma. Secondary antibodies were from Amersham. Detection was performed with ECL system (Amersham, UK).

3.13 - Pull-down assay for RAS

Pull-down assays were performed using the active Ras pull-down and detection Kit (#1611; Thermo Scientific, Rockford, USA). Briefly, cells were lysed with 100 μ L ice-cold lysis buffer together with protease inhibitors. Lysates were kept ice cold, briefly sonicated, and then centrifuged at 14,000 rpm for 10 min to clear the lysate of any unlysed materials and DNA. For standardization purposes, a fraction of the supernatant was collected to measure protein concentrations using the BCA Protein Assay kit (Pierce, Rockford, IL, USA). For each sample, 500 μ g of protein lysate were passed in a spin cup containing 80 μ g of GST-Raf1-RBD bounded to the glutathione resin. The beads and lysates were allowed to incubate for 1 h at 4°C. After incubation, the beads were washed and eluted in loading buffer. 10 μ g of the remaining total protein lysate were run on SDS-PAGE, together with the eluted RAS-GTP. Western blots were probed using anti-RAS primary antibody provided by the kit. GTL16 not treated and treated with JNJ-605 were used as internal controls.

3.14 - Lactate uptake

Lactate uptake was evaluated in a buffered solution (140 mM NaCl, 20 mM Hepes/Na, 2.5 mM MgSO₄, 1 mM CaCl₂, and 5 mM KCl, pH 7.4) containing 0.5 μ Ci/ml [U-¹⁴C] lactate for 15 minutes at 37°C. Cells were subsequently washed with cold PBS and lysed with 0.1 M NaOH. Incorporated radioactive was assayed by liquid scintillation counting (Perkin Elmer, Tri Carb 2800 TR) and normalized on protein content.

3.15 - Lactate production

Lactate was measured in the cultured media with Lactate Assay kit (Source Bioscience Life Sciences) according to the manufacturer's instruction. Briefly, cells supernatant was collected from GTR245, GTR249, GTR164, GTR213, GTR424, GTR165 cells following 48 h of culture. The plated cells were lysed and the protein was extracted and quantified. The collected medium was centrifuged at 1200 rpm for 5 min. Then, 10 μ l of each supernatant sample was added to 50 μ l of lactate reagent solution for 10 min, after which the absorbance was measured at 540 nm in a Multilaber Reader and the values of the absorbance were normalized on protein content.

3.16 - Xenotrials

For the SG16 and GTR245 trials, tumors were passaged and expanded until production of a cohort of mice bearing homogeneous tumors. Mice with established tumors (average volume

250/300 mm³) were randomized to allow the same average volume in each experimental group (n=6) (Figure 10). For the SG16 trial, each experimental group was treated for the indicated days with the following regimens (either single agent or combination): Lapatinib 100 mg/kg, daily, os; Cetuximab 20 mg/Kg, twice weekly ip; Crizotinib 25 mg/kg, daily, os; JNJ-38877605 50mg/kg, daily, os (Table 1). For the GTR245 trial the following drugs were used: Trametinib 1 mg, daily, os; MK-2206 2 mg, 3 times per week, os; Everolimus 0.12 mg, daily, os; Olaparib 1 mg, daily, os (Table 1). Tumor size was evaluated once-weekly by caliper measurements and approximate volume of the mass was calculated using the formula $4/3\pi(D/2)(d/2)^2$, where d is the minor tumor axis and D is the major tumor axis. Experiments were not performed in blind.

SG16, GTR10 and GTR165 spheres (1000 and 10000 cells), obtained as described below in 3.6, were injected s.c. into the right posterior flanks of 5-week-old female NOD-SCID mice. Four animals were used for each condition. Tumor volume was monitored for 7-14 weeks.

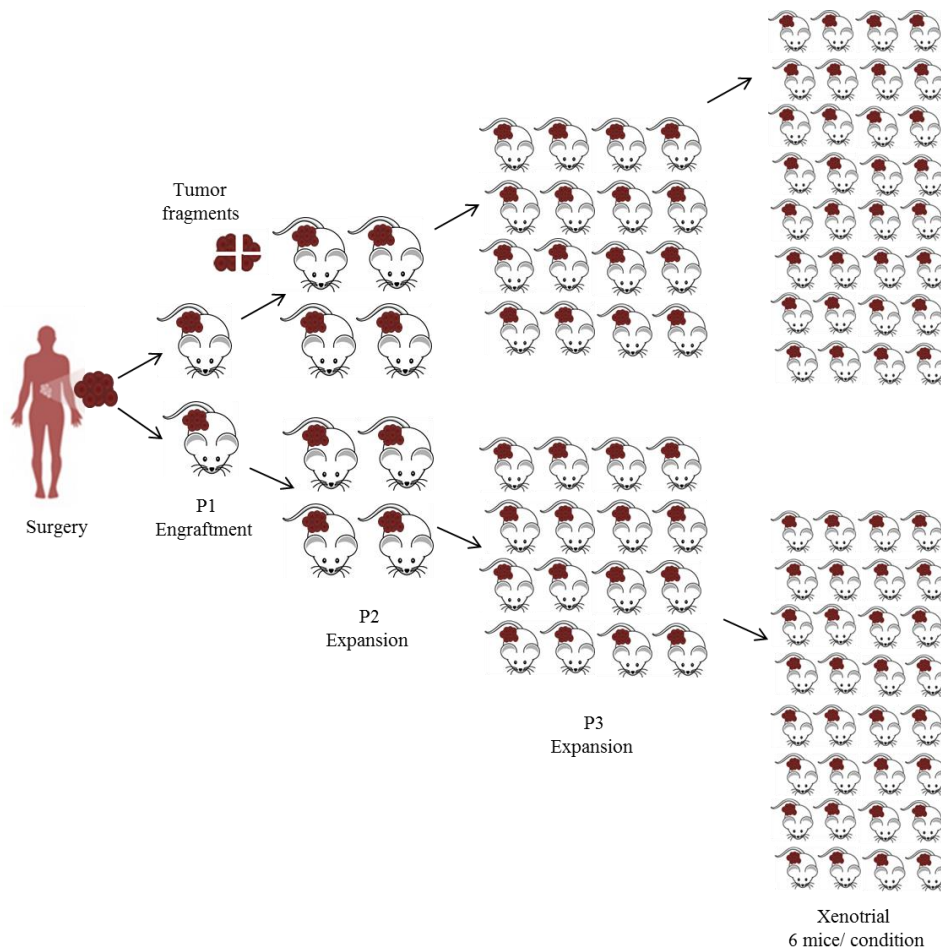


Figure 10 – Xenograft transplantation and expansion. Gastro-esophageal tumors were collected from 16 Italian hospitals and have been used to generate a platform of gastro-esophageal patient-derived xenografts. All the process begins with the collection of patients fresh tumor surgical specimens that are posteriorly transferred in immunocompromised mice. Upon engraftment, the tumors can be divided and re-implanted in several mice allowing a genetic characterization, the generation of *in vitro* models and the realization of xeno-trials.

Table 1 – Drug treatments performed in the xenotrials using the SG16 and GTR245 PDXs. os=by mouth; ip=intraperitoneal.

PDX	Genetic lesion	Single treatments	Doses	Combinational Treatments
SG16	MET amplification	JNJ-38877605	50mg/kg, daily, os	JNJ + Cetuximab
		Cetuximab	20 mg/Kg, twice weekly ip	JNJ + Lapatinib
		Lapatinib	100 mg/kg, daily, os	
GTR245	KRAS mutation	Trametinib	1 mg, daily, os	Trametinib + MK-2206
		MK-2206	2 mg, 3 times per week; os	Trametinib + Everolimus
		Everolimus	0.12 mg, daily, os	Trametinib + Olaparib
		Olaparib	1 mg, daily, os	

3.17 - Immunohistochemistry

Two hours following drug treatments, tumor xenografts were harvested and fixed in formalin for 16h, and then paraffin embedded. Sections were cut (5 μ m) and immunohistochemical analysis was carried out. Briefly, sections were deparaffinized and hydrated. Antigen retrieval was performed using EDTA or Cytrate buffer solution, at 95 °C for 40 min. Endogenous peroxidases were quenched using Metanol-0.3 % H₂O₂. Primary antibodies included MET (C28) antibody from Santa Cruz Biotechnology Inc., Dallas, Texas, USA; P-MET (Tyr1234/1235) antibody AF2480 from R&D Systems (Minneapolis, MN, USA); KRAS antibody (415700) from Invitrogen (Massachusetts, USA); EGFR antibody D38B1, P-EGFR antibody Tyr1173 (53A5); and the P-S6 (Ser235/236) (D57.2.2E) from Cell Signalling (Danvers, MA, USA). Diluted antibodies were applied to the sections overnight and then detected using anti-rabbit reagent and DAB Substrate (Thermo Fisher). Tissues were counterstained with Harris' hematoxylin, dehydrated, cleared, and coverslipped. Agar cytoincluded spheres were fixed, and paraffin embedded. Slices of 5 μ m were cuted, deparafined, hydrated and stained with, hematoxylin and eosin. Images were captured with the AxiovisionLe software (Zeiss, Gottingen, Germany) using an Axio Zeiss Imager 2 microscope (Zeiss).

3.18 - Statistical Analysis

Statistical significance was performed using the two tailed Student's t-test and an unpaired one tailed MannWhitney test or one-way ANOVA analysis of variance followed Bonferroni's post hoc to compare differences between experimental conditions. Error bars represent the S.D., as indicated in each figure legend. Figures show one representative experiment, reporting the average of the technical replicates. Statistical significance: **p* value <0.05; *p* value **<0.01; *p* value ***<0.001; *p* value ****<0.0001.

CHAPTER IV

RESULTS

4- Results

4.1 - The “GEA PLATFORM” project

The work in this thesis is based on the availability of a large collection of gastro-oesophageal tumors implanted in immunocompromised mice (Patient-derived Xenografts, PDX). The GEA Platform (Gastro-Esophageal cancer Annotated Platform) project was generated with the objective of collecting and characterizing at molecular level a wide number of gastro-oesophageal cancers. This platform includes tumors obtained from 16 different Italian hospitals between the end of 2011 and today. The GEA collection was established by processing *ad hoc* surgically removed tumor tissue specimens for pathologic and molecular characterization, by engrafting small fragments (approx. 4mm x 4mm) of the same samples into immunocompromised mice (NOD/SCID), in order to obtain a complete molecular characterization of the original tumor and, at the same time, to generate material to perform preclinical studies.

Samples from 500 gastro-oesophageal cancer patients are included in this platform. Men and women are represented in a 2:1 ratio; patients' median is 68 years. Sixteen per cent of total tumors are classified as gastro-oesophageal junction cancer, 5%, 23% and 48% as cancer of the fundus, body and antrum/pylorus respectively. According to Lauren's classification, intestinal subtype is the most represented (39%), whereas diffuse and mixed types are present in 24% and 9% of cases. 22% of patients were diagnosed at I/II stages and 39% at III/IV stages.

4.1.1 - Establishment of PDX models

Samples included in this platform (n=500) were divided in a variable number of small fragments according to their dimensions and each fragment was implanted in a different mouse. The remaining material was stored for molecular analyses and, when possible, conserved in the vital tumor bank. Success rate of engraftment was 30%. The mean latency period of tumor growth (from implant to the appearance of a palpable tumor) was 73 days (ranging from 31 to 200), but the latency period became progressively shorter along serial passages (a mean of 3 weeks). Histological analysis of tumors grown in mouse models revealed features comparable to their corresponding original tumors.

4.1.2 - Factors influencing PDX generation

Statistical analysis did not show any significant correlation between engraftment and patient characteristics (such as age, gender or neoadjuvant chemotherapy). However, tumors classified as intestinal showed a better grafting (38% of primary tumors were of this subtype versus 57% of PDXs) than those of diffuse type (23% versus 9%; $p=0,002$) or the ones with signet ring morphology (28% versus 15%; $p=0,617$), demonstrating that tumor histological characteristics were associated with success of engraftment, and this can be due to the fact that these tumors display a more aggressive behavior, in absence of proper immune surveillance. The same was true for the MSI status: 15% of primary tumors were MSI+, whereas 28% of PDXs were MSI+ ($p=0,006$). Conversely, tumor location, TNM stage and EBV status did not correlate with engraftment.

Receptor Tyrosine Kinases (RTKs) (specifically HER2, EGFR, MET and FGFR2) and KRAS amplifications had a relevant role in tumor engraftment: indeed, 22% of PDXs presented RTK amplifications, observed in only 12.5% of primary tumors ($p=0,197$). In particular, 4% of primary cancers were HER2 amplified compared to 9% of PDXs ($p=0,072$). 7.4% of collected samples carried EGFR amplification, but this value increased in engrafted tumors (16%; $p=0,079$).

Concerning KRAS, a positive correlation exists between KRAS alterations and engraftment rate, since 3.5 % of the tumors are KRAS amplified vs 5.5% of PDX ($p=0,389$). Concerning KRAS mutations, G12D and G13D are the most frequent in our analyzed PDX (4% and 5%, respectively) however the A146T is present at a frequency much higher than in other studies (3% vs 0.2 %) regarding gastro-esophageal tumors (<http://cbioportal.org>) (204).

4.1.3 - PDX characterization

PDX histological analyses were routinely performed and demonstrated a good correlation with their corresponding original tumors regarding Lauren histological classification. Also, MSI and EBV status remained stable between primary and PDX samples. RT-PCR analyses were performed for each specimen, in order to test and confirm gene amplifications in PDXs tumors. A panel of 243 “gastric cancer specific genes” (as defined by the TCGA consortium) was sequenced to identify DNA alterations. As expected, the sequencing analysis demonstrated that high mutational rates correlate with microsatellite instability.

4.2 - PDX-derived *in vitro* models

A smaller cohort of PDX present in our platform, selected according their molecular characteristics, was used in order to generate *in vitro* models. From this group we established and characterized 31 primary cell lines, 28 organoids and 3 spheres (Table 2). All of our *in vitro* models maintained the molecular (gene amplification or mutations) and histological features (tubular, mucinous or mixed features) of the PDX of origin, demonstrating that they can be successfully used as pre-clinical models to explore and identify target mechanisms in gastric cancer as well as to elucidate mechanisms of response to targeted therapies, as a complement to the respective xenopatients.

Table 2 - Percentage and number of PDX- derived *in vitro* models from the GEA platform.

	Established (n°)	Total (%)
PDX derived cell lines	31	40
PDX derived organoids	28	36
PDX derived stem cells	3	0,4

4.2.1 - Xenospheres characterization

It is described that gastric cancer stem cells can have a role in the response to gastric cancer therapies (285). We aimed at isolating stem cells from our PDX cohort in order to explore if they share the genetic alterations identified in patient tumors and if they respond to targeted therapies as the original tumor.

Three gastric stem-like cell lines were obtained from PDXs: SG16 sph, GTR10 sph and GTR165 sph. These cells were able to grow in serum free medium, in suspension and were able to form spheres ([Figure 11](#)) that reformed upon dissociation. Since these spheres have been isolated from PDXs they can be named “xenospheres”.

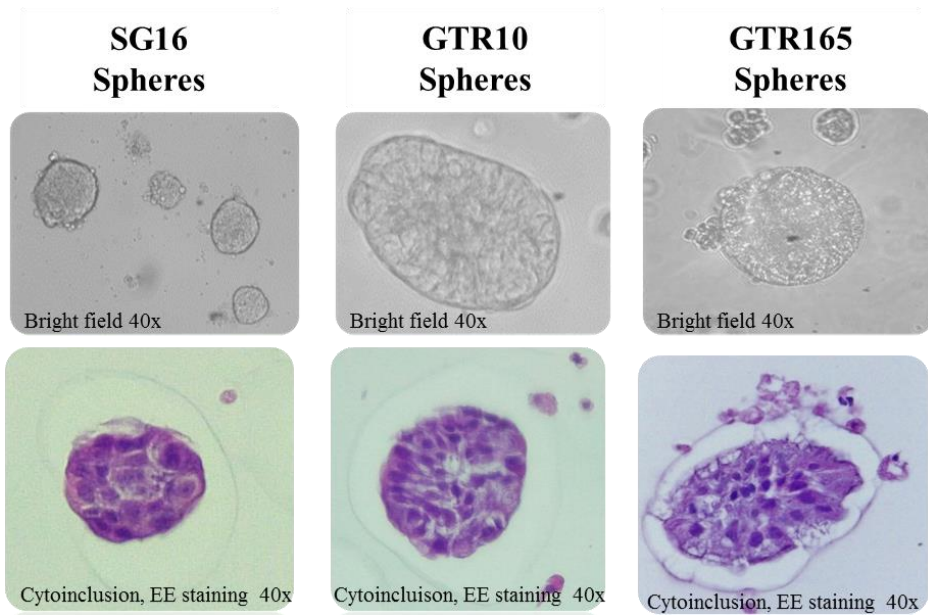


Figure 11 - SG16, GTR10 and GTR165 sphere morphology. Representative images of the spheres observed by phase-contrast light microscopy (upper pictures) and stained with H&E (lower pictures). Amplification 40x.

To date no consensus has been achieved regarding GCSC markers. So, to verify if the isolated spheres display stem features, levels of classical stem markers (ALDH, NANOG, SOX2, OCT4) were explored, in comparison with the respective tumor-derived cells growing in adhesion (indicated as “cells”). Quantitative real time PCR evidenced that SG16 sph, GTR10 sph and GTR165 sph showed higher levels of stem markers in comparison with cells grown in adhesion (Figure 12). As observed in Figure 12, the levels of expression were quite different in the different xenospheres, ALDH level were significantly higher in SG16 and GTR165 spheres compared with GTR10, while SOX2 was more expressed in GTR10 compared to the other two xenospheres.

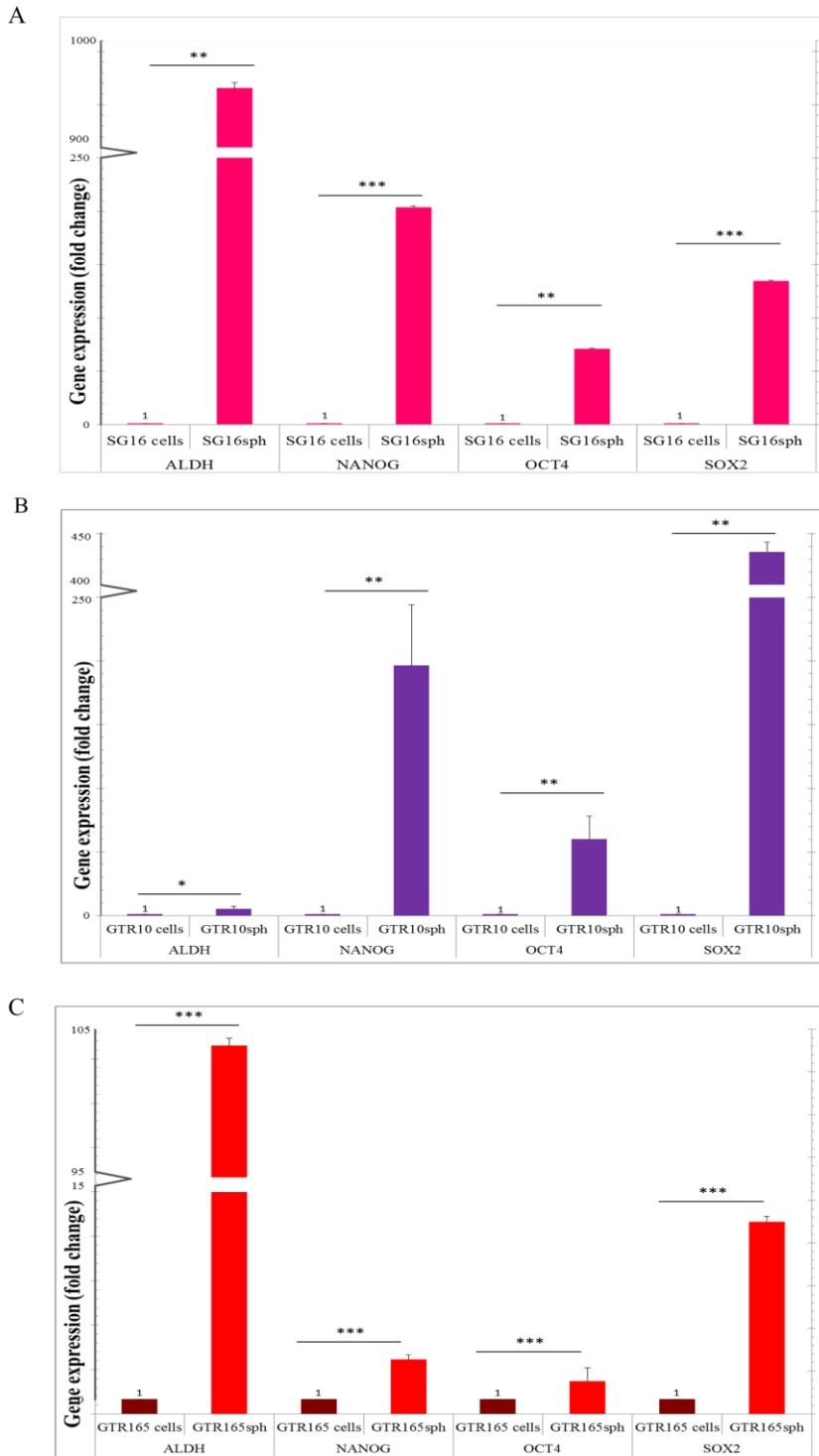


Figure 12- SG16, GTR10 and GTR165 spheres present significantly higher expression of the stem markers ALDH, NANOG, OCT4 and SOX2 compared to the respective cells grown in adhesion. qPCR performed using RNA extracted from SG16, GTR10 and GTR165 spheres and cells. Results are shown as fold change of mRNA expression relative to that of SG16, GTR10 or GTR165 cells. Real time RT-PCR data were obtained using the $\Delta\Delta C_t$ method, with normalization to the reference Actin mRNA. Statistical significance is indicated * $<0,5$; ** $<0,01$; *** $<0,001$.

Anchorage-independent growth is another feature of CSCs. The clonogenic potential of xenosphere-derived cells was assessed by evaluating their ability to grow in soft agar. After 20 days, in all of the 3 cases, we observed an increased clonal ability for the cells derived from the spheres that for those derived from grown in adhesion (Figure 13).

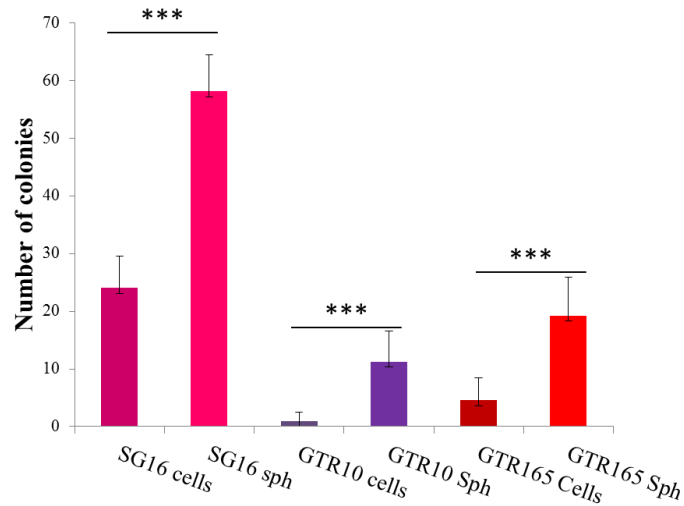


Figure 13 - SG16, GTR10 and GTR165 spheres showed a higher anchorage-independent growth ability compared to the corresponding cells growing in adhesion. The advantageous growth was demonstrated by the increased number of colonies formed in soft agar after 20 days of growth. Statistical significance is indicated $***<0.001$.

Further, the three models of xenospheres were capable of forming tumors starting from a limited number of cells. When 10000 and 1000 cells were s.c. inoculated in NOD/SCID mice both SG16 (Figure 14A) and GTR165 (Figure 14C) spheres were able to form tumors, while GTR10 spheres formed tumors only starting from 10000 cells (Figure 14C).

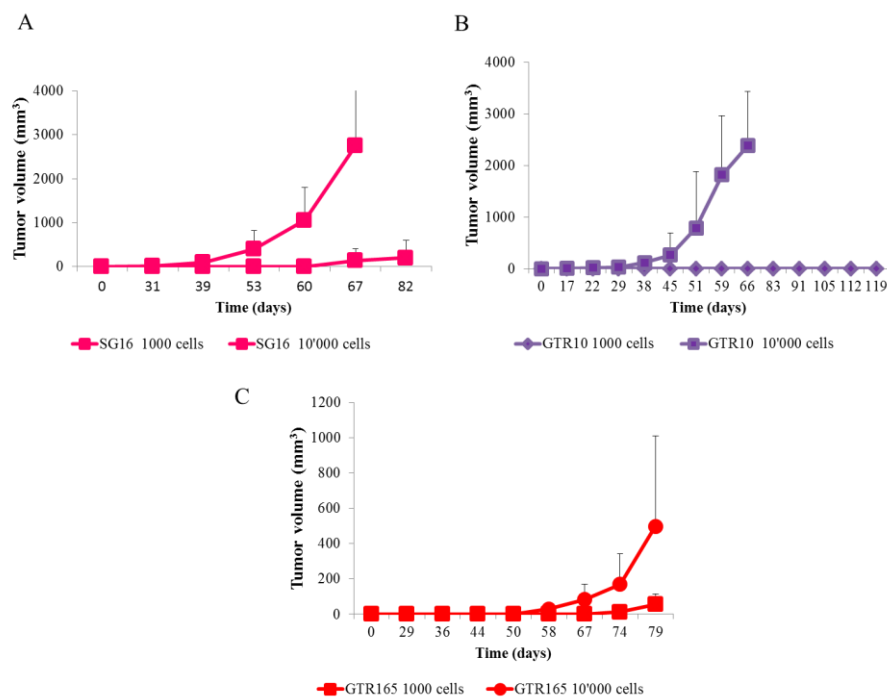


Figure 14 - SG16, GTR10 and GTR165 spheres form tumors when injected in limited number in immunocompromised mice. Spheres were desegregated and 1000 and 10000 cells were s.c. inoculated in NOD-SCID mice. Tumors were monitored and measured with caliper. 4 mice were used per group. Error bars represent SD.

It was previously described that xenospheres are able to faithfully retain the genetic make-up of patients' tumors (286). Indeed, in our group of gastric xenospheres two out of three maintained the genetic molecular alterations of the original tumor. SG16 spheres were derived

from a gastro-esophageal tumor bearing *MET* gene amplification; we observed that spheres, similarly to PDX and cells, maintained *MET* amplification, even though with a lower copy number (Figure 15A). GTR165 spheres were isolated from a tumor bearing *KRAS* amplification that was maintained both in 2D cultured cells and spheres (Figure 15C). On the contrary, GTR10 spheres did not maintain the *HER2* overexpression detected in the gastric tumor from which they derived (Figure 15B). On the bases of these results, at least SG16 and GTR165 stem-like cells can be used as additional *in vitro* models to explore the response to target therapies in gastric cancer.

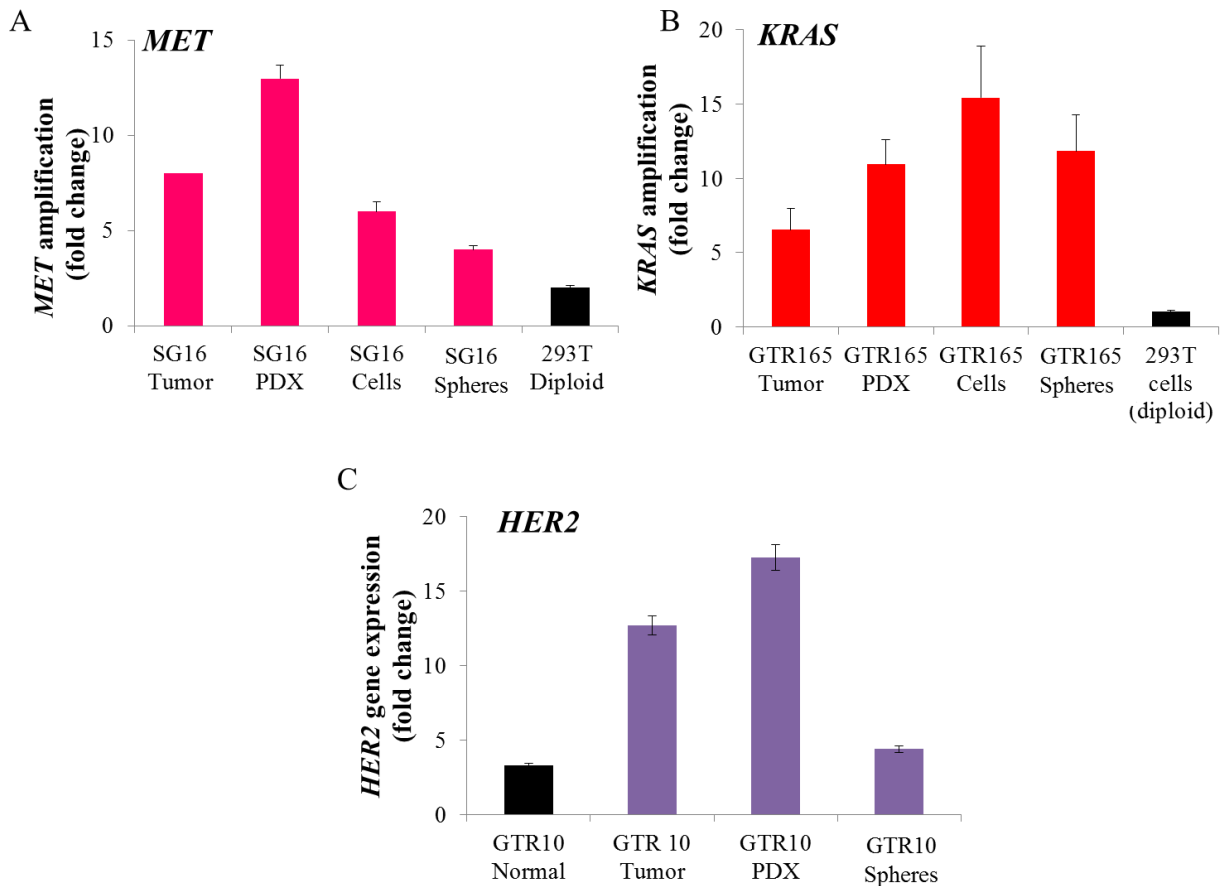


Figure 15 - SG16 and GTR165 spheres maintained *MET* and *KRAS* amplification, respectively, observed in the original tumor. qRT-PCR (performed on gDNA in A and C or on RNA in B) was used to evaluate if SG16, GTR10 and GTR165 xenospheres shared the same molecular alterations observed in the original tumors and PDXs. Contrary to what was seen in SG16 and GTR165 spheres, GTR10 did not show *HER2* overexpression observed in the tumor. 293T cells represent a diploid control.

4.3 - *MET* amplified PDX model

4.3.1 - *MET* amplified PDX model characterization

Among the previously described PDXs available in our platform, we identified one case (named SG16 PDX) bearing a 13-fold amplification of the *MET* gene (Figure 16B). When *MET* amplification was analyzed by quantitative Real Time in the original tumor, the number of *MET*

copies was lower (16 copies) than that found in the PDX (26 copies). This difference between the parental tumor and the PDX can be justified by the lack of dilution with stromal cells derived DNA as the probe used for PCR analysis is human-specific and it does not recognize the murine *MET* gene of stromal cells. *MET* amplification was confirmed also by FISH analysis (Figure 16C) and by Nanostring technology (data not shown). *MET* gene amplification was paralleled by an increase in *MET* mRNA and protein and in *MET* constitutive tyrosine phosphorylation (Figure 16E).

In order to perform biochemical studies, a primary cell line (SG16 cells) was derived from the SG16 PDX. This cell line maintained the molecular features of the original tumor, including *MET* amplification, overexpression and constitutive activation (Figure 16B;D).

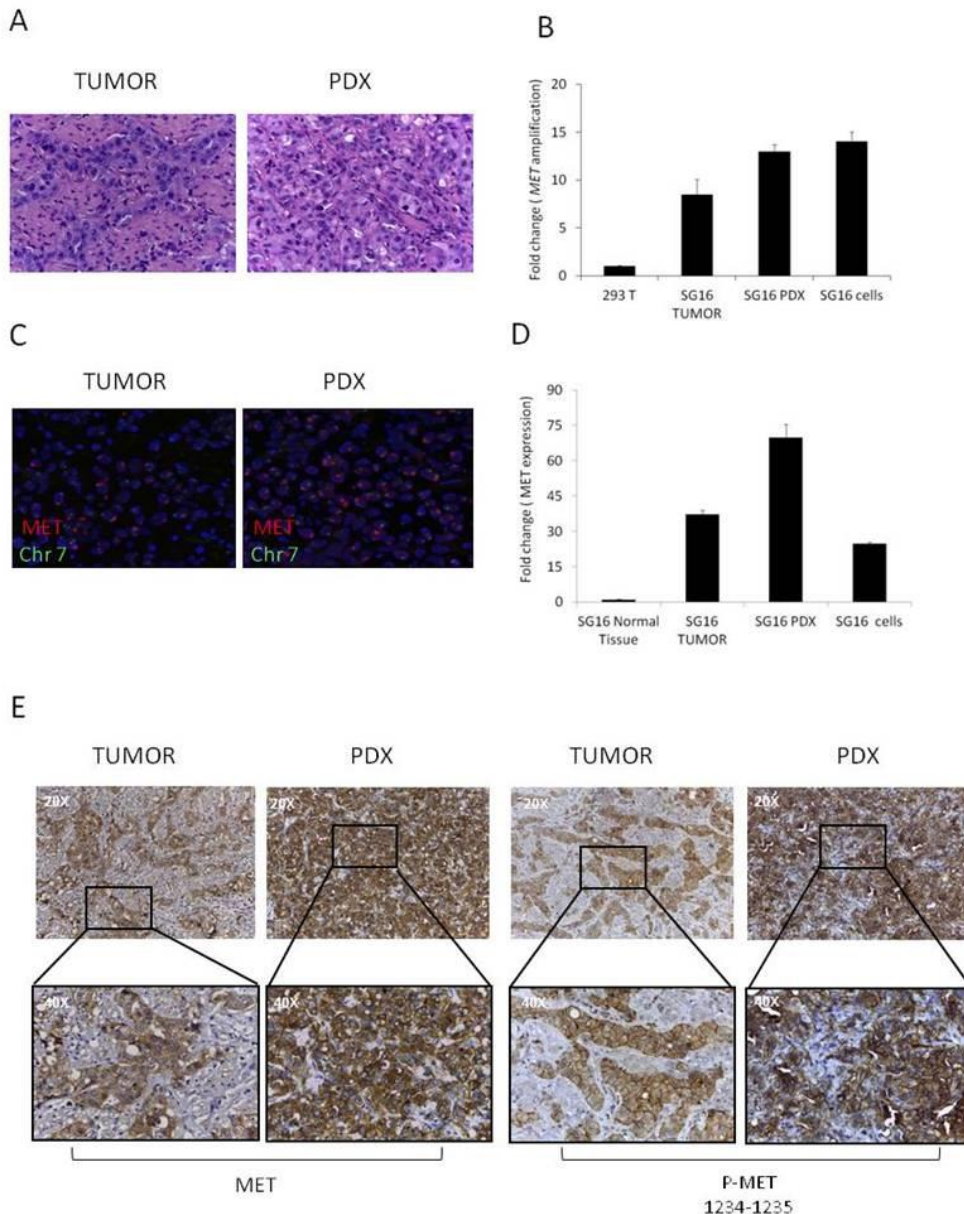


Figure 16 - SG16 tumor and xenopatient (PDX) show amplification and constitutive activation of the MET receptor. A) H&E staining of the primary tumor (left) and PDX (right) demonstrates that xenografted tumors retained the histopathologic characteristics of the original sample Hematoxylin and eosin stain shows clusters of cancer cells infiltrating the muscular layer (left panel). Cells display large eosinophilic cytoplasm and pleomorphic nuclei, with some evident nucleoli. Mitotic figures are frequent. B) qRT-PCR analysis of *MET* gene amplification in the original tumor (SG16), in the PDX and in tumor-derived cells compared to the diploid cell line 293T; C) FISH analysis of the original tumor (left) and of the PDX tumor (right) performed using *MET* (red) and chromosome 7 (green) specific probes; D) qRT-PCR analysis of *MET* expression in the original tumor, in the PDX and in tumor-derived cells in culture compared to the matched normal tissue; E) IHC for *MET* (left panels) and P-*MET* (right panels) in the original tumor and in the PDX. Lower pictures represent enlargement of the framed areas.

4.3.2 - *MET* amplified PDX- derived cells response to *MET* inhibition

Since oncogene amplification, overexpression and constitutive activation are typical characteristics of oncogene addiction, we investigated whether SG16 cells were sensitive to *MET* inhibitors. SG16 cells were treated with JNJ-605, a specific *MET* inhibitor; we observed that SG16 cells were partially resistant to *MET* TKIs as 50% of them were still vital after six days of treatment (Figure 17A). Additionally, western blot analysis in SG16 cells showed that

MET inhibition resulted in abrogation of MET and AKT activation, but only in a partial decrease of MAPK phosphorylation ([Figure 17B](#)). In SG16 spheres, inhibition of the AKT and MAPK pathways was not observed upon treatment with MET monotherapy ([Figure 17D](#)).

Upon these results we explored if EGFR activation could be the cause of partial response to MET inhibition, since it is described in the literature that MET and EGFR can crosstalk, leading to resistance to their respective inhibitors (287). As shown in [Figure 17B](#), EGFR phosphorylation decreased after treatment with JNJ-605, suggesting that it was mainly due to MET trans-phosphorylation. However, a residual EGFR phosphorylation persisted upon MET inhibition. We thus analyzed the effect of EGFR inhibition in these cells, alone or in combination with MET inhibitor JNJ-605. Single treatment with Lapatinib or Cetuximab only partially decreased EGFR phosphorylation (further sustaining the role of MET transphosphorylation) and did not affect P-MAPK levels. On the other side, the concomitant treatment with EGFR and MET inhibitors resulted in complete inactivation of both EGFR and MAPK ([Figure 17B](#)). While single treatment with either Lapatinib or Cetuximab was ineffective, the concomitant inhibition of both MET and EGFR in SG16 cells resulted in a cell viability decrease which was significantly higher compared to that induced by MET inhibition ([Figure 17A](#)).

In order to evaluate if the stem-like spheres isolated from the SG16 PDX responded in a way similar to the cells grown in adhesion, the same treatments were performed in the SG16 spheres. In spite of the fact that these cells were enriched in stem features and grew as spheroids, SG16 spheres showed the same biological behavior ([Figure 17C](#)). However, in these cells the activation of AKT was not abrogated upon the combinational treatments while MAPK and MET activation was completely inactive ([Figure 17D](#)).

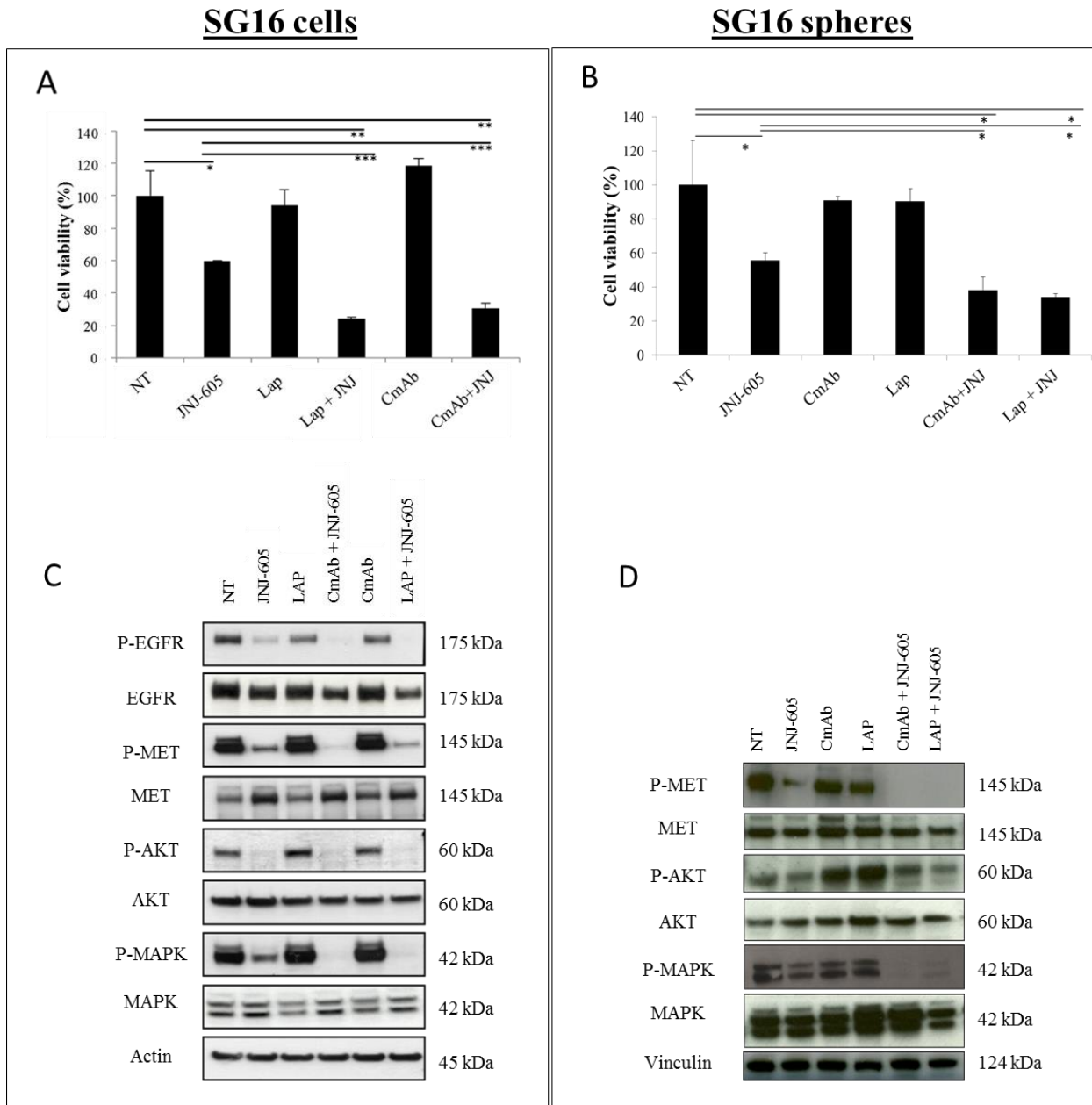


Figure 17 - SG16 Tumor-derived cells and spheres are partially resistant to MET inhibitors and display high sensitivity to combined anti-MET/EGFR treatment. A,C) cell viability assays performed on tumor-derived cells and spheres, upon treatment with the indicated drugs for 6 days. Cell viability was evaluated using Celltiter Glo. B,D) Western blot analysis of tumor-derived cells and spheres, untreated or treated with the indicated drugs. Blots were probed with the indicated antibodies. Actin and vinculin were used as loading controls. SG16 cells display high sensitivity to combined anti-MET/EGFR treatment. NT= untreated; JNJ-605=JNJ-38877605; LAP= lapatinib; CmAb = cetuximab. Statistical significance is indicated * <0.5 ; ** <0.01 ; *** <0.001 .

4.3.3 - MET amplified PDX response to MET inhibition *in vivo*

The results obtained *in vitro* were validated *in vivo*, by a preclinical trial in PDXs. The original SG16 tumor was serially passaged *in vivo* until 6 tumor-bearing animals were produced per experimental group. When xenografts reached an average volume of approximately 250 mm³, mice were randomized into 6 independent treatment cohorts: (i) vehicle (placebo); (ii) the MET inhibitor JNJ-605; (iii) the EGFR mAb Cetuximab, (iv) the dual HER2/EGFR kinase

inhibitor Lapatinib (v) JNJ-605 and Cetuximab; and (vi) JNJ-605 and Lapatinib. As shown in Figure 18A while monotherapy treatment with the MET inhibitor resulted only in a partial response, thus showing a partial primary resistance, the combined use of JNJ-605 and an anti-EGFR drug (either cetuximab or lapatinib) led to a complete and durable response. Intriguingly, treatment with anti-EGFR alone was totally ineffective, thus completely recapitulating the *in vitro* results (Figure 17). Immunohistochemical analysis performed on the tumors showed that, indeed, only the combination was able to completely abrogate tyrosine phosphorylation of both MET and EGFR, as well as the activation of downstream effectors Figure 18B.

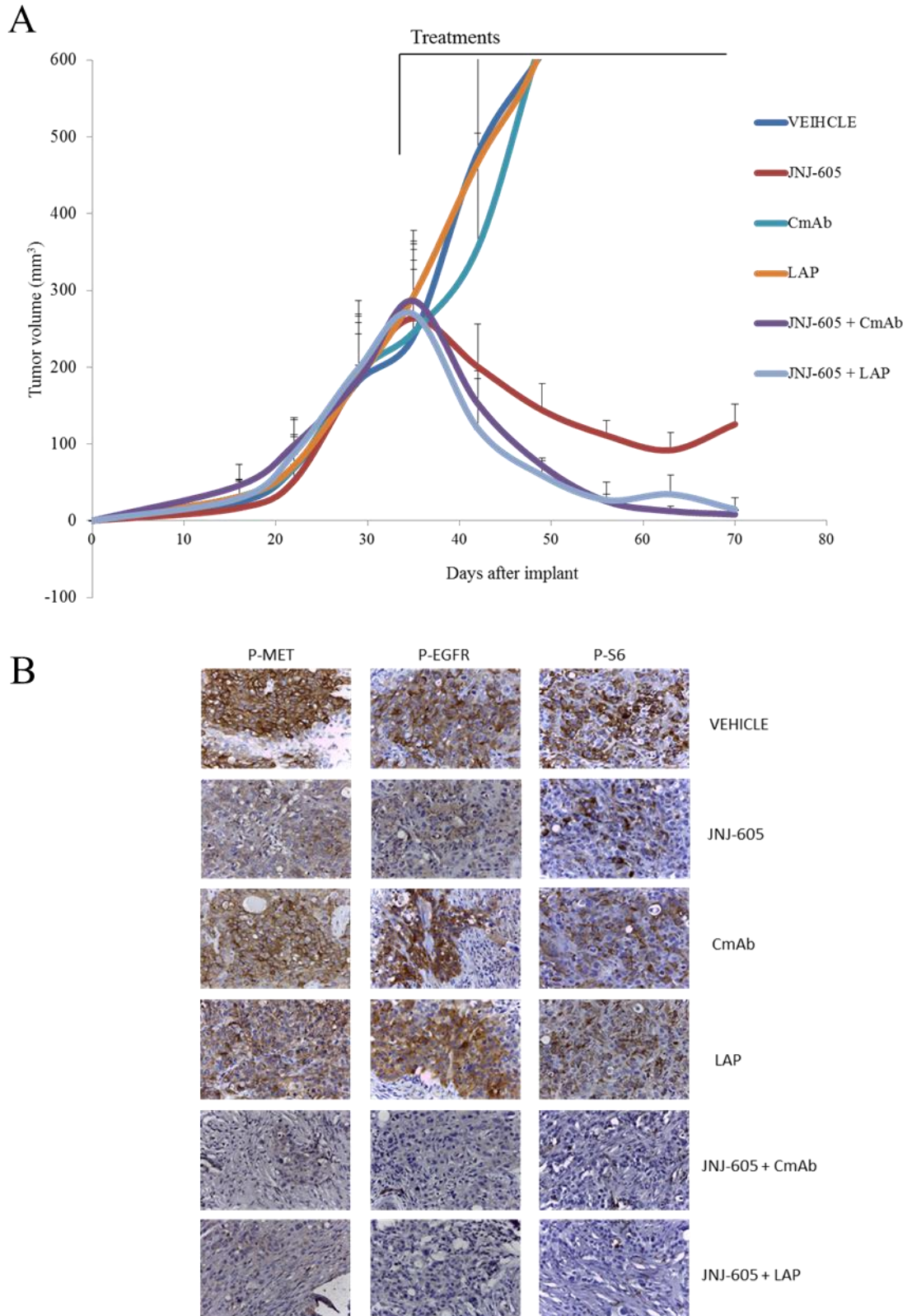


Figure 18- SG16 PDXs show a partial response to MET inhibitors, but a complete response to the combined anti-MET/EGFR treatments. A) SG16 tumors were subcutaneously implanted in NOD SCID mice; when the tumor reached a volume of approximately 250 mm³ the treatment was initiated with the following drugs: the anti-MET inhibitor JNJ-38877605 (JNJ-605); the anti-EGFR drugs Lapatinib (LAP) and Cetuximab (CmAb), alone or in combination, as indicated. The line indicates the day when treatment was started. N = 6 mice for each treatment arm. B) IHC analysis of tumors derived from the mice shown in A. The combined treatment with anti-MET and anti-EGFR drugs completely switched off MET, EGFR and the downstream transducers.

4.3.4 *In vivo* generation of a MET amplified xenopatient model resistant to the MET inhibitor JNJ-605.

After evaluating that the SG16 primary resistance to MET inhibition was due to EGFR activation, we further decided to generate *in vivo* models to study acquired resistance to MET inhibitors. We subcutaneously implanted SG16 tumors in NOD SCID mice and when the tumor reached the approximate volume of 250 mm³, we started a prolonged treatment with JNJ-605 or with a combination of the anti-MET drug and Cetuximab or Lapatinib. After three months we obtained three tumors resistant to JNJ-605 (SG16 RES JNJ), but no tumors resistant to the combination of anti-MET and anti-EGFR drugs (Figure 19). This demonstrates that the combined treatment was more effective not only in inducing a complete (as shown in figure18), but also a durable response.

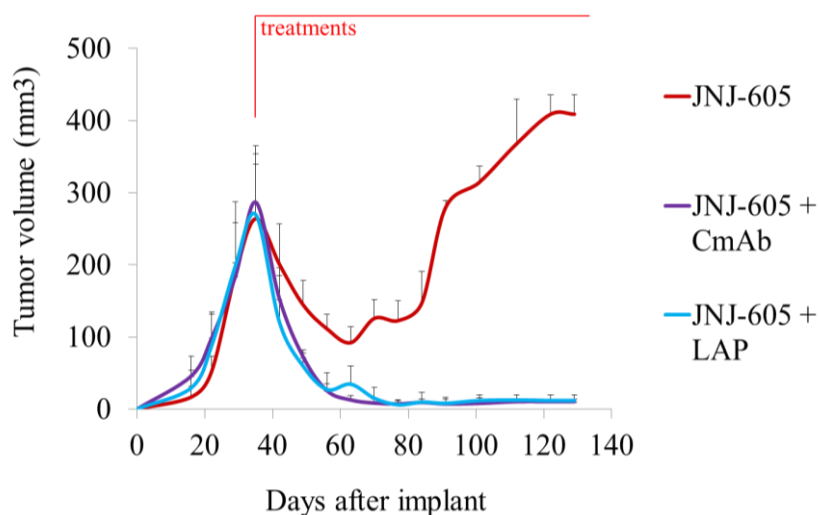


Figure 19 - Generation of SG16 tumors resistant to JNJ-605. Mice were subcutaneously implanted with SG16 tumors and when the tumor reached the approximate volume of 250 mm³ (red line) were treated for three months with the specific anti-MET inhibitor JNJ-38877605 (JNJ-605), alone or in combination with the anti-EGFR drugs cetuximab (CmAb) or lapatinib (LAP), as indicated. As shown, combined anti-MET/EGFR treatment prevented development of resistance.

We then analyzed the SG16 RES JNJ tumors. Since we demonstrated that in SG16 parental cells and tumor EGFR was involved in the primary resistance, we started analyzing if there were alteration in the copy number or expression level of the *EGFR* gene in resistant tumors. We performed a quantitative real time PCR and observed that EGFR was overexpressed (Figure 20A), but not amplified (data not shown) in resistant tumors, compared to parental ones. We confirmed the EGFR overexpression by IHC analysis in resistant SG16 tumors, suggesting that EGFR could be involved not only in the primary resistance, but also in acquired resistance to MET TKIs (Figure 20B). To investigate if the observed EGFR overexpression was involved in sustaining secondary resistance to JNJ-605, we treated SG16 RES JNJ tumors with Cetuximab to evaluate if it could

rescue the sensitivity to the anti-MET drug. Indeed, as shown in Figure 20C, we observed that the resistant tumors underwent a rapid and intense regression when the anti-EGFR mAb was added to the treatment with the MET inhibitor. The immunohistochemical analysis of SG16 RES JNJ tumors revealed that, in presence of JNJ-605, the residual phosphorylation of EGFR was higher in resistant tumors compared to parental tumors. Phosphorylation of EGFR and of its downstream effectors was completely abrogated only upon the combined treatment (Figure 20D).

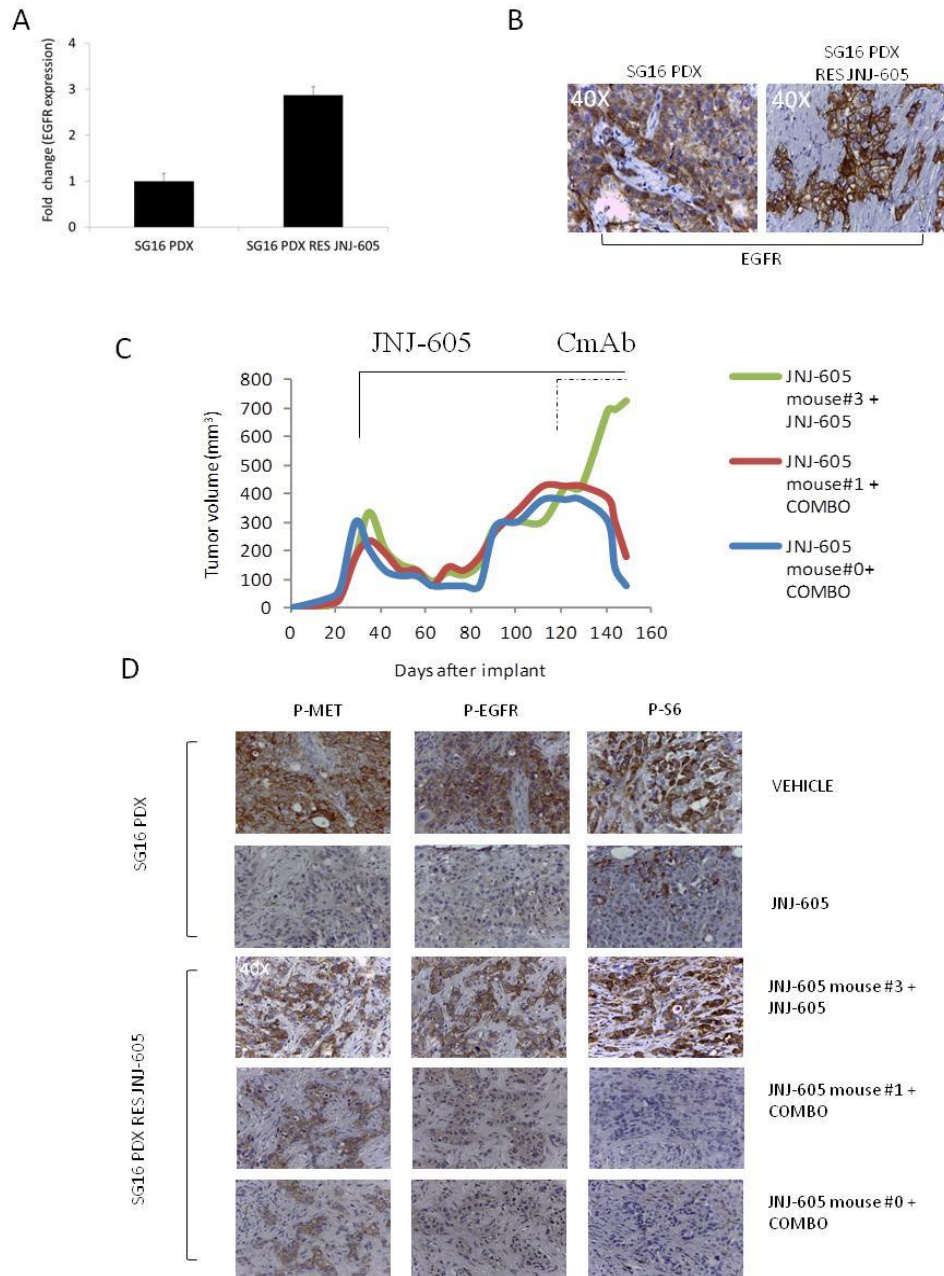


Figure 20 - EGFR is overexpressed and more phosphorylated in SG16 RES JNJ PDX than in the non-resistant parental cells. A) qRT-PCR analysis of EGFR expression in the JNJ-605-resistant PDX, compared to the original PDX. B) IHC analysis of EGFR expression. The analysis was performed after 100 days of treatment on the SG16 PDX and on the SG16 RES JNJ-605. C) Tumor growth curves of the 3 mice (mouse #0;#1;#3) that became resistant to JNJ-605 treatment (shown in Fig.19-Red line). The line indicates the treatment start. The dashed line indicates the day when combined treatment (COMBO= JNJ-605 +

cetuximab) of mice #0 and #1 was started. D) IHC analysis of tumors derived from the mice: SG16 parental PDX treated with vehicle and JNJ-605(SG16 PDX) and the SG16 PDX resistant to JNJ-605 (SG16 RES JNJ-605), treated with the anti-MET drug and with the combined treatment (COMBO= JNJ-605 + Cetuximab).

4.4 - KRAS PDX models

4.4.1 - KRAS amplified and mutated gastric tumors

The molecular characterization of our platform allowed us to identify PDX with KRAS alterations. From our routinely RT-PCR analyses performed on the 500 tumors, we identified KRAS amplification in 9 of them. Only 6 of these tumors engrafted, originating PDXs. (Table 3). To identify KRAS mutations, we performed next generation sequencing on DNA obtained by 100 PDXs; 12 of them presented KRAS mutations (Table 4). The presence of these mutations was then confirmed in the original tumors by Sanger sequencing (as mentioned in the Material and method section, due to economic reasons, only PDX DNAs underwent NGS analysis) . In this way, KRAS mutations account for 12% of our analyzed gastric PDXs, while KRAS gene amplifications 6%. The percentage of KRAS amplified and mutated models in the platform is quite similar to the one described in literature from studies performed in tumor patients, where the frequency of KRAS amplification in gastric tumors is around 5% and the highest percentage of KRAS mutations in studied cohorts is 21% (<http://cbioportal.org>) (204) .

CHAPTER IV - Results

Table 3 - KRAS mutated patients present in our PDX platform. The highlighted red tumors correspond to the models that were used in this work. N.A. = Not Available; heteroz= mutation in heretozigosis; homoz= mutation in homozygosis.

Code	Sex	Diagnosis	Age of diagnosis	Site	Subtype	STAGE	Tumor mutations (COSMIC or Frameshift (Fs); AF>0.3)	Tumor amplifications	PDX	KRAS mutation	Mutant Allele frequency
GTR0164	F	15/07/2015	72	Body	Intestinal	N.A.	FBXW7;PIK3CA; ARID1A (Fs); ARID2 (Fs);PDGFRA (Splice region)	NO AMPL	YES	G13D (heteroz)	0.45
GTR0213	N.A.	N.A.	N.A.	N.A.	N.A.	N.A.	CDH1; RB1;TP53; MTOR	NO AMPL	YES	A146T (heteroz)	0.47
GTR0245	M	05/04/2016	61	Antrum	Intestinal	N.A.	APC;ARID2;ERBB3; ERBB4;MSH6; APC (Fs); AXL (Fs)	NO AMPL	YES	G12D (homoz)	0.99
GTR0249	F	24/04/2016	84	Body	GIST	IB	CDKN2A; NOTCH4;PIK3CA; ERBB3; ARID1A (Fs); BRAF (Fs)	NO AMPL	YES	G12D (heteroz)	0.46
GTR0128	M	10/06/2015	74	Antrum	Intestinal	IIA	B2M;CTNNB1;LRP1 B;PIK3C; RNF43; ALK; ARID1A (Fs); ARID1B (Fs); PTEN (Fs)	FGFR3 (3 copies)	YES	A146T (heteroz)	0.44
GTR0141	F	26/07/2015	60	Body	Diffuse	N.A.	pdx DA METASTASIS;CCND1 ;FBXW7;IRF2;KIT;KRAS;MAP2K2;PIK3CA; ARID1A (Fs); ARID2 (Fs);PDGFRA (Splice region)	FGFR2 (5-8 copies)	YES	G13D (heteroz)	0.48
GTR0194	F	05/2015	59	Body	N.A.	N.A.	ELMO1;FAT4;KMT2; LRP1B;NOTCH3;PIK3CA;TP53; AXL (Fs); BRCA1 (Fs); FGFR4 (Fs)	NO AMPL	YES	G13D (heteroz)	0.52
GTR0202	N.A.	N.A.	N.A.	N.A.	N.A.	N.A.	FAT1;FGFR2;GNAS; KMT2D; PIK3R1; ARID1A (Fs)	NO AMPL	YES	G13D (heteroz)	0.66
GTR0207	M	10/12/2015	76	Cardia	N.A.	N.A.	CDKN2A; PARD3B; TP53;TP53; APC (Fs)	NO AMPL	YES	A146T (homoz)	0.75
GTR0220	M	01/01/2016	69	Antrum/ pylorus	Intestinal	IIIC	ARID2 (del)	NO AMPL	YES	c.11-5p>G NOVEL (heteroz)	0.38
SG54	F	18/02/2014	78	Fundus	Intestinal	IB	ARID1A; TP53	IGF1R (3 copies);EGFR (3 copies)	YES	G12D (heteroz)	0.47
SG26	M	09/07/2012	59	Gastro esophageal junction	Intestinal	IIB	SMO; KDM6A; MTOR	PDGFRB and MET (3 copies)	YES	G12D (heteroz)	0.34

Table 4 - KRAS amplified patients present in our PDX platform. The highlighted blue tumors correspond to the models that were used in this work. N.A. = Not Available.

Code	Sex	Diagnosis	Age of diagnosis	Site	Subtype	STAGE	Tumor mutations (COSMIC or Frameshift (Fs); AF>0.3)	Tumor amplifications	PDX	KRAS mutation
GTR0060	F	10/02/2015	76	Antrum/ pylorus	Diffuse	IIIB	TP53	KRAS (50 copies)	YES	NO
GTR0165	M	11/06/2015	76	Gastro esophageal junction	Intestinal	IIIB	FBXW7;SMAD4;TP53	KRAS (54 copies)	YES	NO
GTR0424	M	10/01/2017	69	Gastro esophageal junction	N.A.	IIB	N.A.	KRAS (90 copies)	YES	NO
GTR0004	M	01/10/2014	62	Antrum/ pylorus	N.A.	IV	N.A.	KRAS (45 copies)	NO	NO
GTR0232	N.A.	N.A.	N.A.	N.A.	N.A.	N.A.	N.A.	KRAS (9 copies)	NO	NO
GTR0237	M	02/03/2016	77	Gastric stump	Intestinal	IIA	N.A.	KRAS (22 copies); MET (4 copies)	NO	NO
GTR0244	M	04/2016	80	Antrum/pylorus	Diffuse	IIIB	N.A.	KRAS (36 copies)	YES	NO
SG12	M	2011	73	Antrum/pylorus	Intestinal	IIIA	ARID1A	KRAS (24 copies)	YES	NO
SG63	M	22/05/2014	77	Antrum/pylorus	Intestinal and diffuse	IIIC	CIC;ARID1A; PTEN (splice region)	KRAS (12 copies)	YES	NO

4.4.2 Characterization of KRAS mutated and amplified models

One of the main objectives of the GEA platform is to explore new targets for gastric cancer therapies. The existence of such a high amount of KRAS altered models in this platform prompted us to explore if KRAS amplification and mutation can drive the same type of biological responses.

From our cohort of 6 KRAS PDXs we also generated cells and organoids, to use them as *in vitro* models for pre-clinical trials. Among the twelve KRAS-mutated PDXs available in the platform, we selected 4 of them to be used in this work. Next generation sequencing (NGS) performed in our cohort of PDXs demonstrated that GTR245, GTR249, GTR213 and GTR164 presented mutations in the *KRAS* gene: i) in GTR245 PDX we detected a G12D mutation, with an allelic frequency of 0.99, indicating that it is present either in homozygosis; or in hemizygotosis ii) GTR249 PDX presented the same G12D mutation, but with an allelic frequency of 0.46, thus in heterozygosis; iii) GTR164 PDX displayed the G13D mutation with an allelic frequency of 0.52 (heterozygosis); iv) GTR213 PDX presented the A146T mutation with an allelic frequency of 0.47 (heterozygosis). This last mutation is quite rare in different cancer types but in our gastric cancer platform represents 3 % percent of KRAS mutations. All these mutations were confirmed by Sanger sequencing in the original tumor and in the PDX-derived cells. Interestingly, the sequencing performed in the original GTR245 tumor showed that the G12D mutation was not in homozygosis as in the PDX and in the cells but in heterozygosis. This fact can be due either to the contamination of human stroma that mislaid the amount of cells with the mutation or to the selection during PDX generation of more aggressive cells characterized by homozygous mutated KRAS in the tumor.

From the 6 models of PDX bearing *KRAS* amplification, we were able to generate three primary cell cultures: GTR60A, GTR165 and GTR424. *KRAS* overexpression/amplification was evaluated by immunohistochemistry on the PDX, and by quantitative real time PCR in the original tumor, PDX and PDX-derived cells (Figure 21B, D and E). Immunohistochemistry performed on the PDX demonstrated elevated levels of *KRAS* expression which correlated with the results obtained by qRT-PCR. As seen in the SG16 model, also in these models there was a significant difference of the levels of gene amplification observed by qPCR between the original tumor and PDXs; this can be explained either by the dilution of cancer DNA with normal DNA derived from human stromal cells or by a positive selection of cells bearing *KRAS* amplification. The first *KRAS* amplified model - GTR60 - is an interesting case within our platform. Similar to what happened for all the other tumors, two immunocompromised mice were implanted with tumor fragments derived from the original specimen and both engrafted. Surprisingly, the analysis of the genomic DNA extracted from each PDX revealed that the two mice developed two tumors different from the molecular point of view: GTR60A PDX carried *KRAS* amplification (50 copies; Figure 21B), while GTR60B showed *EGFR* amplification (100 copies). This can be explained on the basis of tumor heterogeneity, by hypothesizing the presence of two subpopulations of cells carrying the two different amplifications. This was indeed shown by a

double IHC staining of the original tumors that evidenced cells displaying either KRAS or EGFR overexpression/amplification. These two subclones could have been differentially selected in the two mice. For the purpose of our study, only GTR60A tumors were used for in vitro and in vivo experiments. Moreover, qRT-PCR analysis, demonstrated that PDX-derived cells maintained the KRAS amplification (Figure 21B). Regarding the GTR165 PDX, we detected 54 KRAS copies. The level of *KRAS* amplification slightly decreased in the derived cells (40 copies; Figure 21D). The PDX bearing the highest number of *KRAS* copies was GTR424, which presented 56 *KRAS* copies in the original tumor (Figure 21F). The passage in mouse and lately in culture, positively selected the cells with *KRAS* amplification as the number of copies was 90 and 160, respectively.

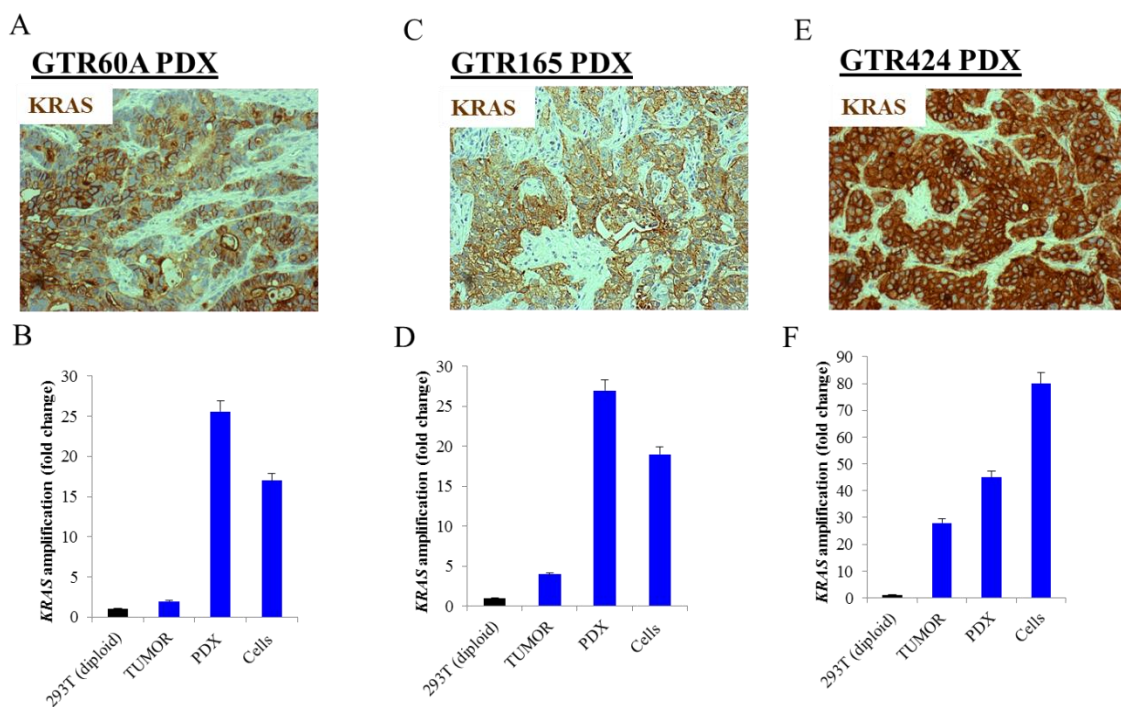


Figure 21 - *KRAS* amplification present in the original tumor was maintained in the PDX and PDX-derived cells. A, C, E) Immunohistochemistry analysis demonstrated high levels of *KRAS* expression in tumors derived from PDX. B, D, F) Quantitative real time PCR analysis performed using DNA extracted from the original tumor, PDX and PDX-derived cells demonstrated that *KRAS* gene amplification was maintained during the different passages. DNA extracted from 293T diploid cells was used as a control. *RNAseP* and *GREB1* were used as housekeeping genes. These two genes are located in different chromosomes. Error bars represent SD.

4.4.3 - RAS activation state in *KRAS* mutated and amplified cells

In order to evaluate the activation state of RAS in *KRAS* amplified and mutated cells we have performed a RAS-GTP pull down, that is based on the use of a GST fusion protein containing the isolated Raf-1 RAS-binding domain (GST-Raf-RBD). The Raf-RBD sequence binds preferentially to activated, GTP-bound RAS. We observed that in the mutated cells, the RAS-GTP/RAS ratio (evaluating the specific activity of RAS), was higher than in *KRAS*

amplified cells. Interestingly, we observed that in the GTR245 cells, where a homozygous G12D mutation is present, KRAS was more active than in GTR249 cells that carry the same mutation in heterozygosis. This suggests that the existence of two mutated alleles leads to a higher specific KRAS activity (Figure 22A,B). KRAS activation state of GTR213 cells, mutated for A146T in heterozygosis, was very similar to that of cells mutated for G12D. This is very interesting as not much is known about this mutated form of KRAS which is quite rare in other tumors. Unexpectedly, mutated RAS protein is generally more active compared to the amplified cells, with the exception of the GTR164 model (bearing a mutation in G13D in heterozygosis) which showed a lower level of activation. As expected, the specific KRAS activity in the *KRAS* amplified cells was inferior to that of the mutated cells.

In order to explore which is the total amount of active KRAS in mutated *vs* amplified cell lines, the level of RAS-GTP was normalized to the total amount of protein loaded. Since we are comparing different cells, from completely different tumors, three housekeepers (HSP70, β -actin and vinculin) were evaluated and quantified, in order to avoid major errors. Interestingly, the total amount of active KRAS present in the cells was greater in KRAS amplified cells compared to KRAS mutated ones, with the exception of GTR245 that demonstrated levels of activation similar to amplified models. These results demonstrate that, in spite of the fact that RAS *per se* is less active in *KRAS* amplified cells, the enormous KRAS expression (due to gene copy number amplification) renders the KRAS pathway more active (Figure 22C). This observation suggests that amplified KRAS can play a driving role in these tumors.

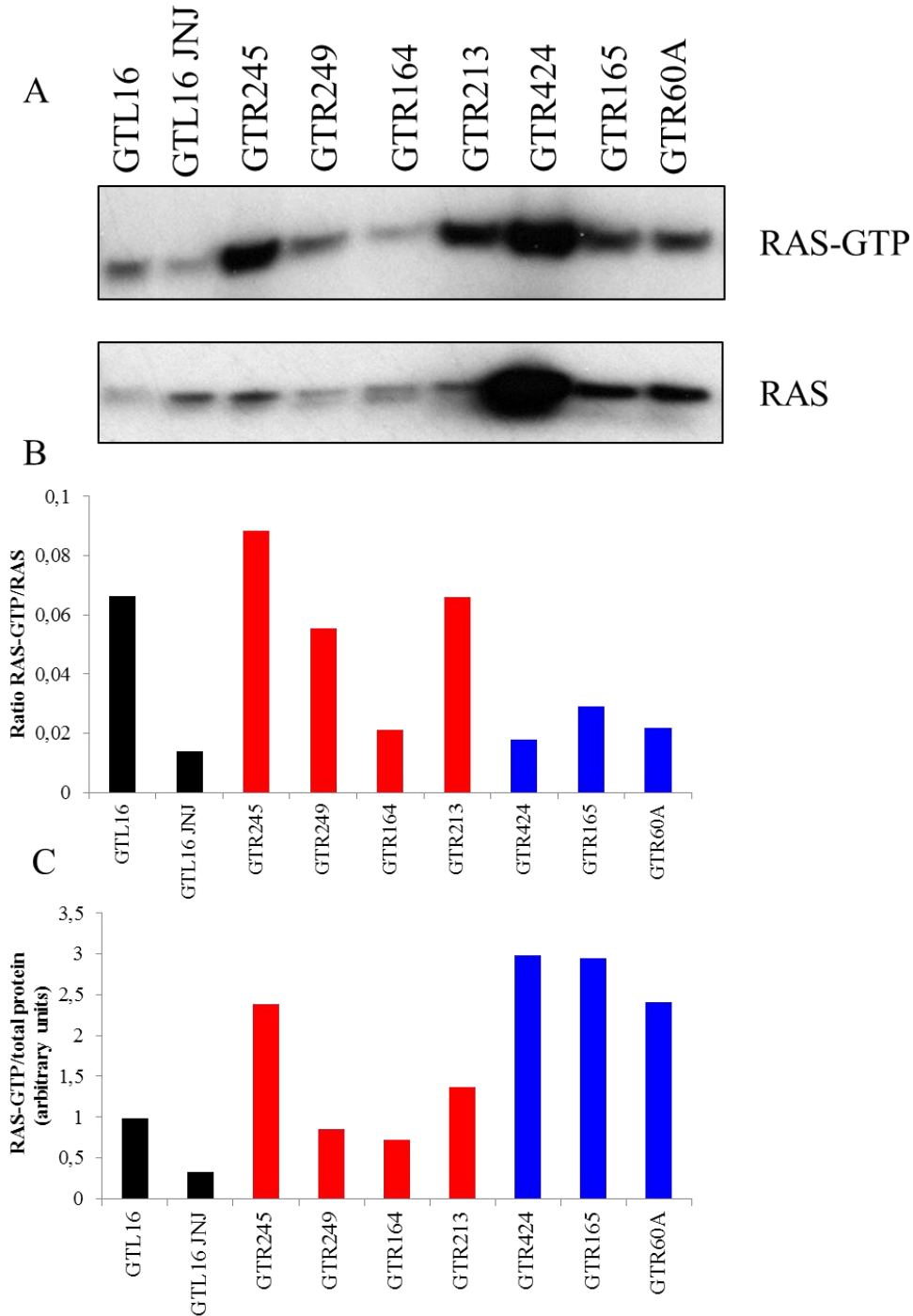


Figure 22 - KRAS mutated models display higher RAS specific activity while KRAS amplified models show more total active RAS. A) Western blot analysis, B) quantification of RAS specific activity and C) RAS total activity was performed in GTR245, GTR249, GTR164, GTR213. Western blot quantification of RAS-GTP, RAS total and housekeepers (HSP70, β -actin and vinculin) was performed. GTL16 was used as positive control and GTL16 treated with JNJ-605 was used as negative control. Blots have been probed with the indicated antibodies. Protein quantification was performed using Image J software.

4.4.4 – Changes in glycolytic metabolism in *KRAS* mutated and amplified *in vitro* models

Previous studies demonstrated that *KRAS* mutated tumors present specific metabolic changes that are required for their maintenance and aggressiveness. Some of these changes are related with increase glucose uptake (192) and a shift in glutamine metabolism (193) (194) (195). Additionally, more recently, it was described in lung cancer models that these changes can be inflated depending on the *KRAS* mutated allele copy number (288). To explore if these changes can also occur in gastric cancer *KRAS* mutated cell models as well as whether *KRAS* amplification is characterized by similar changes, the metabolic activity of GTR245, GTR249, GTR164, GTR213 and GTR165, GTR424 was evaluated.

The glucose transporter 1 (GLUT1), monocarboxylate transporter 4 (MCT4), hexokinase II (HKII) and pyruvate kinase M2 (PKM2), are respectively transporters and glycolytic enzymes that are usually increased following the glycolytic shift. Western blot analysis of our *KRAS* mutated and amplified cells demonstrated that the glycolytic markers were significantly increased in the GTR245 model when compared with the cell line bearing the same mutation, G12D, but in heterozygosis, as well as when compared with other *KRAS* mutated and amplified models (Figure 23A). Additional experiments are required including cells without *KRAS* amplification or mutation, as controls.

In an aerobic metabolism, the final product of glycolysis is pyruvate, however when glycolysis is not followed by Krebs cycle (for example in anoxic conditions), lactate is the final product. In this way, lactate production is an indicator that cells are not performing oxidative metabolism but instead are regenerating the NAD⁺ pool through lactate dehydrogenase. In order to evaluate the glycolytic state of the cells, lactate production and uptake was evaluated. After 48h of culture, cell supernatant was collected and upon lactate quantification it was observed that the GTR245 present higher levels of lactate in the medium compared with the other models (Figure 23B), while the lactate uptake was inversely proportional (Figure 23C). The *KRAS* amplified models showed similar level of glycolytic markers and lactate production/uptake relatively to the *KRAS* mutated cells in heterozygosis.

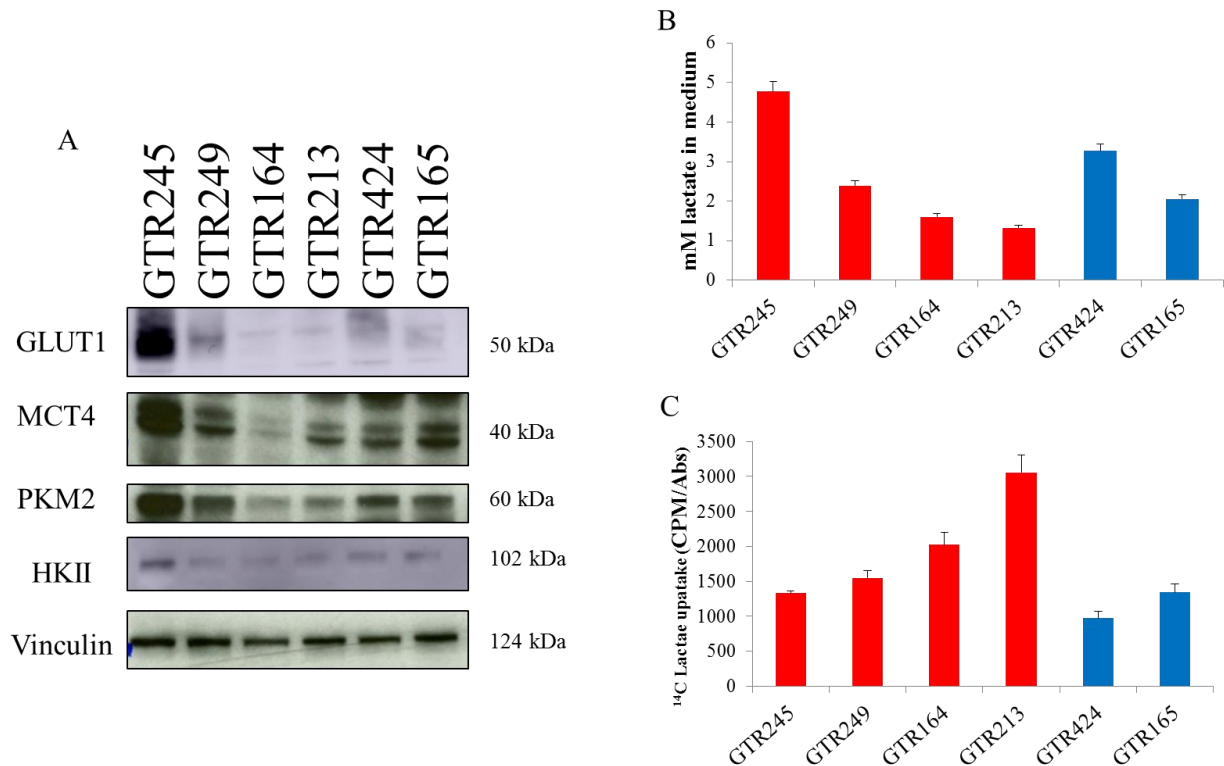


Figure 23 - GTR245 cells show increased levels of glycolytic markers as well as major release of lactate in the medium. A) Glucose transporters 1 (GLUT1), monocarboxylate transporter 4 (MCT4), hexokinase II (HKII) and pyruvate kinase M2 (PKM2) protein expression was evaluated by western blot in GTR245, GTR249, GTR164, GTR213, GTR424 and GTR165 cells. B) The quantity of lactate present in the cell medium was quantified after 48h of cell culture; C) Lactate uptake was also evaluated using radioactive [U-¹⁴C] lactate. Western blots were probed with the indicated antibodies. Vinculin was used as loading control

4.4.5 - KRAS mutated and amplified models are addicted to KRAS

Cancer cells growth and survival can often be impaired by the inactivation of a single oncogene. In order to explore if *KRAS* can be a target in gastric cancer *KRAS* altered models, we evaluated if cells presenting *KRAS* mutation or amplification were addicted to *KRAS*. For this purpose, two of our mutated cell models, GTR245 and GTR213 were transduced with a short hairpin RNA (shRNA) to silence *KRAS*. After overnight transduction, cells were harvested and plated for evaluation of cell viability, protein and RNA expression. After 72h, cell viability was measured and a significant decrease in cell viability was observed in all the cells lines used (Figure 24A,D). To control silencing efficacy, *KRAS* gene and protein expression was evaluated by qPCR and western blot, respectively. As it can be observed in the graphics below (Figure 24B, C, E,F) *KRAS* expression was effectively abrogated upon *KRAS* gene silencing. These results indicate that, as expected, the growth and survival of GTR245 and GTR213 mutated *KRAS* cells is dependent on *KRAS* expression, indicating that cells are addicted to this gene and that its inhibition could lead to a therapeutic response.

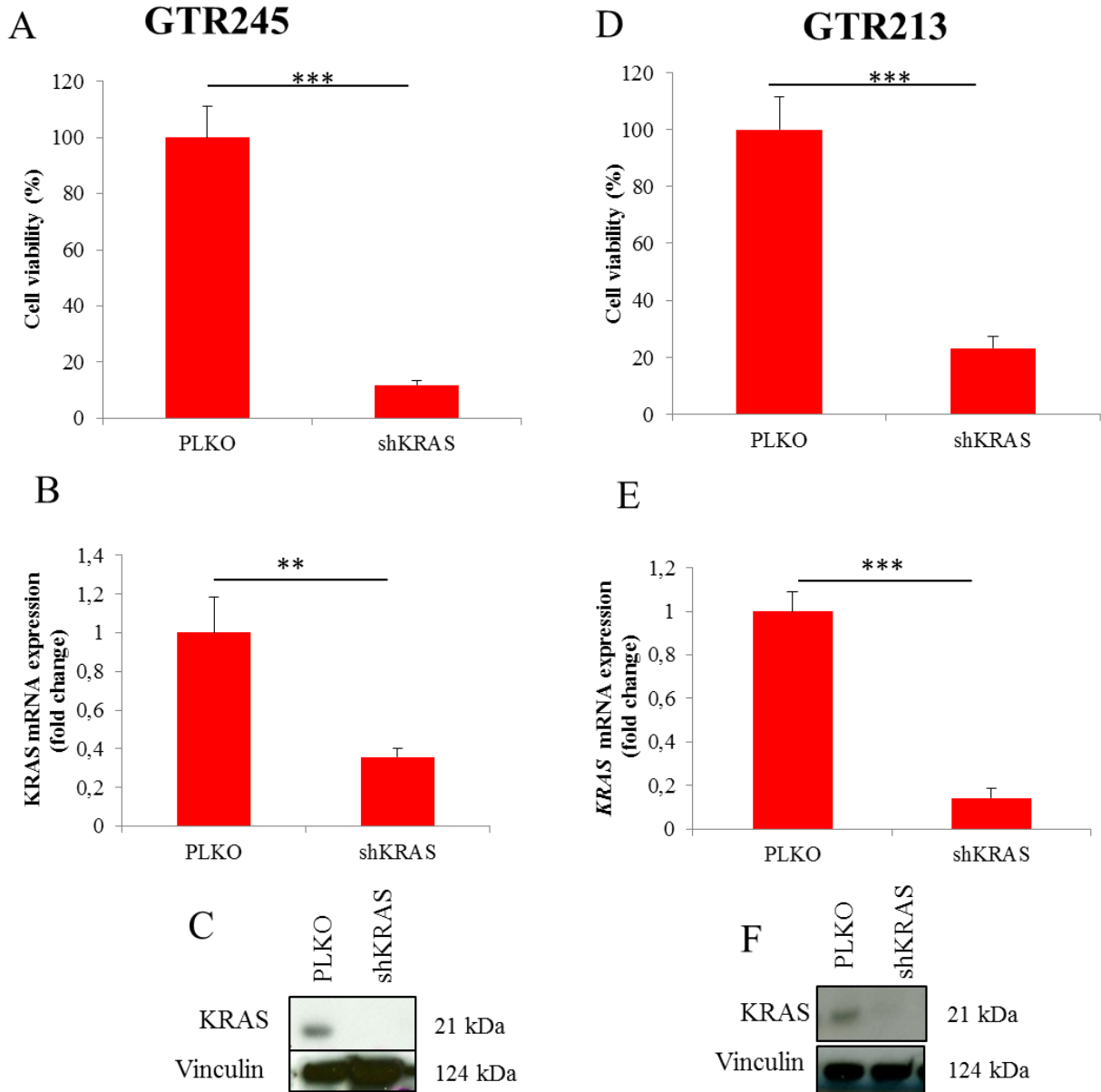


Figure 24 - GTR245 and GTR213 cells are addicted to the *KRAS* oncogene. A, D) Upon transfection GTR245 and GTR213 cell viability was measured using CellTiter Glo after 72h. B, E) *KRAS* gene expression was quantified by qRT-PCR, after 72h; C, F) Western blot analysis was performed to evaluate *KRAS* protein expression. Blots have been probed with the indicated antibodies. Vinculin was used as loading control. shPLKO was used as negative control. Statistical significance is indicated **<0.01; ***<0.001. Error bars represent SD.

Not much is known about the role of amplified WT *KRAS* in tumor cells. To explore if GTR60A, GTR165 and GTR424 are also addicted to *KRAS*, these cells were transfected using a small interfering RNA (siRNA) specific for *KRAS*. Cells were transfected overnight and after 72h cell viability was evaluated. In all the three cell lines *KRAS* gene expression was significantly decreased, compared with control (SicC) and cell viability was decreased as well (Figure 25). These results demonstrate that *KRAS* amplified cells are addicted to the *KRAS* gene.

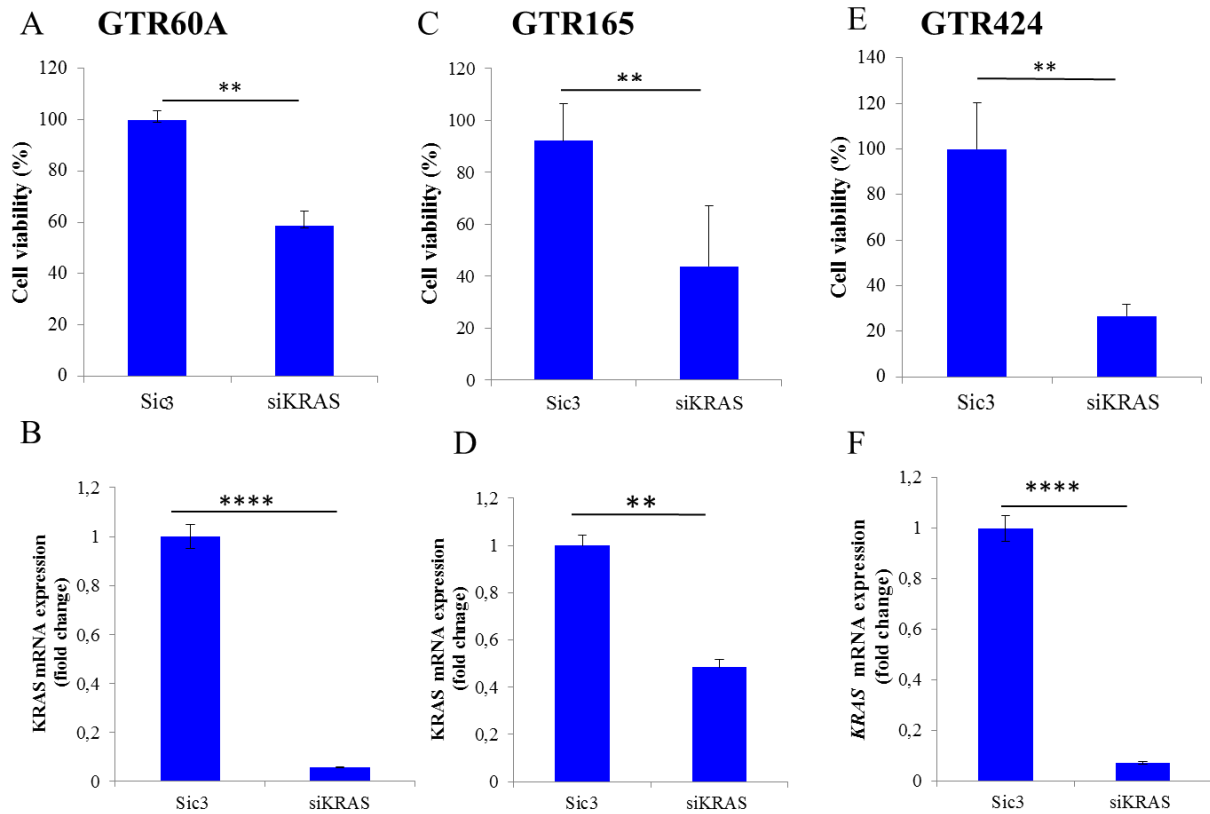


Figure 25 - GTR60A, GTR165 and GTR424 *KRAS* amplified cells are addicted to *KRAS*. A, C, E) 72h upon *KRAS* silencing GTR60A, GTR165 and GTR424 viability was measured using cellTiter Glo . B, D, F) *KRAS* gene expression was quantified by qPCR, 72h after silencing. Sic3 (siRNA control) was used as negative control. Statistical significance is indicated **<0,01; ***<0,001; ****<0,0001. Error bars represent SD.

4.4.6 - *In vitro* response to *KRAS* downstream inhibitors of *KRAS* mutated and amplified models

To date, no drug that can inhibit oncogenic *KRAS* has been approved by FDA. *KRAS* activation drives downstream pathways, such as RAF/MEK/ERK and PI3K/AKT/mTOR pathways, which play an important role in cell proliferation and survival (129) (130). Taking into consideration the fact that both *KRAS* mutated and amplified cells are addicted to *KRAS*, we explored if they were sensible to inhibitors of the *KRAS* pathway (MEK, AKT and mTOR inhibitors). In addition to these inhibitors, in our experiments we also used Olaparib –a PARP inhibitor-, based on the evidences that PARP and MEK inhibitors can synergize in RAS mutant tumors (289). GTR165 and GTR424 (*KRAS* amplified), GTR245 and GTR213 (*KRAS* mutated) cells were treated with i) Trametinib, a dual MEK inhibitor; ii) MK-2206, an AKT inhibitor; Everolimus, a mTOR inhibitor; OSI-027, a dual mTORC1/2 inhibitor; olaparib, a PARP inhibitor. After 96 hours of treatment, cell viability was evaluated. While treatment with Trametinib alone led to a significant decrease in cell viability in both amplified (Figure 26A,B)

and mutated models (Figure 26C,D), AKT and mTOR inhibitors determined only a small impairment of cell growth, Moreover, the combo treatment with Trametinib + AKT or mTOR inhibitors resulted in significant reduction in cell viability of KRAS altered cells. These data suggest that *KRAS* mutated and amplified cells similarly depend on KRAS pathway activation.

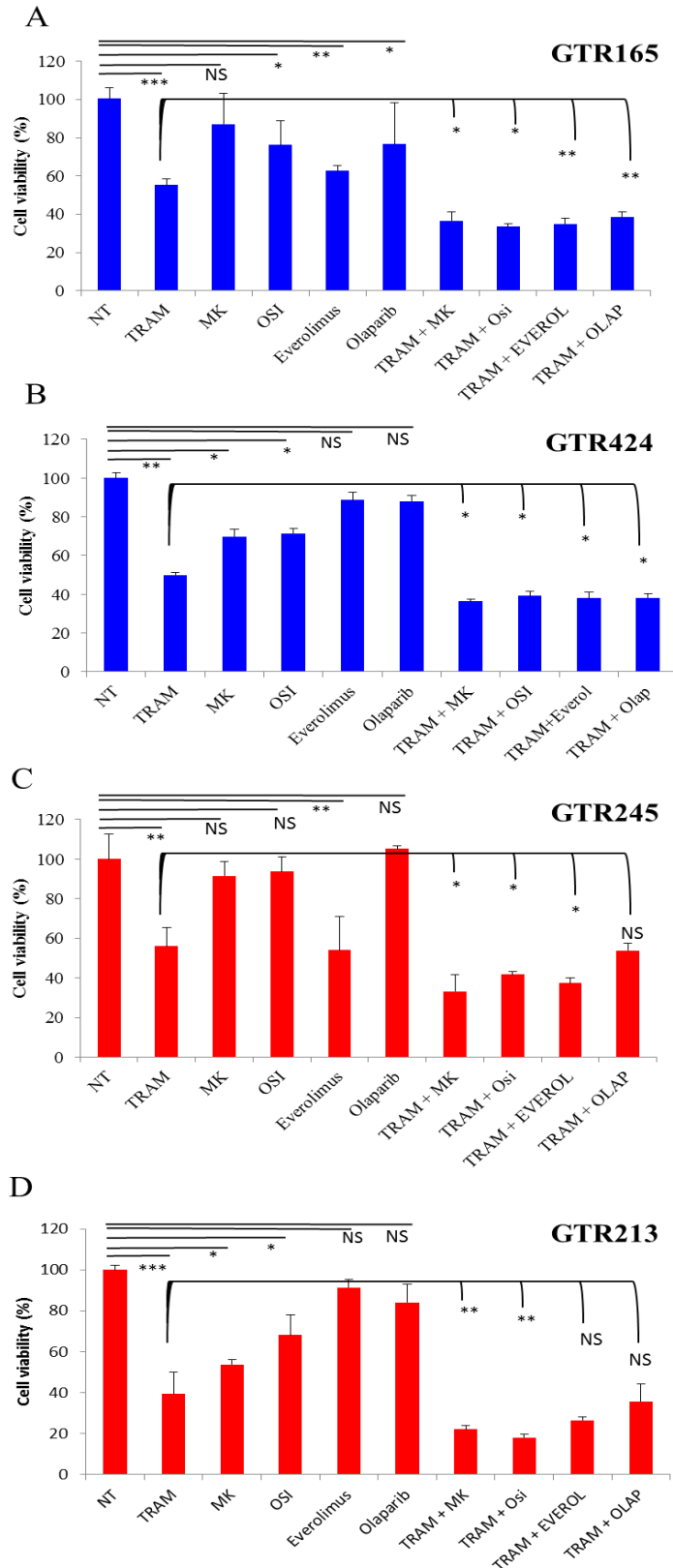


Figure 26 - KRAS amplified and mutated cells respond to KRAS downstream pathway inhibition. A) GTR165, B) GTR424, C) GTR245 and D) GTR213 cell viability was evaluated by CellTiter Glo after 96h of treatment with Trametinib (TRAM=5 nM); MK-2206 (MK=1 μ M); OSI-027 (OSI=250 nM); Everolimus (Everol=25 nM) and Olaparib (Olap=3 μ M). Statistical significance is indicated NS: not significant; *<0,05; **<0,01; ***<0,001.

On the same cells we also performed biochemical analyses after 96h treatment with the Trametinib, MK-2206, OSI-027, Everolimus and Olaparib. Regarding the GTR424 (KRAS amplified) model, single treatments with AKT, mTOR and PARP inhibitors did not change the MAPK phosphorylation, but led to a decrease in AKT phosphorylation. On the other side, single treatment with Trametinib showed a significant decrease in MAPK phosphorylation, but not of AKT. AKT activation was decreased to the untreated basal levels when cells were treated with the combo Trametinib + MK-2206 or Trametinib + Everolimus (Figure 27A). In turn, in the GTR245 (KRAS mutated) model, treatment with Trametinib alone or in combination with the other inhibitors only partially inhibited MAPK activation (Figure 27B). Similar to what was observed in the GTR424 cells, also in the GTR245 mutated model Trametinib (alone or in combination with MK-2206) did not inhibit AKT activation.

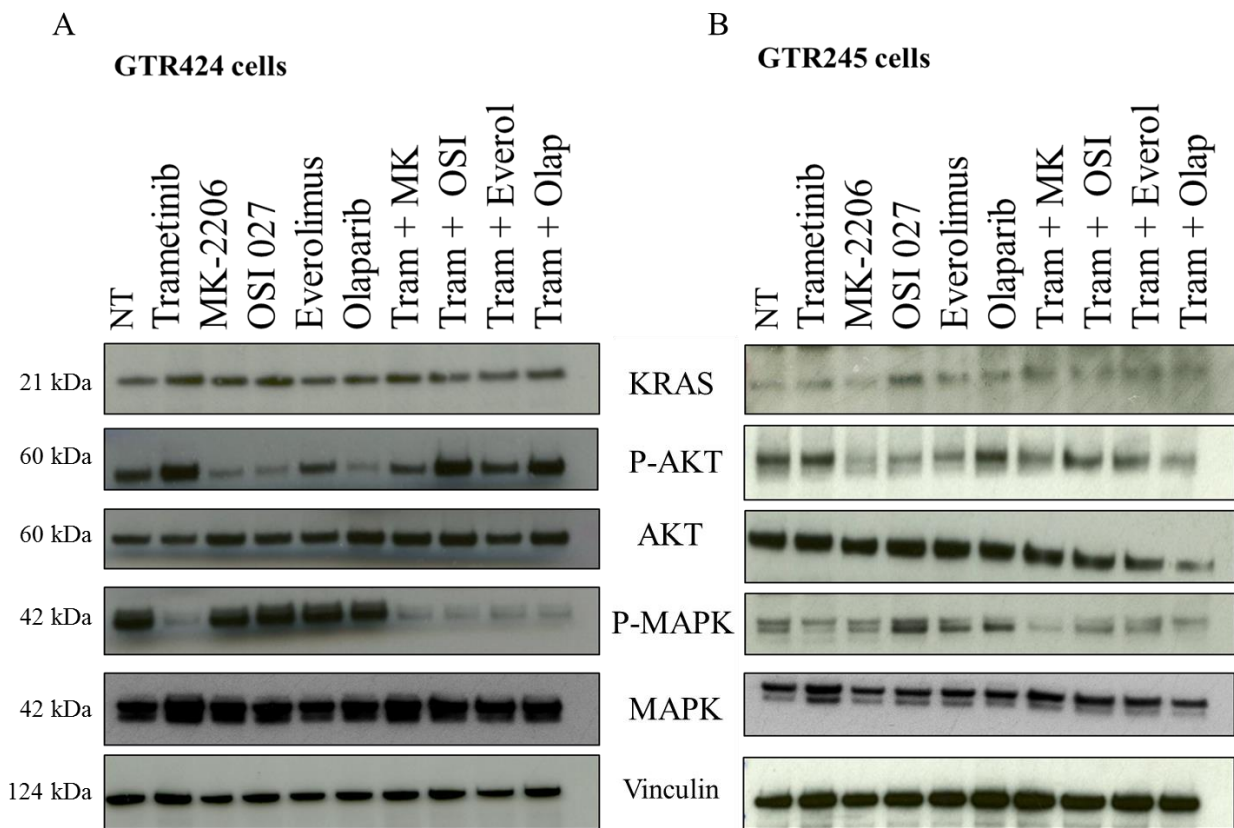


Figure 27 - MEK inhibition together with AKT or mTOR inhibition decreases MAPK activation in KRAS amplified and mutated cells. Western blot analysis was performed in GTR424 and GTR245 cells after 96h of treatment with the indicated drugs. Western blots were probed with the indicated antibodies. Vinculin was used as loading control.

4.4.7 - KRAS mutated model *in vivo* response to KRAS downstream inhibitors

To validate the results obtained *in vitro*, we performed an *in vivo* preclinical trial on PDXs. GTR245 tumors were randomized in 8 independent treatment cohorts: (i) vehicle (placebo); (ii) Trametinib (1 mg, daily, os); (iii) MK-2206 (2 mg, 3 times per week), (iv)

Everolimus (0.12 mg, daily, os), (v) Olaparib; (vi) Trametinib and MK, (vii) Trametinib and Everolimus, and (viii) Trametinib and Olaparib (1 mg, daily, os). As shown in Figure 28A, the single treatment with Trametinib and Everolimus and their combinations led to a delay in tumor growth while single treatments with MK-2206 and Olaparib were ineffective. The effects of the single *in vivo* treatments thus recapitulated those obtained *in vitro*; however, the combos *in vitro* induced a stronger inhibitory effect.

At the end of the trial the mice were sacrificed and the blood was collected for analysis, in order to evaluate possible toxic effects of the above indicated treatments. Results from blood analysis (Table 5) demonstrated that both the single treatments and the combinations did not induce hepatic damage, since in general, the levels of aspartate aminotransferase and total bilirubin detected in the blood of treated mice were not statistically higher from the levels of the vehicles.

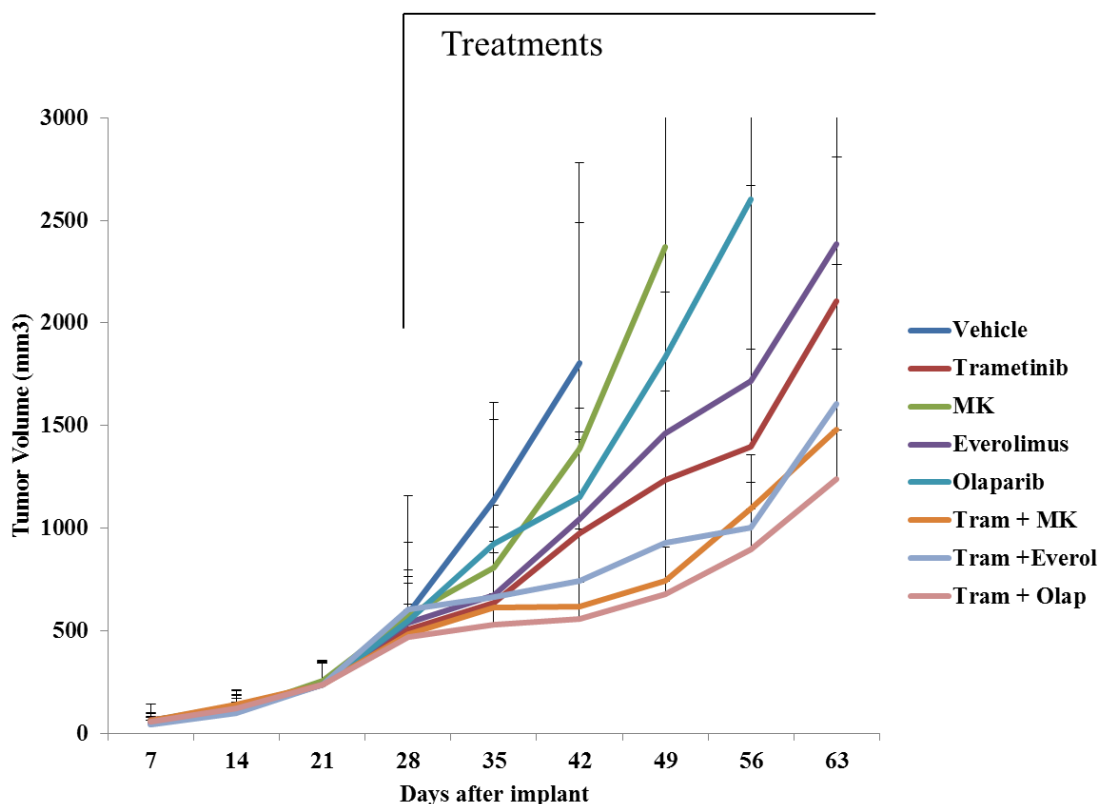


Figure 28 - GTR245: response to KRAS downstream inhibitors *in vivo*. A) GTR245 tumors were subcutaneously implanted in NOD SCID mice; when the tumor reached a volume of approximately 250 mm³ the treatment was started with the indicated drugs: the MEK1/2 inhibitor Trametinib (Tram; 1 mg, daily, os); the AKT1/2 inhibitor MK-2206 (MK; 2 mg, 3 times per week, os); the mTOR inhibitor Everolimus (Everol; 0.12 mg, daily, os) and the PARP inhibitor Olaparib (1 mg, daily, os), alone or in combination. The line indicates the day when treatments were started. N = 6 mice for each treatment arm. Error bars represent SD

CHAPTER IV - Results

Table 5 – Evaluation of Liver function following drug treatments. Blood was collected from the animals submitted to the treatments and aspartate aminotransferase and total bilirubin, two biomarkers of liver function were evaluated. Results are presented as mean ± SD. Statistical significance is indicated NS: not significative; *<0,05, comparing the different treatment values with the vehicle values.

Exerimental group (n=6)	Aspartate aminotransferase (U/L)	Bilirubin total (mg/dl)	
Vehicle	18,6 (±4,028)	0,013 (±0,01)	mean ± SD
	1	1	<i>P</i>
Trametinib	24 (± 7)	0,023 (±0,012)	mean ± SD
	0,33 NS	0,17 NS	<i>P</i>
MK-2206	16,8 (± 1,72)	0,012 (±0,004)	mean ± SD
	0,41 NS	0,75 NS	<i>P</i>
Everolimus	19 (± 3)	0,016 (± 0,001)	mean ± SD
	0,90 NS	0,44 NS	<i>P</i>
Olaparib	19,5 (± 6)	0,026 (± 0,007)	mean ± SD
	0,84 NS	0,04 *	<i>P</i>
Tram + MK	17 (± 2)	0,018 (± 0,0075)	mean ± SD
	0,47 NS	0,37 NS	<i>P</i>
Tram + Everol	16,8 (± 3,2)	0,015 (± 0,0077)	mean ± SD
	0,44	0,73	<i>P</i>
Tram + Olap	18,8 (± 4)	0,022 (± 0,009)	mean ± SD
	0,95	0,14	<i>P</i>

Immunohistochemical analysis performed on the tumors showed that all the single treatments were able to decrease the phosphorylation of the downstream effector S6K. This effect was more accentuated in tumors treated with the combinations (Figure 29). However, even if the S6K pathway was inactive, tumor growth was just partially slowed down, which suggests that other pathways responsible for cell survival were still active.

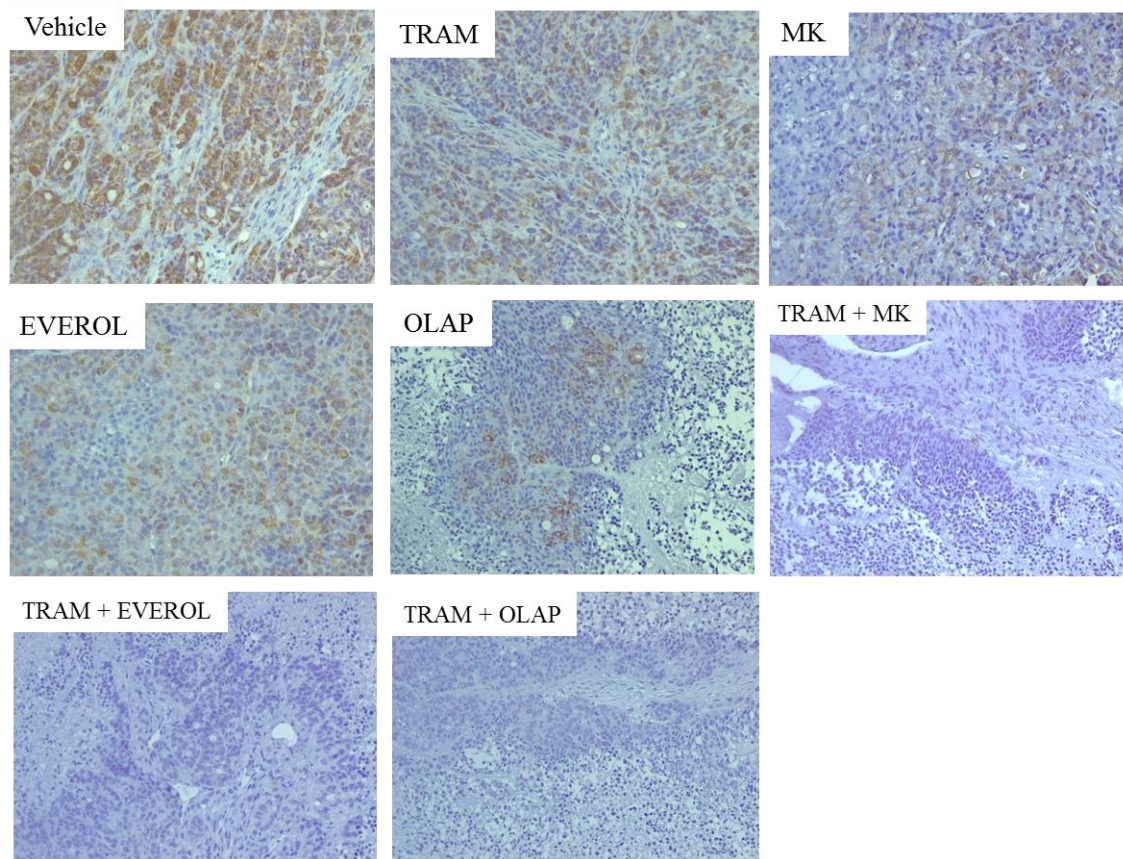


Figure 29 - Combinational drug treatment in GTR245 tumors led to inactivation of the downstream effector P-S6. IHC analysis of tumors treated for two days with the following drugs: the MEK1/2 inhibitor Trametinib (Tram); the AKT1/2 inhibitor MK-2206 (MK); the mTOR inhibitor Everolimus (Everol) and PARP inhibitor Olaparib, alone or in combination, as indicated. While the single treatments led to a decrease in phosphorylation of the downstream effector P-S6, only the combinational treatment was able to switch off the pathway. 6 mice were used per group.

CHAPTER V

DISCUSSION

5- Discussion

In this study we aimed to isolate and characterize *in vivo* and *in vitro* preclinical models of gastroesophageal cancer as well as to explore their response to potential target therapies, taking advantage of the gastroesophageal annotated platform generated in our lab.

In the last decade, the use of PDX platforms has been widely exploited in the field of cancer research (290). In fact, PDX models usually retain the histologic and genetic features of the original tumor and have been shown to be predictive of clinical outcome (214). These features made PDXs a widely successful tool to be used in preclinical trials to evaluate drug response and to identify biomarkers and novel therapeutic targets. In our PDX platform 30% of gastroesophageal tumors received from several hospitals of north Italy and subcutaneously transplanted into NOD/SCID mice, were successfully established. The percentage of successful engraftment as well as the period of latency of engraftment, that in our case was 73 days, were consistent with previous studies of PDX models using surgical tissues of gastric cancer (291) (292), where the success rate was between 24 and 34% and the period of latency was of 65 – 94 days. After establishment, our PDX models could be serially passaged to maintain tumors *in vivo* and could be frozen and thawed maintaining all their growth characteristics.

The generation of the PDX platform made possible to evaluate specific parameters that can influence gastro-esophageal tumor engraftment in NOD/SCID mice. Patients characteristics such as age, gender or neoadjuvant chemotherapy did not correlate with the engraftment success. However, Lauren classification was shown to be related with a different grafting, since tumors classified as intestinal experimented a better engraftment than those of diffuse type or the ones with signet ring morphology. The diffuse type of gastric cancer was also correlated with low success rate in another report involving a platform of gastro-esophageal PDXs (292). The low engraftment of these types of tumors can be explained by the limited number of tumor cells per unit area, since tumor cells are dispersed into the stromal tissue, making it a detrimental factor for successful engraftment. MSI, EBV status and gene amplifications remained stable between primary and PDX samples. The maintenance of the molecular characteristics was also reported in other studies involving gastro-esophageal PDX platforms (291) (292) though it has been described that some molecular lesions, such as HER2 positivity, can be lost during the passage in mice (291). The conservation of the architecture of original tumors as well as of their molecular lesions is essential for evaluation of drugs response in these preclinical models. Few studies have evaluated the relationship between preclinical models and clinical outcomes in gastric cancer (291). Nevertheless, when five gastro-esophageal PDX were treated with the same drugs as the

paired patients, the results demonstrated that four out of five PDX models had comparable therapeutic responses. The failure of the fifth case seemed to be explained by the change in Lauren classification during the passage in mice.

The generation of PDX-derived primary cell cultures and organoids within our platform presented a significant success rate. These models maintained the molecular and biological features of the PDX of origin, demonstrating that they can be successfully used as pre-clinical models. As an additional *in vitro* model, in this study, we aimed to identify, isolate and characterize the CSCs population based on functional selections *in vivo* and *in vitro*. While GCSCs isolation is mainly performed starting from already established gastric cancer cell lines (293), in this work we directly isolated cancer stem-like cell population from PDXs. In this way, we were able to mimic the native status of the patient tumor cells, having more heterogeneity of the tumor cell population. Moreover, since selecting the cells based on putative markers could be biased, since no consensus has yet been reached regarding specific gastric cancer stem cell markers (294), our GC stem cell populations were isolated and enriched by functional selection through sphere cultures *in vitro* and tumor growth *in vivo*. Indeed, we found that the stem-like cell populations grown under sphere conditions (SG16, GTR10 and GTR165) displayed upregulation of a panel of stem-cell related genes. This panel included *ALDH*, *NANOG*, *OCT4* and *SOX2*. *NANOG*, *OCT4* and *SOX2* are well known embryonic stem cell factors essential for pluripotency and self-renewal; similarly, they were also found overexpressed in many cancers, and correlated with histological grade and survival of the patients (295) (296) (297) (298). *ALDH* was recently identified as a potential marker for gastric cancer stem cells (271). Interestingly, two of the three isolated spheres maintained the molecular alterations present in the original tumor, such as *KRAS* and *MET* amplification. The fact that cells with stem-like features present the molecular lesions known to be responsible for tumorigenesis supports the hypothesis that targeting of these lesions can impact on tumor growth. The ability of xenospheres to retain the molecular and histological proprieties of the original tumor was previously described in xenospheres isolated from colorectal PDX-tumors (299). Additionally, in our study, *MET* amplified SG16 spheres, not only maintained the characteristics of the tumor and PDX but were also responsive to *MET* inhibition, as reported for CRC xenospheres harboring *EGFR* amplification which recapitulate the response to Cetuximab treatments observed in the patients from which they derived (299).

The xenosphere model bearing *MET* amplification (SG16 spheres) was isolated from a PDX derived from a *MET*-amplified gastroesophageal cancer. This *MET* amplified model showed to be partially resistant to *MET* inhibition, since even in the presence of more than 26

MET gene copies (a condition that many experimental models have shown to be typical of oncogene addiction) (300) (301) (302), in the absence of amplification of other RTKs or of KRAS mutation/amplification, MET inhibition induced only a partial response, that was shortly followed by relapse. However, treatment with a combined anti-MET/anti-EGFR therapy resulted in a durable, complete response and prevented the onset of resistance, explained by the increased EGFR expression acquired by the resistant tumors. As already described in the literature, the activation of EGFR is particularly frequent in acquired resistance to MET inhibitors (108) (287) (303), and it usually results in maintenance of downstream PI3K-AKT and MEK-ERK signaling in the presence of the MET inhibitor (287) (304). Several studies have shown the presence of a biochemical and functional interaction between MET and the HER family of RTKs (305) (306) (307) (308). In EGFR-mutant, non-small cell lung cancer patients, MET amplification is involved in both *de novo* and acquired resistance to Gefitinib, and pharmacologic inhibition of MET was proven to be able to restore sensitivity to Gefitinib (309) (310). Additionally, our laboratory and collaborators have shown that in MET-addicted gastric cancer cell lines, activation of HER family members contributes to overwhelm MET inhibition (287) (304), demonstrating an increased cell viability *in vitro*, and recovering tumorigenicity *in vivo*. Since MET and HER family share some of their downstream signaling pathways (311) (312), it is plausible that the effect of MET inhibition could potentially be neutralized or attenuated by the parallel activation of receptors of the HER family, reinforcing that combinatorial inhibition of both MET and HER could likely improve the therapeutic effect.

In our PDX platform we have also identified PDX models with KRAS genetic alterations. Indeed we have generated both KRAS mutated and amplified models.

Apart from common mutations in codon 12 and 13, we have surprisingly found that the rare A146T mutation is present in around 30% of our KRAS mutated PDXs. It is interesting to note that this mutation was described to be present just in 0.2% of gastro-esophageal studied cases (<http://cbiportal.org>) (204).

KRAS alterations have been extensively studied in several types of tumors (142) (143) especially the gain of function mutations that are more commonly observed. In general, KRAS activating mutations lead to constitutive RAS activation, blocking it in a GTP-bound state that render the protein insensitive to the activity of GTPase-activating proteins. KRAS gene amplification has been described in a limited number of primary tumors, including gastric, lung, pancreatic and colorectal cancers (205) (206) (207).

Recent studies involving gastric cancer samples provided evidences that KRAS gene amplification (greater than 4 fold) leads to KRAS activation. Usually, less than 10% of wild-type

and over 50% of mutant KRAS is in the GTP-bound state in cells (208). It can be potentially hypothesized that amplification and overexpression of wild-type KRAS could induce biological effects similar to those of KRAS mutated alleles. Studies involving KRAS amplified gastric cancer cell lines demonstrated that serum stimulation could increase the activation of KRAS overexpressing cells, while the KRAS mutated ones were constitutively active (208), suggesting that KRAS amplification can provide a growth advantage to cancer cells by conferring adaptability to changes in microenvironment.

In our study we observed that KRAS amplified cells not only demonstrated high levels of KRAS activation but were also addicted to KRAS and responded to *in vitro* KRAS downstream inhibition as the KRAS mutated cells. Although, *in vitro* studies conducted in KRAS mutated and amplified established gastric cancer cell lines had demonstrated that KRAS mutated cells were more sensitive to MEK inhibition compared with amplified ones (313), we found that Trametinib, a potent MEK inhibitor, led to a significant impairment in cell viability in both mutated and amplified models.

Inhibiting KRAS downstream pathways is the most explored strategy to target KRAS oncogenic activation, yet it is not very effective. In line, single MEK inhibition in our KRAS mutated and amplified models was not totally effective either *in vitro* or *in vivo*. The presence of residual activation of the downstream effectors S6K and of AKT demonstrated that our KRAS mutated and amplified models were partially resistant to Trametinib. Resistance to MEK inhibitors can be mediated by many mechanisms, such as reactivation of RAS/RAF/MEK/ERK signals, increases in the RAS or RAF protein levels, as well as increased signals through alternative pathways, including the PI3K/AKT pathways (314). Indeed, it was described that KRAS amplified and mutated gastric cancer cell lines treated with MEK inhibitors demonstrate a decrease in the activation of MAPK but not in AKT phosphorylation (313). MEK inhibition can also lead to ERK activation by upregulation of receptor tyrosine kinase activity (161) or by amplification of upstream activators that enhance flux through the pathway to elevate ERK activity (161). A deeper mechanistic evaluation of the reasons of this partial resistance is planned.

Extensive studies of PI3K-AKT-mTOR inhibitors, used in monotherapy, have shown disappointing activity against RAS-mutant cancers, both in preclinical and clinical settings (161). Nevertheless, combined inhibition of MEK and AKT/PI3K/mTOR pathways, attempting to overcome the resistance to MEK inhibitors, has been tested in preclinical trials (315) (316) as well as in humans, in advanced solid tumors (317). KRAS mutations are known to significantly contribute to resistance to mTOR and AKT inhibitors (315) (318), but no data are available in

tumors presenting *KRAS* amplification. In our experiments, the effect of both AKT inhibitor (MK-2206) and mTOR inhibitors (Osi-027 and Everolimus) alone was significantly lower than that obtained with Trametinib. Combined MEK/mTOR or MEK/AKT inhibition potentiated the effect of Trametinib, as it decreased Trametinib-triggered AKT activation and led to P-S6K abrogation and slower tumor growth. However the fact that a complete regression was not observed can be due to feedback loops in alternative pathways. A recent study involving *KRAS* mutant cell lines from different tumors, demonstrated that PTEN loss plays an important role in the synergistic interactions between MAPK and PI3K pathway inhibitors (315). An increase in PTEN activation, which lies at the intersection of MAPK and PI3K pathways, could justify the poor results obtained with the association of Trametinib+Everolimus.

Synthetic lethality strategies have been extensively explored in *KRAS* mutated tumors (176) (177) (178) (183). In this study we explored whether inhibiting cell damage repair could be lethal for *KRAS* mutated and amplified cells treated with MEK inhibitors. Small molecule inhibitors of polyADP-ribose polymerase (PARP) are thought to mediate their antitumor effects as catalytic inhibitors that block repair of DNA single strand breaks. *KRAS* mutations can contribute to PARP inhibitor resistance, that can be reversed following MEK inhibition, since it leads to an increase in apoptotic sensitivity and DNA damage, and a decrease in homologous recombination DNA repair capacity (289). In spite of the described synergistic effect of MEK and PARP inhibitors in *KRAS* mutated tumors (ovarian, pancreatic and breast cancer models without BRCA1/2 mutations), the same effect was not observed in our *KRAS* mutated and amplified models. Nonetheless, cell viability *in vitro* and tumor growth *in vivo*, as well as S6K activation was decreased with the combination of Trametinib and Olaparib, compared with the single treatment with Trametinib, but no synergic effect was seen. This lack of synergy could be due to the fact that the ability of PARP and MEK inhibitors combinations to synergize is dependent on the amount of PARP1. This aspect will be carefully investigated.

Overall, the inhibition of cell viability (or tumor growth) observed in the *in vivo* xenotrial was less effective than that observed *in vitro*. This could be due to several reasons. First, the *in vivo* investigated PDX model (GTR245) is characterized by a G12D mutation in homozygosis. Tumors with both alleles mutated have been recently described as more aggressive (288). In fact, inside our group of mutated cells, GTR245, the only one with the mutation in homozygosis, was the cell model with highest levels of RAS activation. This agrees with what was recently reported for cell lines harboring G13D mutation in homozygosis (155). Additionally, *KRAS* mutant tumors in homozygosis have been demonstrated to go through metabolic changes that include upregulation and reprogramming of glucose metabolism and enhanced ROS production

that lead to increased metastatic potential and resistance to inhibition (288). Actually, we have showed in this study that the GTR245 cells express higher levels of the glucose transporter 1 (GLUT1), monocarboxylate transporter 4 (MCT4), hexokinase II (HKII) and pyruvate kinase M2 (PKM2), as well as an increased lactate production, demonstrating that also in *KRAS* mutated gastric cancer models the existence of two mutated alleles can increase the glycolytic phenotype of the cells.

While in some cases tumor resistance can be overcome with a double combination of target therapy, as we demonstrated in the xenopatient SG16, in other cases the use of double target combination therapies is not enough. In the case of *KRAS* altered tumors, the inhibition of all the effector pathways is hard due to compensatory mechanisms, necessitating inhibition at multiple points. Several research groups are beginning to prove that the use of triple target drug combinations could be potentially more effective than double combinations, in tumors like melanoma (319). However, cell toxicity can be too heavy for normal cells and may cause loss of the therapeutic window. Nevertheless, given the increasing evidences in the metabolic changes of *KRAS* mutated tumors, the use of metabolism-targeting drugs, such as metformin (320), known to be less aggressive for the patients, can be an encouraging strategy for targeting *KRAS* oncogenic pathway.

CHAPTER VI

CONCLUSIONS AND FUTURE

PERSPECTIVES

6- Conclusions

In conclusion this work sustains the importance of the use of tumor derived xenografts to better study possible mechanisms of resistance to targeted therapies which could exist or develop in patients. On one side, our model of MET addicted gastric-xenopatients demonstrated the need of preclinical studies to better understand the molecular features of each single patient, in order to give the right molecule to the right patient. On the other side, the preclinical evaluation of KRAS altered models suggests that a precise and systematic analysis of tumor characteristics may identify patients who could benefit from MEK, AKT or mTOR targeted therapy. Further, in this study it was shown that a restricted stem like population of cells within the tumor, can share the molecular lesions of original tumor, and be targeted.

6.1 - Future perspectives

The results of this work pose the basis for a deeper and more detailed research.

Concerning the gastric xenospheres, it is important to confirm the *in vitro* results and to understand whether targeted therapies can be efficient also on gastric stem cells enriched tumors. For this purpose, *in vivo* experiments involving targeted drugs will be performed in tumors originated from gastric stem cells.

The preliminary study of KRAS alterations in gastric cancer had just opened a window on future research aimed at: 1) exploring if KRAS amplified gastric cancer models are addicted to this oncogene and how the microenvironment (providing ligands and cytokines) can influence KRAS activation; 2) studying how the different KRAS mutations and their allelic frequency (hemi or heterozygous) in cancer cells as well as the WT KRAS copy number, can influence tumor metabolism and response to KRAS downstream inhibitors *in vivo*; 3) investigating the response of KRAS amplified models to MEK, AKT and/or mTOR inhibitors *in vivo*.

CHAPTER VII

REFERENCES

7- References

1. Ferlay J, Soerjomataram I, Dikshit R, Eser S, Mathers C, Rebelo M, et al. Cancer incidence and mortality worldwide: Sources, methods and major patterns in GLOBOCAN 2012. *Int. J. Cancer*. 2015; 136: p. E359–E386.
2. Siegel R, Miller K, Jemal A. Cancer statistics. *CA Cancer J Clin*. 2016; 66(1): p. 7-30.
3. Siegel R, Miller K, Jemal A. Cancer Statistics. *CA Cancer J Clin*. 2017; 67(1): p. 7-30.
4. SEER Cancer Stat Facts: Stomach Cancer. National Cancer Institute. Bethesda, MD. [Online]. Available from: <http://seer.cancer.gov/statfacts/html/stomach.html>.
5. Global Burden of Disease Cancer Collaboration. Global, Regional, and National Cancer Incidence, Mortality, Years of Life Lost, Years Lived With Disability, and Disability Adjusted Life-years for 32 Cancer Groups, 1990 to 2015 A Systematic Analysis for the Global Burden of Disease Study. *JAMA Oncol*. 2017; 3(4): p. 524-548.
6. Venerito M, Link A, Rokkas T, Malfertheiner T. Gastric cancer – clinical and epidemiological aspects. *Helicobacter*. 2016; 21(S1): p. 39–44.
7. Wagner AD, Unverzagt S, Grothe W, Kleber G, Grothey A, Haerting J, et al. Chemotherapy for advanced gastric cancer. *Cochrane Database Syst Rev*. 2010; 17(3).
8. Ahmad S, Xia B, Bailey C, Abbott D, Helmink B, Daly M, et al. An update on gastric cancer. *Curr Probl Surg*. 2016; 53: p. 449-490.
9. van der Post R, Vogelaar I, Carneiro F, Guilford P, Huntsman D, Hoogerbrugge N, et al. Hereditary diffuse gastric cancer: updated clinical guidelines with an emphasis on germline CDH1 mutation carriers. *J Med Genet*. 2015; 52(6): p. 361-374.
10. Worthley D, Phillips K, Wayte N, Schrader K, Healey S, Kaurah P, et al. Gastric adenocarcinoma and proximal polyposis of the stomach (GAPPS): a new autosomal dominant syndrome. *Gut*. 2012; 61(5): p. 774-779.
11. Corso G, Carvalho J, Marrelli D, Vindigni C, Carvalho B, Seruca R. Somatic Mutations and Deletions of the E-Cadherin Gene. *J Clin Oncol* 31. 2013; 31: p. 868-875.
12. Oliveira C, Pinheiro H, Figueiredo J, Seruca R, Carneiro F. Familial gastric cancer: genetic susceptibility, pathology, and implications for management. *Lancet Oncol*. 2015; 16(2): p. 60-70.
13. Schistosomes, liver flukes and *Helicobacter pylori*. In IARC Working Group on the Evaluation of Carcinogenic Risks to humans; 7-14 June 1994; Lyon. p. 1-241.
14. Eslick G. *Helicobacter pylori* infection causes gastric cancer? A review of the epidemiological, meta-analytic, and experimental evidence. *World J Gastroenterol*. 2006; 12: p. 2991-2999.
15. El-Omar E, Rabkin C, Gammon M, Vaughan T, Risch H, Schoenberg J, et al. Increased risk of noncardia gastric cancer associated with proinflammatory cytokine gene polymorphisms. *Gastroenterology*. 2003; 124(5): p. 1193-1201.
16. Cho J, Kang MS, Kim KM. Epstein-Barr Virus-Associated Gastric Carcinoma and Specific Features of the Accompanying Immune Response. *J Gastric Cancer*. 2016; 16(1): p. 1-7.
17. Berretta M, Cappellani A, Lleshi A, Di Vita M, Lo Menzo E, Bearz A, et al. The role of diet in gastric cancer: still an open question. *Front Biosci*. 2012; 17: p. 1640-1647.
18. D'Elia L, Rossi G, Ippolito R, Cappuccio F, Strazzullo P. Habitual salt intake and risk of gastric cancer: A meta-analysis of prospective studies. *Clin Nutr*. 2012; 31(4): p. 489-498.
19. Wang X, Terry P, Yan H. Review of salt consumption and stomach cancer risk: Epidemiological and biological evidence. *World J Gastroenterol*. 2009; 15(18): p. 2204-2213.
20. Liu C, Russell R. Nutrition and gastric cancer risk: an update. *Nutr Rev*. 2008; 66(5): p. 237-249.
21. Hecht S, Caramella S, Foiles P, Murphy S, Peterson L. Tobacco-specific nitrosamine adducts: studies in laboratory animals and humans. *Environ Health Perspect*. 1993; 99: p. 57-63.
22. Ladeiras-Lopes R, Pereira A, Nogueira A, Pinheiro-Torres T, Pinto I, Santos-Pereira R, et al. Smoking and

- gastric cancer: systematic review and meta-analysis of cohort studies. *Cancer Causes Control*. 2008; 19(7): p. 689-701.
23. Smyth E, Verheij M, W A, Cunningham D, Cervantes A, Arnold D. Gastric cancer: ESMO Clinical Practice Guidelines for diagnosis, treatment and follow-up. *Annals of Oncology*. 2016;(27 (Supplement 5)): p. v38–v49.
 24. Hunt R, Camilleri M, Crowe S, El-Omar E, Fox J, Kuipers E, et al. The stomach in health and disease. *Gut*. 2015; 64(10): p. 1650-1668.
 25. Ngamruengphong S, Abe S, Oda I. Endoscopic Management of Early Gastric Adenocarcinoma and Preinvasive Gastric Lesions. *Surg Clin N Am*. 2017; 97: p. 371-385.
 26. Nakajima T, Ota K, Ishihara S, Oyama S, Nishi M. Indication for the lymph node dissection of gastric cancer based on the pattern analysis small of lymphatic spread (in Japanese). *Gan to Kagaku Ryoho*. 1994; 21(11): p. 1751-1757.
 27. Karpeh M, Leon L, Klimstra D, Brennan M. Lymph node staging in gastric cancer: is location more important than Number? An analysis of 1,038 patients. *Ann Surg*. 2000; 232(3): p. 362-371.
 28. Wagner P, Ramaswamy A, Ruschoff J, Schmitz-Moormann P, Rothmund M. Lymph node counts in the upper abdomen: anatomical basis for lymphadenectomy in gastric cancer. *Br J Surg*. 1991; 78(7): p. 825-827.
 29. Roukos D, Kappas A. Targeting the optimal extent of lymph node dissection for gastric cancer. *J Surg Oncol*. 2002; 81(2): p. 59-62.
 30. D'Angelica M, Gonen M, Brennan M, Turnbull A, Bains M, Karpeh M. Patterns of initial recurrence in completely resected gastric adenocarcinoma. *Ann Surg*. 2004; 240(5): p. 808-816.
 31. Cunningham D, Allum W, Stenning S, Thompson J, Van de Velde C, Nicolson M, et al. MAGIC trial participants. Perioperative chemotherapy versus surgery alone for resectable gastroesophageal cancer. *N Engl J Med*. 2006; 355: p. 11-20.
 32. Ychou M, Boige M, Pignon J, Conroy T, Bouchè O, Lebreton G, et al. Perioperative chemotherapy compared with surgery alone for resectable gastroesophageal adenocarcinoma: an FNCLCC and FFCO multicenter phase III trial. *J Clin Oncol*. 2011; 29: p. 1715-1721.
 33. De Manzoni G, Marrelli D, Baiocchi G, Morgagni P, Saragoni L, Degiuli M, et al. The Italian Research Group for Gastric Cancer (GIRCG) guidelines for gastric cancer staging and treatment:2015. *Gastric Cancer*. 2017; 20: p. 20-30.
 34. Jou E, Rajdev L. Current and emerging therapies in unresectable and recurrent gastric cancer. *World J Gastroenterol*. 2016; 22(20): p. 4812-4823.
 35. Apicella M, Corso S, Giordano S. Targeted therapies for gastric cancer: failures and hopes from clinical trials. *Oncotarget*. 2017.
 36. Roviello G, Ravelli A, Fiaschi AI, Cappelletti MR, Gobbi A, Senti C, et al. Apatinib for the treatment of gastric cancer. *Expert Rev Gastroenterol Hepatol*. 2016; 10(8): p. 887-892.
 37. Bartley AN, Washington MK, Ventura CB, Ismaila N, Colasacco C, Benson III AB, et al. HER2 Testing and Clinical Decision Making in Gastroesophageal Adenocarcinoma: Guideline From the College of American Pathologists, American Society for Clinical Pathology, and American Society of Clinical Oncology. *Am J Clin Pathol*. 2016; 146(6): p. 647-669.
 38. Nagini S. Carcinoma of the stomach: A review of epidemiology, pathogenesis, molecular genetics and chemoprevention. *World J Gastrointest Oncol*. 2012; 4: p. 156-169.
 39. Lauren P. The two histological main types of gastric carcinoma: diffuse and so-called intestinal-type carcinoma. An attempt at a histo-clinical classification. *Acta Pathol Microbiol Scand*. 1965; 64: p. 31-49.
 40. el-Zimaity H, Itani K, D G. Early diagnosis of signet ring cell carcinoma of the stomach: role of the Genta stain. *J Clin Pathol*. 1997; 50(10): p. 867-868.
 41. Hyung W, Noh S, Lee J, Huh J, Lah K, Choi S, et al. Early gastric carcinoma with signet ring cell histology. *Cancer*. 2002; 94(1): p. 78-83.
 42. Graziano F, Humar B, Guilford P. The role of the E-cadherin gene (CDH1) in diffuse gastric cancer susceptibility: from the laboratory to clinical practice. *Ann Oncol*. 2003; 14(12): p. 1705-1713.

43. Pedrazzani C, Marrelli D, Pacelli F, Di Cosmo M, Mura G, Bettarini F, et al. Gastric linitis plastica: which role for surgical resection? *Gastric Cancer*. 2012; 15(1).
44. WHO. *Histological Typing of Oesophageal and Gastric Tumours*. World Health Organization. 1990.
45. Kajitani T. The general rules for the gastric cancer study in surgery and pathology. Part I. Clinical classification. *Jpn J Surg*. 1981; 11(2): p. 127-139.
46. Corso S, Giordano S. How Can Gastric Cancer Molecular Profiling Guide Future Therapies? *Trends Mol Med*. 2016; 22(7): p. 534-544.
47. The Cancer Genome Atlas Research Network. Comprehensive molecular characterization of gastric adenocarcinoma. *Nature*. 2014; 513: p. 202-209.
48. Cristescu R, Lee J, Nebozhyn M, Kim K, Ting J, Wong S, et al. Molecular analysis of gastric cancer identifies subtypes associated with distinct clinical outcomes. *Nat Med*. 2015; 21: p. 449-456.
49. Cristescu R, Lee J, Nebozhyn M, Kim KM, Ting JC, Wong SS, et al. Molecular analysis of gastric cancer identifies subtypes associated with distinct clinical outcomes. *Nat. Med*. 2015; 21: p. 449-456.
50. Bang Y, Van Cutsem E, Feyereislova A, Chung H, Shen L, Sawaki A, et al. Trastuzumab in combination with chemotherapy versus chemotherapy alone for treatment of HER2-positive advanced gastric or gastro-oesophageal junction cancer (ToGA): a phase 3, open-label, randomised controlled trial. *Lancet*. 2010; 376(9742): p. 687-697.
51. Fuchs CS, Tomasek J, Yong CJ, Dumitru F, Passalacqua R, Goswami C, et al. Ramucirumab monotherapy for previously treated advanced gastric or gastro-oesophageal junction adenocarcinoma (REGARD): an international, randomised, multicentre, placebo-controlled, phase 3 trial. *Lancet*. 2014; 383: p. 31-39.
52. Wilke H, Muro K, Van Cutsem E, Oh SC, Bodoky G, Shimada Y, et al. Ramucirumab plus paclitaxel versus placebo plus paclitaxel in patients with previously treated advanced gastric or gastrooesophageal junction adenocarcinoma (RAINBOW): a double-blind, randomised phase 3 trial. *Lancet Oncol*. 2014; 15: p. 1224-1235.
53. Maron S, Catenacci D. Novel Targeted Therapies for Esophagogastric Cancer. *Surg Oncol Clin N Am*. 2017; 26: p. 293-312.
54. Linggi B, Carpenter G. ErbB receptors: new insights on mechanisms and biology. *Trends Cell Biol*. 2006; 16(12): p. 649-656.
55. Yarden Y, Sliwkowski MX. Untangling the ErbB signalling network. *Nat Rev Mol Cell Biol*. 2001; 2: p. 127-137.
56. Cho J, Jeong J, Sung J, Sung C, Kim K, Park C, et al. A large cohort of consecutive patients confirmed frequent HER2 positivity in gastric carcinomas with advanced stages. *Ann Surg Oncol*. 2013; 20: p. 477-484.
57. Park S, Park Y, Ryu MH, Ryoo BY, Woo C, Jung HY, et al. Extra-gain of HER2-positive cases through HER2 reassessment in primary and metastatic sites in advanced gastric cancer with initially HER2-negative primary tumours: Results of GASTric cancer HER2 reassessment study 1 (GASTHER1). *European Journal of Cancer*. 2016; 53: p. 42-50.
58. Moorcraft SY, Chau I. Investigational therapies targeting the ErbB family in oesophagogastric cancer. *Expert Opin. Investig. Drugs*. 2014; 23(10): p. 1349-1363.
59. Desai Dandona M, Saroya BS, Lockhart AC. Investigational therapies targeting the ErbB (EGFR, HER2, HER3, HER4) family in GI cancers. 2013; 22(3): p. 341-356.
60. Kang YK, Shah MA, Ohtsu A, Van Cutsem E, Ajani JA, van der Horst T, et al. A randomized, open-label, multicenter, adaptive phase 2/3 study of trastuzumab emtansine (T-DM1) versus a taxane (TAX) in patients with previously treated HER2-positive locally advanced or metastatic gastric/gastroesophageal junction adenocarcinoma. *J Clin Oncol*. 2016; 34((suppl 4S; abstr 5)).
61. Franklin M, Carey K, Vajdos F, Leahy D, de Vos A, Sliwkowski M. Insights into ErbB signaling from the structure of the ErbB2-pertuzumab complex. *Cancer Cell*. 2004; 5(4): p. 317-328.
62. Scheuer W, Friess T, Burtscher H, Bossenmaier B, Endl J, Hasmann M. Strongly enhanced antitumor activity of trastuzumab and pertuzumab combination treatment on HER2-positive human xenograft tumor models.

- Cancer Res. 2009; 69(24): p. 9330-9336.
63. Yamashita-Kashima Y, Iijima S, Yorozu K, Furugaki K, Kurasawa M, Ohta M, et al. Pertuzumab in combination with trastuzumab shows significantly enhanced antitumor activity in HER2-positive human gastric cancer xenograft models. *Clin Cancer Res.* 2011; 17(15): p. 5060-5070.
 64. Tabernero J, Hoff P, Shen L, et al. Pertuzumab (P) + trastuzumab (H) + chemotherapy (CT) for HER2-positive metastatic gastric or gastro-oesophageal junction cancer (mGC/GEJC): final analysis of a phase III study (JACOB). In European Society for Medical Oncology (ESMO) 2017 Congress; September 8-12, 2017; Madrid, Spain.
 65. Tynan CJ, Lo Schiavo V, Zanetti-Domingues L, Needham SR, Roberts SK, Hirsch M, et al. A tale of the epidermal growth factor receptor: The quest for structural resolution on cells. *Methods.* 2016; 95: p. 86-93.
 66. Dragovich Tea. Anti-EGFR-Targeted Therapy for Esophageal and Gastric Cancers: An Evolving Concept. *J Onc.* 2009; 804108.
 67. Dragovich T, McCoy S, Fenoglio-Preiser CM, Wang J, Benedetti JK, Baker AF. Phase II Trial of Erlotinib in Gastroesophageal Junction and Gastric Adenocarcinomas: SWOG 0127. *J Clin Oncol.* 2006; 24(30): p. 4922-4927.
 68. Ferry DR, Anderson M, Beddard K, Tomlinson S, Atherfold P, Obszynska J, et al. A Phase II Study of Gefitinib Monotherapy in Advanced Esophageal Adenocarcinoma: Evidence of Gene Expression, Cellular, and Clinical Response. *Clin Cancer Res.* 2007; 13(19): p. 5869-5875.
 69. Dutton SJ, Ferry DR, Blazeby JM, Abbas H, Dahle-Smith A, Mansoor W, et al. Gefitinib for oesophageal cancer progressing after chemotherapy (COG): a phase 3, multicentre, double-blind, placebo-controlled randomised trial. *Lancet Oncol.* 2014; 15(8): p. 894–904.
 70. Janjigian YY, Capanu M, Imtiaz T, Kelsen DP, Ku GY, Schattner M, et al. A phase II study of afatinib in patients (pts) with metastatic human epidermal growth factor receptor (HER2)-positive trastuzumab-refractory esophagogastric (EG) cancer. *J Clin Oncol.* 2014; 32(suppl 3; abstr 52).
 71. Kimura H, Sakai K, Arai T, Shimoyama T, Tamura T, Nishio K. Antibody-dependent cellular cytotoxicity of cetuximab against tumor cells with wild-type or mutant epidermal growth factor receptor. *Cancer Sci.* 2007; 98(8): p. 1275-1280.
 72. Lordick F, Lubber P, Lorenzen S, Hegewisch-Becker S, Folprecht G, Wöll E, et al. Cetuximab plus oxaliplatin/leucovorin/5-fluorouracil in first-line metastatic gastric cancer: a phase II study of the Arbeitsgemeinschaft Internistische Onkologie (AIO). *Br J Cancer.* 2010; 102(3): p. 500-505.
 73. Kim C, Lee JL, Ryu MH, Chang HM, Kim TW, Lim HY, et al. A prospective phase II study of cetuximab in combination with XELOX (capecitabine and oxaliplatin) in patients with metastatic and/or recurrent advanced gastric cancer. *Invest New Drugs.* 2011; 29(2): p. 366-373.
 74. Han SW, Oh DY, Im SA, Park SR, Lee KW, Song HS, et al. Phase II study and biomarker analysis of cetuximab combined with modified FOLFOX6 in advanced gastric cancer. *Br J Cancer.* 2009; 100(2): p. 298-304.
 75. Pinto C, Di Fabio F, Barone C, Siena S, Falcone A, Cascinu S, et al. Phase II study of cetuximab in combination with cisplatin and docetaxel in patients with untreated advanced gastric or gastro-oesophageal junction adenocarcinoma (DOCETUX study). *Br J Cancer.* 2009; 101(8): p. 1261-1268.
 76. Lordick F, Kang YK, Chung HC, Salman P, Oh SC, Bodoky G, et al. Capecitabine and cisplatin with or without cetuximab for patients with previously untreated advanced gastric cancer (EXPAND): a randomised, open-label phase 3 trial. *Lancet Oncol.* 2013; 14(6): p. 490–499.
 77. Chan JA, Blaszczak LS, Enzinger PC, Ryan DP, Abrams TA, Zhu AX, et al. A multicenter phase II trial of single-agent cetuximab in advanced esophageal and gastric adenocarcinoma. *Ann Oncol.* 2011; 22(6): p. 1367-1373.
 78. Schønnemann KR, Yilmaz M, Bjerregaard JK, Nielsen KM, Pfeiffer P. Phase II study of biweekly cetuximab in combination with irinotecan as second-line treatment in patients with platinum-resistant gastro-oesophageal cancer. *Eur J Cancer.* 2012; 48(4): p. 510-517.

79. Luber B, Deplazes J, Keller G, Walch A, Rauser S, Eichmann M, et al. Biomarker analysis of cetuximab plus oxaliplatin/leucovorin/5-fluorouracil in first-line metastatic gastric and oesophago-gastric junction cancer: results from a phase II trial of the Arbeitsgemeinschaft Internistische Onkologie (AIO). *BMC Cancer*. 2011; 11: p. 509.
80. Lordick F, Kang YK, Salman P, Oh SC, Bodoky G, Kurteva GP. Clinical outcome according to tumor HER2 status and EGFR expression in advanced gastric cancer patients from the EXPAND study. *Journal of Clinical Oncology*. 2013; 15_suppl: p. 4021.
81. Robert Jr R. The ErbB/HER family of protein-tyrosine kinases and cancer. *Pharmacological Research*. 2014; 79: p. 34-74.
82. Waddell T, Chau I, Cunningham D, Gonzalez D, Okines AF, Okines C, et al. Epirubicin, oxaliplatin, and capecitabine with or without panitumumab for patients with previously untreated advanced oesophagogastric cancer (REAL3): a randomised, open-label phase 3 trial. *Lancet Oncol*. 2013; 14(6): p. 481-489.
83. Wang JW, Chi Y, Zheng ZX, Tao Qu ZAP, Yang L, Jiang WC. Randomized, single-centered, phase II clinical trial of nimotuzumab plus cisplatin and S-1 as first-line therapy in patients with advanced gastric cancer. *J Clin Oncol*. 2012; 30(suppl; abstr e14668).
84. Aprile G, Giampieri R, Bonotto M, Bittoni A, Ongaro E, Cardellino GG, et al. The challenge of targeted therapies for gastric cancer patients: the beginning of a long journey. *Expert Opin. Investig. Drugs*. 2014; 23(7): p. 925-942.
85. Qin S. Phase III study of apatinib in advanced gastric cancer: A randomized, double-blind, placebo-controlled trial. *J Clin Oncol*. 2014; 32(5s(suppl; abstr 4003)).
86. Van Cutsem E, de Haas S, Kang YK, Ohtsu A, Tebbutt NC, Ming Xu J, et al. Bevacizumab in combination with chemotherapy as first-line therapy in advanced gastric cancer: a biomarker evaluation from the AVAGAST randomized phase III trial. *J Clin Oncol*. 2012; 30(17): p. 2119-2127.
87. Shen L, Li J, Xu J, Pan H, Dai G, Qin S, et al. Bevacizumab plus capecitabine and cisplatin in Chinese patients with inoperable locally advanced or metastatic gastric or gastroesophageal junction cancer: randomized, double-blind, phase III study (AVATAR study). *Gastric Cancer*. 2015; 18(1): p. 168-176.
88. Shah MA, Wainberg ZA, Catenacci DV, Hochster HS, Ford J, Kunz P, et al. Phase II study evaluating 2 dosing schedules of oral foretinib (GSK1363089), cMET/VEGFR2 inhibitor, in patients with metastatic gastric cancer. *PLoS One*. 2013; 8(3): p. e54014.
89. Trusolino L, Bertotti A, Comoglio PM. MET signalling: principles and functions in development, organ regeneration and cancer. *Nat Rev Mol Cell Biol*. 2010; 11(12): p. 834-848.
90. Gherardi E, Birchmeier W, Birchmeier C, Vande Woude G. Targeting MET in cancer: rationale and progress. *Nat Rev Cancer*. 2012; 12(2): p. 89-103.
91. Gordon M, et al. Safety, pharmacokinetics, and pharmacodynamics of AMG 102, a fully human hepatocyte growth factor-neutralizing monoclonal antibody, in a first-in-human study of patients with advanced solid tumors. *Clin Cancer Res*. 2010; 16: p. 699-710.
92. Wen P, et al. A phase II study evaluating the efficacy and safety of AMG 102 (rilotumumab) in patients with recurrent glioblastoma. *Neuro Oncol* 13. 2011;: p. 437-446.
93. Iveson T, et al. Rilotumumab in combination with epirubicin, cisplatin, and capecitabine as first-line treatment for gastric or oesophagogastric junction adenocarcinoma: an open-label, dose de-escalation phase 1b study and a double-blind, randomised phase 2 study. *Lancet Oncol*. 2014; 15: p. 1007-1018.
94. Cunningham D, Tebbutt NC, Davidenko I, Murad AM, Al-Batran SE, Ilson DH, et al. Phase III, randomized, double-blind, multicenter, placebo-controlled trial of rilotumumab plus epirubicin, cisplatin and capecitabine as firstline therapy in patients with advanced MET-positive gastric or gastroesophageal junction cancer: RILOMET-1 study. *J Clin Oncol*. 2015; 33((suppl; abstr 4000)).
95. D'Arcangelo M, F C. Focus on the potential role of ficlatuzumab in the treatment of non-small cell lung cancer. *Biologics*. 2013; 7: p. 61-68.
96. Mok T, Geater S, Su WC, Tan EH, JC-H Y, Chang GC, et al. A randomized phase 2 study comparing the

- combination of ficlatuzumab and gefitinib with gefitinib alone in Asian patients with advanced stage pulmonary adenocarcinoma. *J Thorac Oncol.* 2016; 11: p. 1736–1744.
97. Okamoto W, Okamoto I, Tanaka K, Hatashita E, Yamada Y, Kuwata K, et al. TAK-701, a humanized monoclonal antibody to hepatocyte growth factor, reverses gefitinib resistance induced by tumor-derived HGF in non-small cell lung cancer with an EGFR mutation. *Mol Cancer Ther.* 2010; 9.
 98. Jones S, Cohen R, Bendell J, Denlinger C, Harvey R, Parasuraman S, et al. Safety, tolerability, and pharmacokinetics of TAK-701, a humanized anti-hepatocyte growth factor (HGF) monoclonal antibody, in patients with advanced nonhematologic malignancies: first-in-human phase I dose-escalation study. *J Clin Oncol.* 2010; 28(3081).
 99. Martens T, et al. A novel one-armed anti-c-Met antibody inhibits glioblastoma growth in vivo. *Clin Cancer Res.* 2006; 12: p. 6144-6152.
 100. Comoglio P, Giordano S, Trusolino L. Drug development of MET inhibitors: targeting oncogene addiction and expedience. *Nat Rev Drug Discov.* 2008 504-516; 7.
 101. Spiegel. *Annals of Oncology.* 218th ed.; 2010.
 102. Koeppen H, et al. Biomarker analyses from a placebo-controlled phase II study evaluating erlotinib±onartuzumab in advanced non-small cell lung cancer: MET expression levels are predictive of patient benefit. *Clin Cancer Res.* 2014; 20: p. 4488-4498.
 103. Rosen L, Goldman J, Algazi A, Turner P, Moser B, Hu T, et al. A first-in-human phase I study of a bivalent MET antibody, Emibetuzumab (LY2875358), as monotherapy and in combination with erlotinib in advanced cancer. *Clin Cancer Res.* 2017.
 104. Cepero V, Sierra J, Giordano S. Tyrosine kinases as molecular targets to inhibit cancer progression and metastasis. *Curr Pharm Des.* 2010; 16: p. 1396-1409.
 105. Kwak E, LoRusso P, Hamid O, et al. Clinical activity of AMG 337, an oral MET kinase inhibitor, in adult patients (pts) with MET-amplified gastroesophageal junction (GEJ), gastric (G), or esophageal (E). *J Clin Oncol.* 2015; 33(1).
 106. Kazandjian D, et al. FDA approval summary: crizotinib for the treatment of metastatic non-small cell lung cancer with anaplastic lymphoma kinase rearrangements. *Oncologist.* 2014; 19: p. e5-11.
 107. Camidge D, et al. Activity and safety of crizotinib in patients with ALK-positive non-small-cell lung cancer: updated results from a phase 1 study. *Lancet Oncol.* 2012; 13: p. 1011-1019.
 108. Shaw A, et al. Crizotinib in ROS1-rearranged non-small-cell lung cancer. *N Engl J Med.* 2014; 371: p. 1963-1971.
 109. Lennerz JK, Kwak EL, Ackerman A, Michael M, Fox SB, Bergethon K, et al. MET amplification identifies a small and aggressive subgroup of esophagogastric adenocarcinoma with evidence of responsiveness to crizotinib. *J Clin Oncol.* 2011; 29(36): p. 4803-4810.
 110. Frampton G, Ali S, Rosenzweig M, et al. Activation of MET via diverse exon 14 splicing alterations occurs in multiple tumor types and confers clinical sensitivity to MET inhibitors. *Cancer Discov.* 2015; 5: p. 850-9.
 111. Lee J, Ou S, Lee J, et al. Gastrointestinal malignancies harbor actionable MET exon 14 deletions. *Oncotarget.* 2015; 6: p. 28211-22.
 112. Asaoka Y, Tada M, Ikenoue T, et al. Gastric cancer cell line Hs746T harbors a splice site mutation of c-Met causing juxtamembrane domain deletion. *Biochem Biophys Res Commun.* 2010; 394: p. 1042-6.
 113. Zang Z, Ong C, Cutcutache I, et al. Genetic and structural variation in the gastric cancer kinome revealed through targeted deep sequencing. *Cancer Res.* 2011; 71: p. 29-39.
 114. Eder J, Vande Woude G, Boerner S, LoRusso P. Novel Therapeutic Inhibitors of the c-Met Signaling Pathway in Cancer. *Molecular Pathways.* 2009; 15(7).
 115. Su X, Zhan P, Gavine PR, Morgan S, Womack C, Ni X, et al. FGFR2 amplification has prognostic significance in gastric cancer: results from a large international multicentre study. *Br J Cancer.* 2014; 110: p. 967-975.
 116. Bang YJ, Van Cutsem E, Mansoor W, Petty R, Chao Y, Cunningham D, et al. A randomized, open-label phase II study of AZD4547 (AZD) versus paclitaxel (P) in previously treated patients with advanced gastric cancer

- (AGC) with fibroblast growth factor receptor 2(FGFR2) polysomy or gene amplification (amp): SHINE study. *J Clin Oncol.* 2015; (Suppl 20): 4014.
117. Smyth EC, Turner NC, A P. Phase II study of AZD4547 in FGFR amplified tumours: gastroesophageal cancer (GC) cohort pharmacodynamic and biomarker results. In *ASCO Annual Meeting Proceedings*; 2016; Chicago.
 118. Doi T, Kang YK, Muro K, Jiang Y, Jain RK, Lizambri R. A phase 3, multicenter, randomized, doubleblind, placebo-controlled study of rilotumumab in combination with cisplatin and capecitabine as firstline therapy for Asian patients with advanced METpositive gastric or GEJ adenocarcinoma: The RILOMET-2 trial. *J Clin Oncol.* 2015; 33((suppl 3; abstr TPS226)).
 119. Ohtsu A, Ajani JA, Bai YX, Bang YJ, Chung HC, Pan HM, et al. Everolimus for previously treated advanced gastric cancer: results of the randomized, double-blind, phase III GRANITE-1 study. *J Clin Oncol.* 2013; 31: p. 3935-3943.
 120. Ramanathan RK, McDonough SL, Kennecke HF, Iqbal S, Baranda JC, Seery TE, et al. Phase 2 study of MK-2206, an allosteric inhibitor of AKT, as second-line therapy for advanced gastric and gastroesophageal junction cancer: A SWOG cooperative group trial (S1005). *Cancer.* 2015; 121: p. 2193-2197.
 121. Ribas A, Robert C, Hodi F, Wolchok J, Joshua A, Hwu WJ, et al. Association of response to programmed death receptor 1 (PD-1) blockade with pembrolizumab (MK-3475) with an interferon-inflammatory immune gene signature. *J Clin Oncol.* 2015; 33.
 122. Derks S, Liao X, Chiaravalli A, Xu X, Camargo MC, Solcia E, et al. Abundant PD-L1 expression in Epstein-Barr Virus-infected gastric cancers. *Oncotarget.* 2016; 7(22): p. 32925-32932.
 123. Ma C, Patel K, Singhi AD, Ren B, Zhu B, Shaikh F, et al. Programmed Death-Ligand 1 Expression Is Common in Gastric Cancer Associated With Epstein-Barr Virus or Microsatellite Instability. *Am J Surg Pathol.* 2016; 40(11): p. 1496-1506.
 124. Muro K, Chung HC, Shankaran V, Geva R, Catenacci D, Gupta S, et al. Pembrolizumab for patients with PD-L1-positive advanced gastric cancer (KEYNOTE-012): a multicentre, open-label, phase 1b trial. *Lancet Oncol.* 2016; 17: p. 717-726.
 125. Le DT, Bendell JC, Calvo E, Kim JW, Ascierto PA, Sharma P, et al. Safety and activity of nivolumab monotherapy in advanced and metastatic (A/M) gastric or gastroesophageal junction cancer (GC/GEC): Results from the CheckMate-032 study. *J Clin Oncol.* 2016; 34((suppl 4S: abstr 6).).
 126. Chung HC, Arkenau HT, Wyrwicz L, Oh DY, Lee KW, Infante JR, et al. Avelumab (MSB0010718C; anti-PD-L1) in patients with advanced gastric or gastroesophageal junction cancer from JAVELIN solid tumor phase Ib trial: Analysis of safety and clinical activity. *J Clin Oncol.* 2016; 34(abstr 4009).
 127. Moehler MH, Cho JY, Kim YH, Kim JW, Di Bartolomeo M, Ajani JA, et al. A randomized, open-label, two-arm phase II trial comparing the efficacy of sequential ipilimumab versus best supportive care following first-line chemotherapy in patients with unresectable, locally advanced/metastatic gastric or GEJ cancer. *J Clin Oncol.* 2016; 34((suppl; abstr 4011)).
 128. Ralph C, Elkord E, Burt DJ, O'Dwyer JF, Austin EB, Stern PL, et al. Modulation of Lymphocyte Regulation for Cancer Therapy: A Phase II Trial of Tremelimumab in Advanced Gastric and Esophageal Adenocarcinoma. *Clin Cancer Res.* 2010; 16(5): p. 1662-1672.
 129. Seger R, Krebs E. The MAPK signaling cascade. *FASEB J.* 1995; 9: p. 726–735.
 130. Engelman J, Luo J, Cantley L. The evolution of phosphatidylinositol 3-kinases as regulators of growth and metabolism. *Nat Rev Genet.* 2006; 7: p. 606–619.
 131. Wolthuis R, Bos J. Ras caught in another affair: the exchange factors for Ral. *Curr Opin Genet Dev.* 1999; 9: p. 112-117.
 132. Lambert J, Lambert Q, Reuther G, al e. Tiam1 mediates Ras activation of Rac by a PI (3)K-independent mechanism. *Nat Cell Biol.* 2002; 4: p. 621–625.
 133. Gonzalez-Garcia A, Pritchard C, Paterson H, al e. RalGDS is required for tumor formation in a model of skin Carcinogenesis. *Cancer Cell.* 2005; 7: p. 219–226.
 134. Malliri A, van der Kammen R, Clark K, al e. Mice deficient in the Rac activator Tiam1 are resistant to Ras-

- induced skin tumours. *Nature*. 2002; 417: p. 867–871.
135. Mitin N, Rossman K, Der C. Signaling Interplay in Ras Superfamily Function. *Current Biology*. 2005; 15: p. R563–R574.
136. Hunter J, al e. Biochemical and structural analysis of common cancer-associated KRAS mutations. *Mol Cancer Res*. 2015; 13: p. 1325–1335.
137. Smith Mea. NMR-based functional profiling of RASopathies and oncogenic RAS mutations. *Proc Natl Acad Sci U. S. A*. 2013; 110: p. 4574–4579.
138. Donovan S, al e. GTPase activating proteins: critical regulators of intracellular signaling. *Biochim Biophys Acta*. 2002; 1602: p. 23–45.
139. Schubert S, al e. Biochemical and functional characterization of germ line KRAS mutations. *Mol Cell Biol*. 2007; 27: p. 7765–7770.
140. Pai E, al e. Refined crystal structure of the triphosphate conformation of H-ras p21 at 1.35 Å resolution: implications for the mechanism of GTP hydrolysis. *EMBO J*. 1990; 9: p. 2351–2359.
141. Feig L, Cooper G. Relationship among guanine nucleotide exchange, GTP hydrolysis, and transforming potential of mutated ras proteins. *Mol Cell Biol*. 1988; 8: p. 2472–2478.
142. Edkins S, al e. Recurrent KRAS codon 146 mutations in human colorectal cancer. *Cancer Biol Ther*. 2006; 5: p. 928–932.
143. Cerami E, al e. The cBio cancer genomics portal: an open platform for exploring multidimensional cancer genomics data. *Cancer Discov*. 2012; 2: p. 401–404.
144. Hingorani S, al e. Trp53R172H and KrasG12D cooperate to promote chromosomal instability and widely metastatic pancreatic ductal adenocarcinoma in mice. *Cancer Cell*. 2005; 7: p. 469–83.
145. Ji H, al e. LKB1 modulates lung cancer differentiation and metastasis. *Nature*. 2007; 448: p. 807–810.
146. Haigis K, al e. Differential effects of oncogenic K-Ras and N-Ras on proliferation, differentiation and tumor progression in the colon. *Nat Genet*. 2008; 40: p. 600–608.
147. Chin L, al e. Essential role for oncogenic Ras in tumour maintenance. *Nature*. 1999; 400: p. 468–72.
148. Collins M, al e. Metastatic pancreatic cancer is dependent on oncogenic Kras in mice. *PLoS One*. 2012; 7: p. e49707.
149. Fisher G, al e. Induction and apoptotic regression of lung adenocarcinomas by regulation of a K-Ras transgene in the presence and absence of tumor suppressor genes. *Genes Dev*. 2001; 15: p. 3249–3262.
150. Kwong L, al e. Oncogenic NRAS signaling differentially regulates survival and proliferation in melanoma. *Nat Med*. 2012; 18: p. 1503–1510.
151. Ying H, al e. Oncogenic Kras maintains pancreatic tumors through regulation of anabolic glucose metabolism. *Cell*. 2012; 149: p. 656–670.
152. Zhang Z, et al. Wildtype Kras2 can inhibit lung carcinogenesis in mice. *Nat Genet*. 2001; 29: p. 25–33.
153. To Mea. Interactions between wild-type and mutant Ras genes in lung and skin carcinogenesis. *Oncogene*. 2013; 32: p. 4028–4033.
154. Junttila M, al e. Selective activation of p53-mediated tumour suppression in high-grade tumours. *Nature*. 2010; 468: p. 567–571.
155. Burgess M, al e. KRAS Allelic imbalance enhances fitness and modulates MAP kinase dependence in cancer. *Cell*. 2017; 168: p. 817–829 e15.
156. Grant B, al e. Novel allosteric sites on Ras for lead generation. *PLoS One*. 2011; 6(e25711).
157. Buhrman G, al e. Analysis of binding site hot spots on the surface of Ras GTPase. *J Mol Biol*. 2011; 413: p. 773–789.
158. Taveras A, al e. Ras oncoprotein inhibitors: the discovery of potent, ras nucleotide exchange inhibitors and the structural determination of a drug-protein complex. *Bioorg Med Chem*. 1997; 5: p. 125–133.
159. Peri F, al e. Design, synthesis and biological evaluation of sugar-derived Ras inhibitors. *ChemBiochem*. 2005; 6: p. 1839–1848.

160. Karaguni I, et al. The new sulindac derivative IND 12 reverses Ras-induced cell transformation. *Cancer Res.* 2002; 62: p. 1718–1723.
161. Cox A, et al. Drugging the undruggable Ras: mission possible? *Nat Rev Drug Discov.* 2014; 13(11): p. 828–851.
162. Shima F, et al. In silico discovery of small-molecule Ras inhibitors that display antitumor activity by blocking the Ras-effector interaction. *Proc Natl Acad Sci USA.* 2013; 110: p. 8182–8187.
163. Ostrem J, Peters U, Sos M, Wells J, Shokat K. K-Ras(G12C) inhibitors allosterically control GTP affinity and effector interactions. *Nature.* 2013; 503: p. 548–551.
164. Athuluri-Divakar S. A small molecule RAS-Mimetic disrupts RAS association with effector proteins to block signaling. *Cell.* 2016; 165: p. 643–655.
165. Takashima A, et al. Targeting the Ras oncogene. *Expert Opin Ther Targets.* 2013; 17: p. 507–531.
166. Zimmermann G, et al. Small molecule inhibition of the KRAS-PDEdelta interaction impairs oncogenic KRAS signalling. *Nature.* 2013; 497: p. 638–642.
167. Lyons J, Wilhelm S, Hibner B, Bollag G. Discovery of a novel Raf kinase inhibitor. *Endocr Relat Cancer.* 2001; 8: p. 219–225.
168. Lito P, Rosen N, Solit D. Tumor adaptation and resistance to RAF inhibitors. *Nat Med.* 2013; 19: p. 1401–1409.
169. Hatzivassiliou G, et al. RAF inhibitors prime wild-type RAF to activate the MAPK pathway and enhance growth. *Nature.* 2010; 464: p. 431–435.
170. Heidorn S, et al. Kinase-dead BRAF and oncogenic RAS cooperate to drive tumor progression through CRAF. *Cell.* 2010; 140: p. 209–221.
171. Poulikakos P, Zhang C, Bollag G, Shokat K, Rosen N. RAF inhibitors transactivate RAF dimers and ERK signalling in cells with wild-type BRAF. *Nature.* 2010; 464: p. 427–430.
172. Gilmartin A, et al. GSK1120212 (JTP-74057) is an inhibitor of MEK activity and activation with favorable pharmacokinetic properties for sustained in vivo pathway inhibition. *Clin Cancer Res.* 2011; 17: p. 989–1000.
173. Bollag G, et al. Clinical efficacy of a RAF inhibitor needs broad target blockade in BRAF-mutant melanoma. *Nature.* 2010; 467: p. 596–599.
174. Ebi H, et al. Receptor tyrosine kinases exert dominant control over PI3K signaling in human KRAS mutant colorectal cancers. *J Clin Invest.* 2011; 121: p. 4311–4321.
175. Engelman J, et al. Effective use of PI3K and MEK inhibitors to treat mutant Kras G12D and PIK3CA H1047R murine lung cancers. *Nat Med.* 2008; 14: p. 1351–1356.
176. Kim J, et al. XPO1-dependent nuclear export is a druggable vulnerability in KRAS-mutant lung cancer. *Nature.* 2016; 538: p. 114.
177. Wang J, et al. Suppression of KRAS-mutant cancer through the combined inhibition of KRAS with PLK1 and ROCK. *Nature Communications.* 2016; 7(11363).
178. Sarthy A, et al. Survivin depletion preferentially reduces the survival of activated K-Ras-transformed cells. *Mol Cancer Ther.* 2007; 6: p. 269–276.
179. Morgan-Lappe S, et al. Identification of Ras-related nuclear protein, targeting protein for xenopus kinesin-like protein 2, and stearyl-CoA desaturase 1 as promising cancer targets from an RNAi-based screen. *Cancer Res.* 2007; 67: p. 4390–4398.
180. Luo J, et al. A genome-wide RNAi screen identifies multiple synthetic lethal interactions with the Ras oncogene. *Cell.* 2009; 137: p. 835–848.
181. Vicent S, et al. Wilms tumor 1 (WT1) regulates KRAS-driven oncogenesis and senescence in mouse and human models. *J Clin Invest.* 2010; 120: p. 3940–3952.
182. Corcoran R, et al. Synthetic lethal interaction of combined BCL-XL and MEK inhibition promotes tumor regressions in KRAS mutant cancer models. *Cancer Cell.* 2013; 23: p. 121–128.
183. Kumar M, et al. The GATA2 transcriptional network is requisite for RAS oncogene-driven non-small cell lung cancer. *Cell.* 2012; p. 642–655.

184. Wang Y, al e. Critical role for transcriptional repressor Snail2 in transformation by oncogenic RAS in colorectal carcinoma cells. *Oncogene*. 2010; 29: p. 4658–4670.
185. Manchado E, al e. A combinational strategy for treating KRAS-mutant lung cancer. *Nature*. 2016; 534: p. 647–651.
186. Barbie D, al e. Systematic RNA interference reveals that oncogenic KRAS-driven cancers require TBK1. *Nature*. 2009; 462: p. 108–112.
187. Singh A, al e. TAK1 inhibition promotes apoptosis in KRAS-dependent colon cancers. *Cell*. 2012; 148: p. 639–650.
188. Hanahan DWR. Hallmarks of cancer: the next generation. *Cell*. 2011; 144: p. 646–674.
189. Guo J, al e. Activated Ras requires autophagy to maintain oxidative metabolism and tumorigenesis. *Genes Dev*. 2011; 25: p. 460–470.
190. Yang S, al e. Pancreatic cancers require autophagy for tumor growth. *Genes Dev*. 2011; 25: p. 717–729.
191. Kamphorst J, al e. Hypoxic and Ras-transformed cells support growth by scavenging unsaturated fatty acids from lysophospholipids. *Proc Natl Acad Sci USA*. 2013; 110: p. 8882–8887.
192. Yun J, al e. Glucose deprivation contributes to the development of KRAS pathway mutations in tumor cells. *Science*. 2009; 325: p. 1555–1559.
193. Son J, al e. Glutamine supports pancreatic cancer growth through a KRAS-regulated metabolic pathway. *Nature*. 2013; 496: p. 101–105.
194. Gaglio D, al e. Oncogenic K-Ras decouples glucose and glutamine metabolism to support cancer cell growth. *Mol Syst Biol*. 2011; 7: p. 523.
195. Weinberg F, al e. Mitochondrial metabolism and ROS generation are essential for Kras-mediated tumorigenicity. *Proc Natl Acad Sci USA*. 2010; 107: p. 8788–8793.
196. Thornburg J, al e. Targeting aspartate aminotransferase in breast cancer. *Breast Cancer Res*. 2008; 10: p. R84.
197. Bos J, MV-d V, Marshall C, Veeneman G, van Boom J, van der Eb A. A human gastric carcinoma contains a single mutated and an amplified normal allele of the Ki-ras oncogene. *Nucleic Acids Res*. 1986; 14: p. 1209–1217.
198. Hewit L, al e. KRAS, BRAF and gastric cancer. *Translational Gastrointestinal Cancer*. 2015; 4(6).
199. Victor T, Du Toit R, Jordaan A, Bester A, van Helden P. No evidence for point mutations in codons 12, 13 and 61 of the ras gene in a high-incidence area for esophageal and gastric cancers. *Cancer Res*. 1990; 50: p. 4911–4914.
200. Hongyo T, Buzard G, Palli D, al e. Mutations of the K-ras and p53 genes in gastric adenocarcinomas from a high-incidence region around Florence, Italy. *Cancer Res*. 1995; 55: p. 2665–2672.
201. Corso G, Velho S, Paredes J, al e. Oncogenic mutations in gastric cancer with microsatellite instability. *Eur J Cancer*. 2011; 47: p. 443–451.
202. van Grieken N, Aoyama T, Chambers P, al e. KRAS and BRAF mutations are rare and related to DNA mismatch repair deficiency in gastric cancer from the East and the West: Results from a large international multicentre study. *Br J Cancer*. 2013; 108: p. 1495–1501.
203. Liu Z, Liu L, Li M, Zhang Q, Cheng S, Lu S. Mutation detection of KRAS by high-resolution melting analysis in Chinese gastric cancer. *Oncol Rep*. 2009; 22: p. 515–520.
204. J. G, al e. Integrative Analysis of Complex Cancer Genomics and Clinical Profiles Using the cBioPortal. *Sci Signal*. 2013; 6(269).
205. Weir B, al e. Characterizing the cancer genome in lung adenocarcinoma. *Nature*. 2007; 450(7171): p. 893–898.
206. Martin E, al e. Common and Distinct Genomic Events in Sporadic Colorectal Cancer and Diverse Cancer Types. *Cancer Res*. 2007; 67(22): p. 10736–10743.
207. Roelofs H, al e. Restricted 12p amplification and RAS mutation in human germ cell tumors of the adult testis. *Am J Pathol*. 2000; 157(4): p. 1155–1166.
208. Mita H, Toyota M, Aoki F, Akashi H, al e. A novel method, digital genome scanning detects KRAS gene

- amplification in gastric cancers: involvement of overexpressed wild-type KRAS in downstream signaling and cancer cell growth. *BMC Cancer*. 2009; 9(198).
209. Misale S, et al. Emergence of KRAS mutations and acquired resistance to anti EGFR therapy in colorectal cancer. *Nature*. 2012; 486(7404): p. 532-536.
 210. Valtorta E, et al. KRAS gene amplification in colorectal cancer and impact on response to EGFR-targeted therapy. *Int J Cancer*. 2013; 133(5): p. 1259-1265.
 211. Boyd M. The NCI in vitro antitumor drug discovery screen: concept, implementation, and operation, 1985–1995. In Teicher B. *Anticancer drug development guide: preclinical screening, clinical trials and approval*. Totowa, NJ: Humana Press; 1997.
 212. Venditti JM, Wesley RA, Plowman J. Current NCI preclinical antitumor screening in vivo: results of tumor panel screening, 1976–1982, and future directions. *Adv Pharmacol Chemother*. 1984; 20: p. 1-20.
 213. Abaan OD, Polley EC, Davis SR, Zhu YJ, Bilke S, Walker RL, et al. The exomes of the NCI-60 panel: a genomic resource for cancer biology and systems pharmacology. *Cancer Res*. 2013; 73: p. 4372–4382.
 214. Hidalgo M, Frederic A, Andrew B, Budinská E, Byrne A, Caldas C, et al. Patient-Derived Xenograft Models: An Emerging Platform for Translational Cancer Research. *Cancer Discov*. 2014; 4(9): p. 998-1013.
 215. Gillet JP, Calcagno AM, Varma S, Marino M, Green LJ, Vora MI. Redefining the relevance of established cancer cell lines to the study of mechanisms of clinical anti-cancer drug resistance. *Proc Natl Acad Sci U S A*. 2011; 108: p. 18708–18713.
 216. Némati F, Sastre-Garau X, Laurent C, Couturier J, Mariani P, Desjardins L, et al. Establishment and characterization of a panel of human uveal melanoma xenografts derived from primary and/or metastatic tumors. *Clin Cancer Res*. 2010; 16: p. 2352–2356.
 217. Sivanand S, Pena-Llopis S, Zhao H, Kucejova B, Spence P, Pavia-Jimenez A, et al. A validated tumorgraft model reveals activity of dovitinib against renal cell carcinoma. *Sci Transl Med*. 2012; 4(137ra75).
 218. Keysar SB, Astling DP, Anderson RT, Vogler BW, Bowles DW, Morton JJ, et al. A patient tumor transplant model of squamous cell cancer identifies PI3K inhibitors as candidate therapeutics in defined molecular bins. *Mol Oncol*. 2013; 7: p. 776–790.
 219. Rubio-Viqueira B, Jimeno A, Cusatis G, Zhang X, Iacobuzio-Donahue C, Karikari C, et al. An in vivo platform for translational drug development in pancreatic cancer. *Clin Cancer Res*. 2006; 12: p. 4652–4661.
 220. Hidalgo M, Bruckheimer E, Rajeshkumar NV, Garrido-Laguna I, De Oliveira E, Rubio-Viqueira B, et al. A Pilot Clinical Study of Treatment Guided by Personalized Tumorgrafts in Patients with Advanced Cancer. *Mol Cancer Ther*. 2011; 10(8): p. 1311–1316.
 221. Junttila MR, de Sauvage FJ. Influence of tumour micro-environment heterogeneity on therapeutic response. *Nature*. 2013; 501: p. 346–354.
 222. De Wever O, Mareel M. Role of tissue stroma in cancer cell invasion. *J Pathol*. 2003; 200: p. 429-447.
 223. Walsh N, et al. Humanized mouse models of clinical disease. *Annu Rev Pathol*. 2017; 12: p. 187-215.
 224. Weeber F, et al. Tumor Organoids as a Pre-clinical. *Cancer Model for Drug Discovery*. 2017; 24(9): p. 1092-1100.
 225. Griffith L, Swartz M. Capturing complex 3D tissue physiology in vitro. *Nat Rev Mol Cell Biol*. 2006;: p. 211-224.
 226. Ishiguro T, et al. Tumor-derived spheroids: Relevance to cancer stem cells and clinical applications. 2017; 108(3): p. 283–289.
 227. Sato T, et al. Long-term expansion of epithelial organoids from human colon, adenoma, adenocarcinoma, and Barrett’s epithelium. *Gastroenterology*. 2011; 141: p. 1762–1772.
 228. Clevers H. Modeling development and disease with organoids. *Cell*. 2016; 165: p. 1586–1597.
 229. Boj S, et al. Organoid models of human and mouse ductal pancreatic cancer. *Cell*. 2015; 160: p. 324–338.
 230. Huang L, et al. Ductal pancreatic cancer modeling and drug screening using human pluripotent stem cell- and patient-derived tumor organoids. *Nat Med*. 2015; 21: p. 1364–1371.

231. Bartfeld S, al e. In vitro expansion of humangastric epithelial stem cells and their responses to bacterial infection. *Gastroenterology*. ; 148: p. 126–136.e6.
232. Gao H, al e. High-throughput screening using patient-derived tumor xenografts to predict clinical trial drug response. *Nat Med*. 2015; 21: p. 1318–1325.
233. Karthaus W, al e. Identification of multipotent luminal progenitor cells in human prostate organoid cultures. *Cell*. 2014; 159: p. 163–175.
234. Huch M, Boj S, Clevers H, al e. Lgr5(+) liver stem cells, hepatic organoids and regenerative medicine. *Regen Med*. 2013; 8: p. 385–387.
235. Huch M, al e. Long-term culture of genome-stable bipotent stem cells from adult human liver. *Cell*. 2015; 160: p. 299–312.
236. Drost J, al e. Sequential cancer mutations in cultured human intestinal stem cells. *Nature*. 2015; 521: p. 43–47.
237. Li X, al e. Oncogenic transformation of diverse gastrointestinal tissues in primary organoid culture. *Nat Med*. 2014; 20: p. 769–777.
238. Nadauld L, al e. Metastatic tumor evolution and organoid modeling implicate TGFBR2 as a cancer driver in diffuse gastric cancer. *Genome Biol*. 2014; 15(428).
239. Riffle S, Hegde R. Modeling tumor cell adaptations to hypoxia in multicellular tumor spheroids. *J Exp Clin Cancer Res*. 2017; 36(102).
240. Weiswald L, al e. Spherical Cancer Models in Tumor Biology. *Neoplasia*. 2015; 17(1): p. 1–15.
241. Furth J, Kahn M. The transmission of leukaemia of mice with a single cell. *Am J Cancer*. 1937; 31: p. 276–282.
242. Bonnet D, Dick J. Human acute myeloid leukemia is organized as a hierarchy that originates from a primitive hematopoietic cell. *Nat Med*. 1997; 3: p. 730–737.
243. Al-Hajj M, al e. Prospective identification of tumorigenic breast cancer cells. *Proc Natl Acad Sci USA*. 2003; 100: p. 3983–3988.
244. Collins A, al e. Prospective spective identification of tumorigenic prostate cancer stem cells. *Cancer Res*. 2005; 65: p. 10946–10951.
245. Fang D, al e. A tumorigenic subpopulation with stem cell properties in melanomas. *Cancer Res*. 2005; 65: p. 9328–9337.
246. Yang Z, al e. Identification of local and circulating cancer stem cells in human liver cells. *Hepatology*. 2008 919–928; 47.
247. Li C, al e. Identification of pancreatic cancer stem cells. *Cancer Res*. 2007; 67: p. 1030–1037.
248. Hermann P, al e. Distinct populations of cancer stem cells determine tumor growth and metastatic activity in human pancreatic cancer. *Cell Stem Cell*. 2007; 1: p. 313–323.
249. O’Brien C, al e. A human colon cancer cell capable of initiating tumour growth in immunodeficient mice. *Nature*. 2007; 445: p. 106–110.
250. Ricci-Vitiani L, al e. Identification and expansion of human colon cancer-initiating cells. *Nature*. 2007; 445: p. 111–115.
251. Prince M, al e. Identification of a subpopulation of cells with cancer stem cell properties in head and neck squamous cell carcinoma. *Proc Natl Acad Sci USA*. 2007; 104: p. 973–978.
252. Clarke M, al e. Cancer stem cells-perspectives on current status and future directions: AACR workshop on cancer stem cells. *Cancer Res*. 2006; 66: p. 9339–9344.
253. Reya T, al e. Stem cells, cancer, and cancer stem cells. *Nature*. 2001; 414: p. 105–111.
254. Brabletz S, al e. Gastrointestinal stem cells in development and cancer. *J Pathol*. 2009; 217: p. 307–317.
255. Safa A, al e. Resistance to Cell Death and Its Modulation in Cancer Stem Cells. *Crit Rev Oncog*. 2016; 21(3-4): p. 203–219.
256. Nguyen L, al e. Cancer stem cells: an evolving concept. *Nat Rev Cancer*. 2012; 12(2): p. 133-143.

257. Marjanovic N, al e. Cell Plasticity and Heterogeneity in Cancer. *Clinical Chemistry*. 2013.
258. Cabrera M, al e. Cancer stem cell plasticity and tumor hierarchy. *World Journal of Stem Cells*. 2015; 7(1): p. 27–36.
259. Franco S, al e. In vitro models of cancer stem cells and clinical applications. *BMC Cancer*. 2016; 16(738).
260. Blanpain C, al e. Epithelial stem cells: turning over new leaves. *Cell*. 2007; 128: p. 445–458.
261. Tatematsu M, al e. Stem cells and gastric cancer: role of gastric and intestinal mixed intestinal metaplasia. *Cancer Sci*. 2003; 94: p. 135–141.
262. Satija N, al e. Mesenchymal stem cells: molecular targets for tissue engineering. *Stem Cells Dev*. 2007; 16: p. 7–23.
263. Kavanagh D, Kalia N. Hematopoietic stem cell homing to injured tissues. *Stem Cell Rev*. 2011; 7: p. 672–682.
264. Varon C, al e. Helicobacter pylori infection recruits bone marrow-derived cells that participate in gastric preneoplasia in mice. *Gastroenterology*. 2012; 14: p. 281–291.
265. Bekaii-Saab T, al e. Identifying and targeting cancer stem cells in the treatment of gastric cancer. *Cancer*. 2017; 123(8): p. 1303–1312.
266. Clevers H, al e. The cancer stem cell: premises, promises and challenges. *Nat Med*. 2011; 17: p. 313–319.
267. Singh S, al e. Identification of a cancer stem cell in human brain tumors. *Cancer Res*. 2003; 63: p. 5821–5828.
268. Ginestier Cea. ALDH1 is a marker of normal and malignant human mammary stem cells and a predictor of poor clinical outcome. *Cell Stem Cell*. 2007; 1(5): p. 555–567.
269. Huang CPea. ALDH-positive lung cancer stem cells confer resistance to epidermal growth factor receptor tyrosine kinase inhibitors. *Cancer Lett*. 2013; 328(1): p. 144–151.
270. Fitzgerald Tea. The impact of Aldehyde dehydrogenase 1 expression on prognosis for metastatic colon cancer. *J Surg Res*. 2014; 192((1)): p. 82–89.
271. Nguyen P, al e. Characterization of Biomarkers of Tumorigenic and Chemoresistant Cancer Stem Cells in Human Gastric Carcinoma. *Clin Cancer Res*. 2017; 23(6): p. 1586–1597.
272. Zhang C, Li C, He F, al e. Identification of CD44+ CD24+gastric cancer stem cells. *J Cancer Res Clin*. 2011; 137(11): p. 1679–86.
273. Chen XL, al e. Clinical significance of putative markers of cancer stem cells in gastric cancer: A retrospective cohort study. *Oncotarget*. 2016; 7(38): p. 62049–62069.
274. Brungs D, al e. Gastric cancer stem cells: evidence, potential markers, and clinical implications. *J Gastroenterol*. 2016; 51: p. 313–326.
275. Yoon C, al e. CD44 expression denotes a subpopulation of gastric cancer cells in which Hedgehog signaling promotes chemotherapy resistance. *Clin Cancer Res*. 2014; 20(15): p. 3974–3988.
276. Jiang J, al e. Trastuzumab (herceptin) targets gastric cancer stem cells characterized by CD90 phenotype. *Oncogene*. 2016; 31(6): p. 671–682.
277. Gong X, al e. LGR5-Targeted Antibody–Drug Conjugate Eradicates Gastrointestinal Tumors and Prevents Recurrence. *Large Molecule Therapeutics*. 2016; 15(7).
278. Honjo S, al e. Metformin sensitizes chemotherapy by targeting cancer stem cells and the mTOR pathway in esophageal cancer. *Int J Oncol*. 2014; 45(2): p. 567–574.
279. Nguyen P, al e. All-trans retinoic acid targets gastric cancer stem cells and inhibits patient-derived gastric carcinoma tumor growth. *Oncogene*. 2016; 35(43): p. 5619–5628.
280. Shitara K, al e. Dose-escalation study for the targeting of CD44v+ cancer stem cells by sulfasalazine in patients with advanced gastric cancer (EPOC1205). *Gastric Cancer*. 2017; 20(2): p. 341–349.
281. Chen R, al e. Disruption of xCT inhibits cancer cell metastasis via the caveolin-1/β-catenin pathway. *Oncogene*. 2009; 28: p. 599–609.
282. Yae T, al e. Alternative splicing of CD44 mRNA by ESRP1 enhances lung colonization of metastatic cancer cell. *Nat Commun*. 2012; 3(883).

283. Miyoshi H, Stappenbeck T. In vitro expansion and genetic modification of gastrointestinal stem cells as organoids. *Nat Protoc.* 2013; 8(12): p. 2471–2482.
284. Vigna E, Naldini L. Lentiviral vectors: excellent tools for experimental gene transfer and promising candidates for gene therapy. *J Gene Med.* 2000; 2: p. 308–316.
285. Yashiro M. Gastric Cancer Stem Cells and Resistance to Cancer Therapy. *Chemotherapy.* 2014; 3(135).
286. Luraghi P, al e. A molecularly annotated model of patient-derived colon cancer stem-like cells to assess genetic and non-genetic mechanisms of resistance to anti-EGFR therapy. *Clin Cancer Res.* 2017.
287. Viola D, Cappagli V, Elisei R. Cabozantinib (XL184) for the treatment of locally advanced or metastatic progressive medullary thyroid cancer. *Future Oncol.* 2013; 9: p. 1083-1092.
288. Kerr M, al e. Mutant Kras copy number defines metabolic reprogramming and therapeutic susceptibilities. *Nature.* 2016; 531(7592): p. 110–113.
289. Sun C, al e. Rational combination therapy with PARP and MEK inhibitors capitalizes on therapeutic liabilities in RAS mutant cancers. *Sci Transl Med.* 2017; 9(392).
290. Byrne A, al e. Interrogating open issues in cancer precision medicine with patient-derived xenografts. *Nature Reviews Cancer.* 2017; 17: p. 254–268.
291. Zhu Y, al e. Establishment and characterization of patient-derived tumor xenograft using gastroscopic biopsies in gastric cancer. *SCIENTIFIC REPORTS.* 2015; 5(8542).
292. Choi Y, al e. Establishment and characterisation of patient-derived xenografts as preclinical models for gastric cancer. *Scientific Reports.* 2016; 6(22172).
293. Fukuda Kea. Tumor initiating potential of side population cells in human gastric cancer. *Int J Oncol.* 2009; 34: p. 1201–1207.
294. Hajimoradi M, al e. STAT3 is Overactivated in Gastric Cancer Stem-Like Cells. *Cell J.* 2016; 17(4): p. 617–628.
295. Ruangpratheep C, al e. OCT4 expression on a case of poorly differentiated (insular) carcinoma of the thyroid gland and minireview. *J Med Assoc Thai.* 2005; 88: p. S281–S289.
296. Sanada Y, al e. Histopathologic evaluation of stepwise progression of pancreatic carcinoma with immunohistochemical analysis of gastric epithelial transcription factor SOX2: comparison of expression patterns between invasive components and cancerous intraductal. *Pancreas.* 2006; 32: p. 164-170.
297. Spisek R, al e. Frequent and specific immunity to the embryonal stem cell–associated antigen SOX2 in patients with monoclonal gammopathy. *J Exp Med.* 2007; 204: p. 831–840.
298. Wang Q, al e. Oct3/4 and Sox2 are significantly associated with an unfavorable clinical outcome in human esophageal squamous cell carcinoma. *Anticancer Res.* 2009; 29: p. 1233–1241.
299. Luraghi P, al e. MET signaling in colon cancer stem-like cells blunts the therapeutic response to EGFR inhibitors. *Cancer Res.* 2014; 74(6): p. 1857-1869.
300. Petti C, al e. Truncated RAF kinases drive resistance to MET inhibition in MET-addicted cancer cells. *Oncotarget.* 2015; 6: p. 221-233.
301. Arbiser JL, al e. Isolation of mouse stromal cells associated with a human tumor using differential diphtheria toxin sensitivity. *Am J Pathol.* 1999; 155: p. 723-729.
302. Paraiso K, Smalley K. Fibroblast-mediated drug resistance in cancer. *Biochem Pharmacol* 85. 2013; 85: p. 1033-1041.
303. Martin V, al e. Increase of MET gene copy number confers resistance to a monovalent MET antibody and establishes drug dependence. *Mol Oncol.* 2014.
304. Ponzetto C, al e. c-met is amplified but not mutated in a cell line with an activated met tyrosine kinase. *Oncogene.* 1991; 6: p. 553-559.
305. Smolen G, al e. Amplification of MET may identify a subset of cancers with extreme sensitivity to the selective tyrosine kinase inhibitor PHA-665752. *Proc Natl Acad Sci U S A.* 2006; 103: p. 2316-2321.
306. Lennerz J, al e. MET amplification identifies a small and aggressive subgroup of esophagogastric

- adenocarcinoma with evidence of responsiveness to crizotinib. *J Clin Oncol.* 2010; 29: p. 4803-4810.
307. Bachleitner-Hofmann Tea. HER kinase activation confers resistance to MET tyrosine kinase inhibition in MET oncogene-addicted gastric cancer cells. *Mol Cancer Ther.* 2008; 7: p. 3499-3508.
308. Corso S, Comoglio PM, Giordano S. Cancer therapy: can the challenge be MET? *Trends Mol Med.* 2005; 11(6): p. 284-292.
309. Engelman J, al e. MET amplification leads to gefitinib resistance in lung cancer by activating ERBB3 signaling. *Science.* 2007; 316: p. 1039-1043.
310. Bean J, al e. MET amplification occurs with or without T790M mutations in EGFR mutant lung tumors with acquired resistance to gefitinib or erlotinib. *Proc Natl Acad Sci U S A.* 2007; 104: p. 20932-20937.
311. Puri N, Salgia R. Synergism of EGFR and c-Met pathways, cross-talk and inhibition, in non-small cell lung cancer. *J Carcinog.* 2008; 7(9).
312. Breindel J, al e. EGF receptor activates MET through MAPK to enhance non-small cell lung carcinoma invasion and brain metastasis. *Cancer Res.* 2013; 73: p. 5053-5065.
313. Hirashita Y, Tsukamoto Y, Yanagihara K, Fumoto S, Hijiya N, al e. Reduced phosphorylation of ribosomal protein S6 is associated with sensitivity to MEK inhibition in gastric cancer cells. *Cancer Sci.* 2016; 107: p. 1919-1928.
314. Freeman A, Morrison D. Mechanisms and potential therapies for acquired resistance to inhibitors targeting the Raf or MEK kinases in cancer. *Molecular Mechanisms of Tumor Cell Resistance to Chemotherapy: Targeted Therapies to Reverse Resistance.* Bonavita B. 2013;: p. 47-67.
315. Milella M, al e. PTEN status is a crucial determinant of the functional outcome of combined MEK and mTOR inhibition in cancer. *Scientific Reports.* 2017; 7(43013).
316. Dumble Mea. Discovery of Novel AKT Inhibitors with Enhanced Anti-Tumor Effects in Combination with the MEK Inhibitor. *Plos One.* 2014; 9(6).
317. Tolcher A, al e. Phase I study of the MEK inhibitor trametinib in combination with the AKT inhibitor afuresertib in patients with solid tumors and multiple myeloma. *Cancer Chemother Pharmacol.* 2015; 75(1): p. 183-189.
318. Ng K, al e. Phase II Study of Everolimus in Patients with Metastatic Colorectal Adenocarcinoma Previously Treated with Bevacizumab-, Fluoropyrimidine-, Oxaliplatin-, and Irinotecan-Based Regimens. *Cancer Therapy: Clinical.* 2013.
319. Sullivan R, al e. Atezolizumab (A) + cobimetinib (C) + vemurafenib (V) in BRAFV600-mutant metastatic melanoma (mel): Updated safety and clinical activity. *Journal of Clinical Oncology.* 2017; 35(15 suppl): p. 3063-3063.
320. Ma Y, al e. K-ras gene mutation as a predictor of cancer cell responsiveness to metformin. *Mol Med Rep.* 2013; 8(3): p. 763-768.

Acknowledgments

I would like to express my special appreciation and thanks Professor Silvia Giordano for offering me the opportunity to be part of her group during this last 3 years, for allowing me to grow as a research scientist and for her support during the hard times. Working in Silvia's group made me learn a lot during my PhD and I will always be grateful for the chance she gave me.

I would like to thank also to Professor Claudia Giachino for the chance of performing my PhD under her tutoring, as well as her supervision during these 4 years. I also want to thank Valentina, Clara, Lisa e Silvia, from all their support.

Special thanks to Marilisa, Annalisa, Maria, Simona, Silvia, Elena, Cristina, for friendly welcomed me, for teaching, patience and support. A big thank to Stefano, Laura, Stefania, Giulia e Micchela for helping and supporting me always with a smile.

I would also like to thank every member of the Tamagnone's group, especially to Sabrina, Luca, Chiara, Gabriela and Giulia, for having accepted me in Lilla's group from the first day.

Thanks also to all the people in the Institute who spent some of their time helping me: Stefania Giove, Federica Verginelli, Barbara Martignolo, Francesco Sassi, Emanuel Midonti and Claudio Isella.

Thanks very much to Chiara, Virginia, Anna, Guendalina, Liana, Lavinia, and Ilaria for our scientific conversations, our laughs, their kindness, patience and support, as well as their friendship.

An important thanks to my family, especially to my parents, that even from far always encouraged me with their unconditional love and support. Thank you to be my rocks!

Thanks to all those that passed in my life and directly or indirectly have helped me to get here, supporting me in my personal and professional growth.

PhD Report

Relazione sulle attività svolte nel corso del dottorato e pubblicazioni

Candidata Tânia Isabel de Miranda Capelôa

Docenti responsabili : Prof.ssa Claudia Giachino

Prof.essa Silvia Giordano

PUBLICATIONS

Full papers

- Corso S., Cargnelutti M., Durando S., Menegon S., Apicella M., Migliore C., Capelôa T., Isella C., Medico E., Bertotti A., Sassi F., Sarotto I., Casorzo L., Pisacane A., Mangioni M., Sottile A., Degiuli M., Fumagalli U., Sgroi G., Molfino S., De Manzoni G., Rosati R., De Simone M., Marrelli D., Saragoni L., Rause S., Pallabazzer G., Roviello F., Cassoni P., Sapino A., Bass A. and Giordano S. (2017) Rituximab treatment prevents lymphoma onset in gastric cancer patient-Derived-Xenografts, Manuscript submitted for publication.

- Apicella M., Migliore C., Capelôa T., Menegon S., Cargnelutti M., Degiuli M., Sapino A., Sottile A., Sarotto I., Casorzo L., Cassoni P., De Simone M., Comoglio P.M., Marsoni S., Corso S., Giordano S. (2016) Dual MET/EGFR therapy leads to complete response and resistance prevention in a MET-amplified gastroesophageal xenopatient cohort. *Oncogene*. DOI: 10.1038/onc.2016.283.

- Gallina C., Capelôa T., Saviozzi S., Accomasso L., Catalano F., Tullio F., Martra G., Penna C., Pagliaro P., Turinetto V., Giachino C. (2015) Human mesenchymal stem cells labelled with dye-loaded amorphous silica nanoparticles: long-term biosafety, stemness preservation and traceability in the beating heart. *J Nanobiotechnology*; 13:77. DOI: 10.1186/s12951-015-0141-1.

Abstracts:

- Apicella M., Migliore C., Menegon S., Cargnelutti M., Capelôa T., Cassoni P., Sapino A., Bass A., Corso S., Giordano S.. "Targeting HER2 in gastric cancer: Hints from a gastric PDX platform". Poster presented at the EACR-AACR-SIC Special Conference 2017: The Challenges of Optimizing Immuno- and Targeted Therapies: From Cancer Biology to the Clinic, Florence, Italy, June 24 - 27, 2017

- Tânia Capelôa, Claudia Giachino, Simona Corso, Silvia Giordano. “Gastric cancer stem cells: do they maintain the genetic alterations of driver genes identified in the primary tumor?” Poster presented at the 2nd EACR-OECI conference: MAKING IT PERSONAL Cancer Precision Medicine, Amsterdam, Netherlands, 13-16 March 2017.
- Cristina Migliore, Maria Apicella, Silvia Menegon, Marilisa Cargnelutti, Tânia Capelôa, Paola Cassoni, Anna Sapino, Adam Bass, Simona Corso and Silvia Giordano.”Precision medicine in gastric cancer: identification of negative response predictors for trastuzumab therapy.” Poster presented at the Europdx Workshop 2016: PDX models in clinical oncology and cancer precision medicine, Weggis, Switzerland, 3-5 October 2016.
- Tânia Capelôa, Maria Apicella, Cristina Migliore, Anna Sapino, Paola Cassoni, Simona Corso, Silvia Giordano. “Dual anti-MET/EGFR therapy leads to complete response and resistance prevention in a MET-amplified gastroesophageal xenopatient cohort.” Poster and short talk presentation at the 58th annual meeting of the italian cancer society, Verona, Italy, 5-8 September 2016.
- Silvia Menegon, Maria Apicella, Cristina Migliore, Tânia Capelôa, Marilisa Cargnelutti, Maurizio Degiuli, Anna Sapino, Paola Cassoni, Michele De Simone, Paolo M. Comoglio, Silvia Marsoni, Simona Corso and Silvia Giordano. “Gastric cancer in the age of targeted agents: identification and validation of novel therapeutic strategies through the generation of a patient-derived xenografts platform”. AACR 107th Annual Meeting 2016; New Orleans, LA, USA, 16-20 April, 2016.
- Tânia Capelôa, Maria Apicella, Cristina Migliore, Anna Sapino, Paola Cassoni, Simona Corso, Silvia Giordano.”Dual anti-MET/EGFR therapy leads to complete response and resistance prevention in a MET-amplified gastroesophageal xenopatient cohort.” Poster presented at the VHIO SPECIAL SYMPOSIUM: Towards Predictive Cancer Models, Barcelona, Spain, May 2016,
- Gallina C., Accomasso L., Capelôa T., Saviozzi S., Turinetto V., Penna C., Tullio F., Catalano F., Alberto G., Alloatti G., Pagliaro P., Giachino G. “Human mesenchymal stem cells labeled with fluorescent silica nanoparticles appear to have a differential migratory behavior in an ex vivo rat model of myocardial infarction. Poster presentation at II Meeting of Department of Clinical and Biological Sciences, Turin, Italy, September 16, 2014.

- Period of Collaboration

From 7 to 14 of September 2017, visiting PhD student in the laboratory the of Professor Paola Chiarugi - Department of biomedical, experimental and clinical sciences of the University of Florence

Courses:

- Biostatistics course: Candiolo Cancer Institute, IRCC, Turin, 2017
- Laboratory Assistant Suite (LAS) platform course: Candiolo Cancer Institute, IRCC, Turin, 2017.
- Corso di citofluorimetria, Istituto di Candiolo, IRCC, 18 Marzo. 2016, Torino
- Corso de manipolazione animale, Istituto di Candiolo, IRCC, 6-16 Giugno 2015, Torino

Workshops/congress

- PROMISES AND CHALLENGES OF DEVELOPING NEW DRUGS IN ONCOLOGY, 4th Michelangelo conference, Milan, Italy, July 6-7, 2017
- 2nd EACR-OECI conference: MAKING IT PERSONAL Cancer Precision Medicine, Amsterdam, Netherlands, 13-16 March 2017.
- GIORNATA DI STUDIO GUIDO TARONE, Università di Torino Molecular Biotechnology Center, 22 May 2017
- The 58th annual meeting of the italian cancer society, Verona, Italy, 5-8 September 2016.
- VHIO SPECIAL SYMPOSIUM: Towards Predictive Cancer Models, May 2016, Barcelona - Spain.
- Enabling technologies in 3D cancer organoids - Unito Polito Cancer Conference Series March 8-9, 2016, Torino.
- "Therapeutic strategies based on cancer stem cell targeting", Prof. Ruggero De Maria, IRCC- Torino, 2nd October 2015.
- Corso "Introduzione alla ricerca bibliografica", 18 e 25 settembre 2014, Torino Esposizioni.
- "Essere giovani protagonisti in H2020 (Opportunità di finanziamento: le Azioni Marie Curie e la rete Euraxess, il Cv dalla teoria alla pratica)", 2 luglio, 2014, Torino Esposizioni.
- "Targeted Therapy of Cancer: where we are heading", 27 giugno 2014, Centro di Biotecnologie Molecolari.

Presentazioni Seminari dottorato

- "Biosafety of functionalized silica nanoparticles for human mesenchymal stem cells imaging: Role in regenerative medicine", 28 Novembre 2014
- "Therapeutic approaches for gastric cancer based on genetic and biological analysis", 30 Giugno 2015
- "Therapeutic approaches in gastric cancer based on genetic and biological analysis", 27 Novembre 2015
- "Therapeutic approaches in gastric cancer based on genetic and biological analysis", 30 Giugno 2016
- "Therapeutic approaches in gastric cancer based on genetic and biological analysis", 29 Novembre 2016

Presentazioni Seminari dottorato (Journal club)

- “Glomerular common gamma chain confers B- and T-cell–independent protection against glomerulonephritis”, 9 Ottobre 2017, Turin
- “Normalization and improvement of CNS deficits in mice with Hurler syndrome after long-term peripheral delivery of BBB-targeted iduronidase”. 14 Febbraio 2017, Turin
- “Variations in DNA methylation of interferon gamma and programmed death 1 in allograft rejection after kidney transplantation”, 16 Dicembre 2016
- “Parkinson's disease-associated mutant VPS35 causes mitochondrial dysfunction by recycling DLP1 complexes”, 8 Marzo 2016
- “Towards a therapy for Angelman syndrome by reduction of a long non- coding RNA”, 13 Ottobre 2015
- “An exome study of Parkinson's disease in Sardinia, a Mediterranean genetic isolate”, 19 Maggio 2015
- "Decreasing Cx36 Gap Junction Coupling Compensates for Overactive KATP Channels to Restore Insulin Secretion and Prevent Hyperglycemia in a Mouse Model of Neonatal Diabetes", 9 Dicembre 2014
- "Whole-exome sequencing and imaging genetics identify functional variants for rate of change in hippocampal volume in mild cognitive impairment", 9 Giugno 2014